MAY 16 1929

U. S. DEPARTMENT OF COMMERCE

BUREAU OF STANDARDS JOURNAL OF RESEARCH

Vol. 2 MAY, 1929 No. 5

CONTENTS

RP. No.	TITLE	Page
60	Continuous spectrum X rays from thin targets	837
61	A mutiple-strand test for yarns	871
62	Thermal expansion of tantalum	887
63	Soundproofing of airplane cabins	897
64	Prism refractometry and certain goniometrical requirements for precision	909
65	A new determination of the melting point of palladium	931
66	A new seismometer equipped for electromagnetic damping and electromagnetic and optical magnification (theory, general design, and preliminary results)	963

BUREAU OF STANDARDS JOURNAL OF RESEARCH

PARTIAL CONTENTS OF VOLUME 1

Price of bound volume, $2.75

September, 1928 (Vol. 1, No. 3)

RP11. Standard solar wave lengths (3592-7148A). Price 5 cents.

RP12. Wave lengths and Zeeman effects in yttrium spectra. Price 10 cents.

RP13. Wear and mechanical properties of railroad bearing bronzes at different temperatures. Price 35 cents.

RP14. Steel for casehardening—normal and abnormal steel. Price 35 cents.

RP15. Strain markings in mild steel under tension. Price 15 cents.

October, 1928 (Vol. 1, No. 4)

RP16. Methods for the derivation and expansion of formulas for the mutual inductance of coaxial circles and for the inductance of single-layer solenoids. Price 10 cents.

RP17. Effect of clearance and displacement of attracted disk and also of a certain arrangement of conducting hoops upon the constant of an electrometer. Price 5 cents.

RP18. Mutual inductance of any two circles. Price 5 cents.

RP19. Receiving sets for aircraft beacon and telephony. Price 15 cents.

RP20. Sensitization of photographic emulsions by colloidal materials. Price 10 cents.

RP21. An experimental study of the corona voltmeter. Price 20 cents.

RP22. The International temperature scale. Price 5 cents.

RP23. Tables of theoretical Zeeman effects. Price 15 cents

November, 1928 (Vol. 1, No. 5)

RP24. Mutual inductance and torque between two concentric solenoids. Price 5 cents.

RP25. A study of the hydrogen-antimony-tin method for the determination of oxygen in cast irons. Price 5 cents.

RP26. Note on the effect of repeated stresses on the magnetic properties of steel. Price 5 cents.

RP27. Effect of twist on cotton yarns. Price 5 cents.

Research papers are available as separates for purchase from the Superintendent of Documents United States Government Printing Office, Washington, D. C.

[Continued on page 3 of cover]

U. S. DEPARTMENT OF COMMERCE
BUREAU OF STANDARDS

BUREAU OF STANDARDS JOURNAL OF RESEARCH

May, 1929
Vol. 2, No. 5

UNITED STATES
GOVERNMENT PRINTING OFFICE
WASHINGTON : 1929

For a partial list of previous research papers appearing in Volumes 1 and 2, BUREAU OF STANDARDS JOURNAL OF RESEARCH, see pages 2, 3, and 4 of the cover

SOLD ONLY BY THE SUPERINTENDENT OF DOCUMENTS
U. S. GOVERNMENT PRINTING OFFICE
WASHINGTON, D. C.
AT
$2.75 PER YEAR ON SUBSCRIPTION

CONTINUOUS SPECTRUM X RAYS FROM THIN TARGETS[1]

By Warren W. Nicholas[2]

Technique is described for the use of thin metal foils as anticathodes in X-ray tubes. The continuous radiation from these foils is analyzed by a crystal, the intensities being measured by a photographic comparison method. It is indicated that the high-frequency limit of the continuous spectrum from an infinitely thin target consists of a finite discontinuity. (The corresponding thick target spectrum has only a discontinuity of slope.) The energy distributions on a frequency scale are approximately horizontal, for gold and for aluminum, and for $\psi=40°$, 90°, and 140°, where ψ is the angle between measured X rays and cathode stream; this agrees with Kramer's, but not with Wentzel's, theory. The intensities for these values of ψ are roughly 3:2:1, respectively; theories have not yet been constructed for the variation with ψ of resolved energy, but it is pointed out that the observations do not support a supposed quantum process in which a single cathode ray, losing energy $h\nu$ by interaction with a nucleus, radiates a single frequency ν in the continuous spectrum. The observations do not support the "absorption" process assumed by Lenard, in which cathode rays, in penetrating a metal, suffered large losses of speed not accompanied by radiation. The manner in which thick target spectra are synthesized from thin is discussed, and empirical laws are formulated describing the dependence on ψ of thick target continuous spectrum energy. A structure for the moving electron is proposed which explains classically X ray continuous spectrum phenomena, and seems to have application in other fields as well.

CONTENTS

	Page
I. Introduction	838
II. Method	839
1. Source of X rays	839
2. Spectral analysis of X rays	841
III. Apparatus	842
1. X-ray tube	842
2. Spectrographs	844
IV. Results	845
1. Shape of the high-frequency limit	845
2. Continuous spectrum energy distribution	849
V. Discussion	851
1. Passage of cathode rays through matter	851
2. Synthesis of thick target spectra	851
3. Mechanism of radiation	853
4. Structure of the moving electron	859
VI. Bibliography	870

[1] A preliminary report of these results was presented at a meeting of the American Physical Society, April, 1928.

[2] This work was done while the author was a National Research Fellow at Cornell University.

I. INTRODUCTION

Past experiments performed for the purpose of discovering the laws of X-ray emission have generally utilized the conventional X-ray tubes, with massive anticathodes, for which, unfortunately, experimental conditions are not so simple as could be desired. For example, the cathode rays in such a tube have a definite uniform speed v_0 only at the instant they strike the anticathode; in their impacts with the atoms of the target, they are gradually slowed down to zero, so that, in reality, the X rays are produced by cathode rays of all speeds between zero and v_0. This loss of speed has been corrected for, and the laws of continuous spectrum emission derived (1) [3] for uniform cathode ray speeds on the basis of the Thomson-Whiddington-Bohr law and the total energy law, but this latter is not known for directions other than perpendicular to the cathode stream, and there is some question as to whether the former law is applicable to the present case (2, 3, 4). Perhaps the most serious doubt in this respect is due to the experiments of Lenard (3), who claimed that a large percentage of the cathode rays were not slowed up gradually but suffered large losses of speed ("absorptions") in encountering the atoms of the target.[4]

Another difficulty with experimental conditions inside the conventional X-ray tube is the uncertainty as to the direction of motion of the cathode rays which have penetrated the anticathode. The laws for calculating these changes of direction, which are due to a slow diffusion as well as to sharper deflections (5), have not yet been investigated in such a way as to allow their application to the present problem in the same way as the Thomson-Whiddington-Bohr law was applied to the loss of speed.

A third difficulty with thick targets is due to deflections of the cathode rays inside the target such as to cause a considerable fraction of them to leave the focal spot, reenter the space between cathode and anode, but, due to the field, come back to strike other parts of the anode (2, 6, 7). The X rays produced by these stray cathode rays are not ordinarily included in the measurements, and since their spectrum distribution is different (2) from that of the X rays coming from the focal spot it is evident that even the mathematical form of the laws of emission will be influenced by their neglect. The effect is not at all inappreciable, as this "stray" X-ray energy is of the order of one-fifth of the whole (7).

Other difficulties, such as the correction for absorption in the target, and the determination of the initial direction of the cathode stream

[3] The figures given in parentheses here and throughout the text relate to the reference numbers in the bibliography given at the end of this paper.

[4] For an excellent discussion of these ideas, together with an account of experimental and theoretical work on the continuous spectrum, see Kulenkampff, Handbuch der Physik, **23**, pp. 433–476.

for a target face inclined to the cathode stream are of comparatively small importance, and since these have been adequately discussed in previous papers (1, 2) they will receive only passing mention here.

II. METHOD

1. SOURCE OF X RAYS

The obvious way to simplify these experimental conditions is to use as target a foil so thin that only a very small proportion of the cathode rays in passing through the foil suffer appreciable deflection and loss of speed. This means, for ordinary voltages (of the order of 50 kv), films of a thickness of the order of 10^{-5} cm, depending on the density and atomic number of the metal used.[5]

The outstanding difficulty here is the measurement of X-ray energy from such a foil, since comparatively low current input must be used in order to prevent melting the foil. With a thick target, heat is conducted away from the focal spot to the mass of metal, but with these thin targets the heat must be dissipated chiefly by radiation. Now, the amount of energy (H) generated per unit time per unit area of these foils should be equal to $i\Delta V$ where i is current density; an application of the Thomson-Whiddington-Bohr law shows that H is approximately proportional to $\frac{i\Delta x}{V}$ for a given material. This energy appears mostly as heat energy—the X-ray energy being correspondingly small—thus the thinner the foil the less the heat it must dissipate. But the foil radiates heat proportional to its two surfaces, so the thinner the foil the greater the current density possible without melting the foil; in fact, it appears that for a given material and voltage $i_{max}\Delta x$ is practically constant. (For gold this constant is of the order of 10^{-5} milliamperes cm^{-1} at 40 kv.) Also the X-ray energy per unit area is proportional to $i\Delta x$, other things being equal; thus, no matter how thin the target, there is a definite limit to the X-ray energy obtainable at a given voltage per unit area of thin target of given material.

The relation $H \propto \frac{i\Delta x}{V}$ had a curious consequence in the experiments.

---

[5] For the calculation of the loss of speed the Thomson-Whiddington-Bohr law (8) is used, provisionally, since the experiments performed on metal foils to test this law have so far been applied not to all the cathode rays but only to those which penetrate with the least energy loss. Adopting the form

$$\frac{d(V^2)}{dx} = -b$$

where V is the equivalent voltage of the cathode rays, dx is the thickness of the foil (strictly, for infinitesimal thickness), and b is a constant roughly equal to 40×10^4 times the density of the metal if V is in kilovolts and x is in centimeters. The loss of speed of the cathode rays in the present experiments corresponded usually to a loss of voltage $\left(\Delta V = \frac{b\Delta x}{2V}\right)$ in the neighborhood of 1 kilovolt. The deflections of the cathode rays are also calculable by formula (5) for the case when the foils are so thin as to approximate conditions for single scattering. In the present experiments, however, it was impractical to use such thin foils, and the deflections were estimated by direct experiment (see below).

Where relatively high current densities were used it was found neces-sary in shutting off the power to reduce the filament current before cutting off the voltage. Otherwise, due to the gradual discharge of the condensers of the filter system (see below), there was an instant at which normal current flowed through the tube (the potential being far above the saturation value) at low voltage, with conse-quent melting of the foil. Strictly speaking, this effect will be en-hanced by the increased deflections in the target at lower voltages (5) which will, in general, contribute to the path lengths in the foil and consequently to $i\Delta x$; that is, H really increases faster than $1/V$.

The dependence of H on Δx is readily shown. In one experiment for example, an aluminum foil of 0.05 mm thickness melted for current densities and voltages which did not affect a 0.7 μ foil of the same metal. This dependence, however, holds also only within narrow limits. If the aluminum was still further increased in thickness (to 1 mm), it did not melt, due undoubtedly to the increased conduc-tion (negligible for very thin foils) away from the focal spot to parts of the foil not struck by cathode rays.

Several methods of support for the foils were used. It was essential, of course, that the electrical contact to the foils should be good in order that the foil remain accurately at the positive potential. In some of the experiments the gold foils were suspended from a brass support to which they were soldered with Wood's metal. Usually, however, the foils were suspended from an aluminum frame to which they were clamped.

In order that the source of X rays remain fixed, it was necessary that no fields exist near the foils to deflect them away from their vertical position. Thus, the X-ray tubes were designed so that the foils were practically entirely inclosed in a metal container at the same potential as the foil. The importance of this condition was evident in some experiments in which a part of the metal inclosure had been only insecurely connected electrically. When the cathode-ray current was turned on, the foil began to swing, more and more violently, until it tore itself to pieces.[6]

In these experiments there is a source of error which apparently can not be entirely eliminated. It is due to the fact that there are superposed on the X rays of which a measurement is desired other X rays, generated chiefly by stray cathode rays. Most of these stray cathode rays are those which have penetrated the foil, struck the end wall of the tube, and been "reflected" to strike again the foil and the side walls of the tube. X rays produced on the side walls in the regions which are lined up with the slits necessarily affect the measurements. Apparently no arrangement of fields can entirely

[6] The synchronization of disturbing field with foil position, which is necessary for such an effect, could be caused by a variation with foil position of cathode-ray deflections, which, in turn, affected the charging of the partially insulated metal piece.

diminate the reflection from the end walls of the tube, but by increasing the distance from the foil to the end wall the effect may be made as small as desired. The errors are further reduced by coating the inner walls of the tube with a substance of low atomic number, which reduces both the reflections from the end wall and the production of X rays in the side walls. However, all the undesired X rays mentioned above are generated practically uniformly over areas which are large compared with the focal spot. Thus, these X rays, if appreciable, can be measured independently and suitable correction applied to the measurements of X rays from the focal spot.

Duane (9, 10) has recently used a most ingenious method, in which a stream of mercury vapor forms the target. This method has the advantage over the one used in the present experiments, in that by varying the vapor density the deflections and loss of speed should be capable of being made negligibly small for any given voltage. The chief inherent difficulty would seem to be the somewhat large dimensions of the focal spot, which is sometimes a disadvantage, especially in measuring or comparing absolute spectral intensities (2).

Another method for investigating thin target spectra has been proposed by Bergen Davis (11). Since X-ray efficiency is proportional to the atomic number of the anticathode material, a target of beryllium would produce comparatively few X rays. If this target were now plated with a thin coating of heavy metal, the increment of X-ray energy would be practically due to the X rays produced in the heavy metal. Davis suggested[7] the use of tungsten as the heavy metal, since it is known that the "plating" of the beryllium could be carried out at will simply by evaporating part of the tungsten cathode filament. An objection to the method seems to be that, due to deflections inside the target, many of the cathode rays will return to the anode surface, to strike heavy atoms with reduced speed and indefinite direction. For example, the "stray cathode rays" discussed above will, in general, have penetrated the heavy metal twice before striking the anode the second time. Since most of these secondary effects will be superposed directly on the focal spot, it would seem that a satisfactory correction for them would be difficult.

2. SPECTRAL ANALYSIS OF X RAYS

The X rays produced in the thin targets were analyzed spectrally by a crystal grating, and the intensities were recorded photographically; the photographic method was used on account of its sensitiveness and flexibility. In order to interpret the photographic record in terms of energy distribution in the spectrum, it was necessary to standardize the films and spectrographs. This was done by substituting for the thin target a thick one and repeating the experiment

[7] Not published.

under identical conditions. Since the energy distribution in the thick target spectrum is known, a comparison of the two photographic records, which were treated simultaneously in the development, should permit an estimation of the energy distribution in the thin target spectrum. It is obvious that in this comparison most of the corrections (for example, absorption in windows, etc., variation of crystal reflecting efficiency, variation of sensitivity of photographic film) ordinarily so troublesome in such measurements are automatically taken care of. Absorption in the target is not thus taken care of, but in the present experiments it was negligible.

III. APPARATUS

1. X-RAY TUBE

Figure 1 shows a horizontal section and Figure 2 a vertical section of the tube used. The brass parts *S*, *T*, *B*, *A*, *W*, *F* are all at the

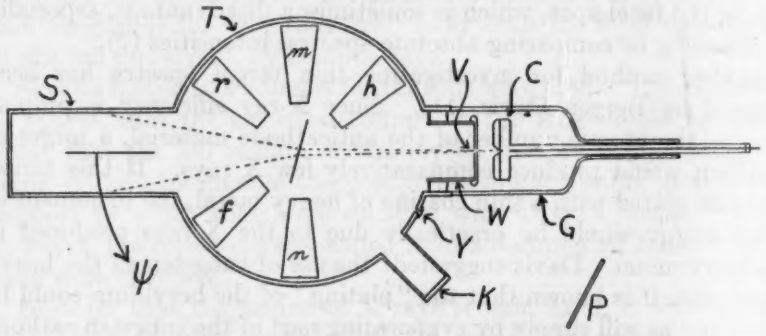

FIGURE 1.—*Horizontal section of thin target tube*

E, Thin target; *C*, cathode; *S*, chamber to reduce number of "reflected" cathode rays; *n*, *f*, *r*, *m*, *h*, spectrographs; *K*, glass window

positive potential, together with the thin foil *E* and the spectrographs *n*, *f*, *r*, *m*, *h*. *G* is of glass and is fastened to the brass with De Khotinsky; it supports and insulates the cathode *C*. The main part of the beam of cathode rays is included between the dotted lines. After being accelerated through the space between *C* and *W* they pass through the slit *V*, strike the thin foil *E*, and are finally stopped in the chamber *S*, designed to reduce the number of "reflected" cathode rays striking the foil. The spectrographs were arranged so as to analyze the X rays produced in *E*. The thin foil is inclined at the angle shown in Figure 1 to reduce absorption in the target of the X rays to be measured by spectrographs *m*, *n*.

The cover *B* was sealed to *A* with soft De Khotinsky and was easily removed by heating with a blowtorch. This permitted the renewal of thin foils, the insertion of spectrographs, the removal of the cathode for adjustment or renewal of filament (since *W* was

removable). A was a brass cylinder fastened to T with hard De Khotinsky. The poor conduction of heat from A to T permitted the ready removal and replacement of the cover without the necessity of supplying enough heat to warm the mass of metal T. To replace B, it was inverted over a blowtorch and heated to a temperature at which the bottom of the groove was easily wet with soft De Khotinsky, whereupon it was immediately placed on A. A very thin layer of the composition sufficed.

The glass tube H led to the evacuating system, consisting of an air-cooled mercury vapor pump and a Hyvac forepump. The

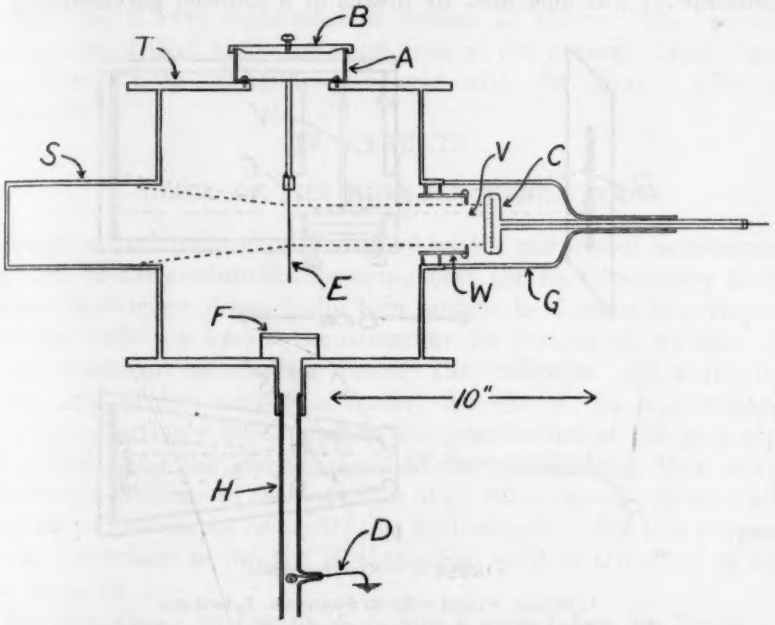

FIGURE 2.—*Vertical section of tube*

B, Removable cover, sealed with De Khotinsky; *D*, grounded wire to prevent discharges to forepump; *F*, small table to prevent discharges between *E* and *D*

grounded wire D was found necessary in case the potential was applied before a sufficiently high vacuum had been attained, to prevent a discharge through the mercury vapor pump to the forepump with possible damage to the motor commutator. Other discharges were found to occur between D and E, with damage to the foil, until the metal disk F was inserted. F also served to divert the air stream through H, which otherwise might have torn the foil when air was let into the apparatus.

The cathode C was designed and adjusted (filament behind a narrow slit) so that a focal spot on E was obtained which was about 4 mm wide and 3 cm long and of very approximately uniform intensity

distribution over this area. A pinhole photograph on plate P (pinhole at Y) served to indicate the dimensions and uniformity of the focal spot.

Protection from X rays is simple with this type of tube; the metal chamber was simply wrapped with sheet lead. The source of high potential used in the present work was patterned after the one at Stanford University (1), and the capacitances and inductances of the filter system were of the same order. The voltage was held steady by means of an electrostatic voltmeter which had been calibrated by spark gap, and the current (usually of the order of 0.1 milliampere) was measured by means of a shunted galvanometer.

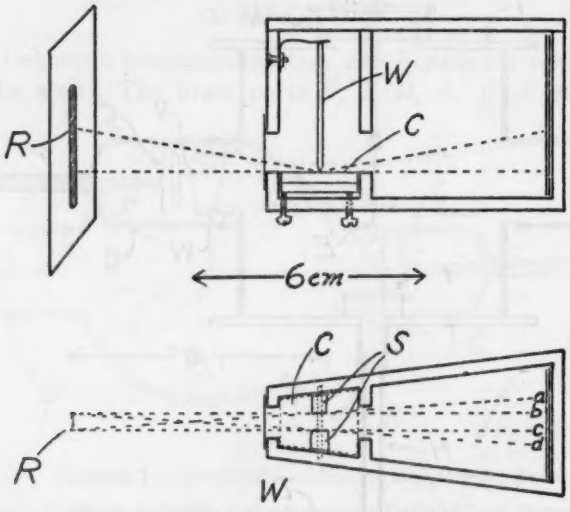

FIGURE 3.—*Spectrographs*

C, Crystal; *W*, lead wedge for Seeman slit; *R*, focal spot
Note that the design permitted an estimate, in the region outside *ad*, of the X rays due to stray cathode rays

2. SPECTROGRAPHS

The spectrographs (fig. 3) were of the Seeman type, a lead wedge W being pressed against two 0.06 mm pieces of lead S which rested on the face of the calcite crystal C. The ordinary features of design and necessary adjustments are obvious from the figure. It is evident that, if the focal spot R is of uniform intensity throughout its length and the thin target is of uniform thickness, the arrangement of Figure 3 is equivalent to one in which the crystal is rotated. But for the quantitative comparison of thin and thick target spectra mentioned above it is not necessary that the focal spot be of uniform intensity, if the intensity distribution does not change from experiment to experiment, which actually proved to be the case.

The length of the Seeman slit, governed by the distance between the lead pieces S, was 4 mm. Thus, from the geometry of the arrangement, it is seen that with the 4 mm focal spot used the part of the film *bc* would be blackened uniformly, since it is affected equally by radiation from all parts of the focal spot R. It is this part of the film that was photometered. Sections of film *ab* and *cd* will not receive uniform blackening, but the part of the film outside *ad* will be blackened uniformly by any X rays generated uniformly over the outer parts of the thin foil, as well as by X rays produced on the walls of the tube. Consequently, the spectral intensity outside the region *ad* is a measure of the energy in the various sources of undesired X rays mentioned in Section II above. The spectrograms showed that, under the conditions of the present experiments, these X rays were negligible compared with the X rays affecting the region *bc*.

IV. RESULTS

1. SHAPE OF THE HIGH-FREQUENCY LIMIT

Special experiments were performed for the purpose of ascertaining the form of the continuous spectrum near the high-frequency limit, a direct knowledge of which, for thin targets, is of prime importance. The chief difficulty here is the correction for various slit widths. It would be difficult to calculate directly the "effective" slit width due to the slits of the microphotometer, the slit of the spectrograph (which is effectively broadened by the penetration of the rays into the crystal), and the idiosyncrasies of the photographic film, but a satisfactory estimate of the net effect of all these factors can be made from either line shapes or absorption limit shapes. For this purpose it was convenient to use the K absorption limit of the silver of the film ($\lambda_{Ag K}$, fig. 4).

The data shown in Figures 4, 5, and 6 were taken for $V=32$ kv and $\psi=90°$. The thin target was of 0.086 μ gold foil, and a thick target of gold was used for the comparison spectrum. In Figure 4 the ordinates of the upper curves are proportional to transmission, since they are direct microphotometer readings. The lower curves represent photographic density (logarithm of reciprocal of transmission); this quantity is directly proportional to X-ray intensity (12) for a given wave length and for the low densities used here, but the constant of proportionality varies with wave length. The high-frequency limit (λ_0) of the thin target continuous spectrum is seen to have a shape and width much like that of the absorption limit. This suggests that the former may consist of a finite discontinuity, just like the absorption limit does, and as was suggested by Webster (13) from his analysis of thick target data.

For purposes of comparison curve A is duplicated in Figure 5, and dotted curve C is a reproduction of the absorption limit shape, reversed and magnified vertically. Now, practically, the "effective slit width" due to the factors mentioned above will be the same here for the absorption limit as for the continuous spectrum limit; for since the wave lengths have been (purposely) chosen fairly near together the slit width of the spectrometer will not change much, and the densitometer slit width will not change at all. Thus, if the continuous spectrum limit were perfectly sharp, curves A and C

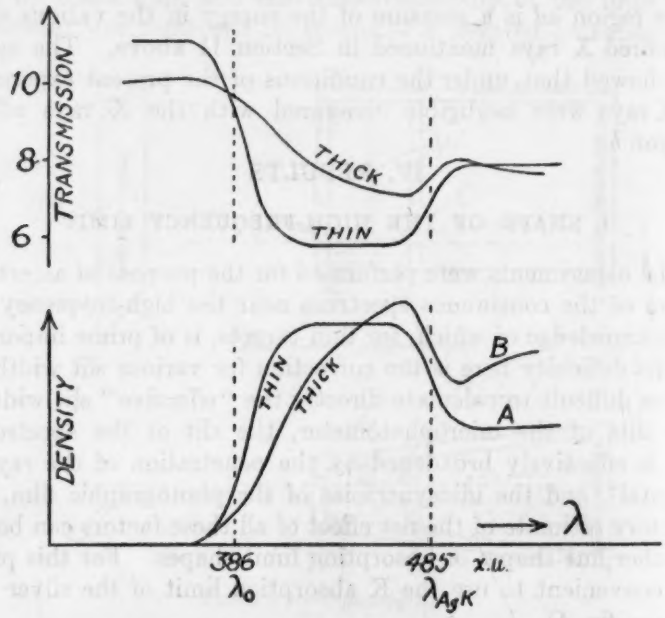

FIGURE 4.—*Comparison of thin and thick target spectra for gold at 32 kv and an angle (ψ) between cathode rays and measured X rays of 90°*

The two density curves are on different scales of ordinates
λ_0 high-frequency limit of continuous spectrum
λ_{AgK} absorption limit due to silver of photographic film

should coincide. However, this perfectly sharp discontinuity can only be anticipated for an infinitely thin target and for perfectly steady voltages; these conditions are impossible experimentally. The result of the finite thickness of foil is to cause finite losses of velocity of the cathode rays, so that in reality the atoms of the foil are bombarded by cathode rays with a range of speeds instead of a uniform speed. An analogous result is caused by an unsteadiness of voltage. Consequently, there is produced in the thin target not a spectrum with a definite high-frequency limit (λ_0), but rather a continuous succession of such spectra with different λ_0's. The result

is an apparent broadening of the limit, much as would have been caused by an increase of slit width.

It is desirable to calculate whether this broadening is of such an amount as to be accountable for by the known thickness of foil and the estimated variations of voltage, or whether the continuous spectrum limit is in reality not a sharp discontinuity. For this purpose the limit for the infinitely thin target will first be assumed perfectly sharp, as in *D*. (Fig. 5.) Further, assuming all but a negligible fraction of the cathode rays to be uniformly distributed through a definite range of voltages between V and $V-\Delta V$, it is obvious that the final shape of the limit will be closely approximated by substituting for the ordinate of *C* at λ an ordinate proportional to the area under the curve *C* between $\lambda-\Delta\lambda/2$ and $\lambda+\Delta\lambda/2$, where $\Delta\lambda$ corresponds to ΔV. The crosses of Figure 5 represent the result of this calculation for $\Delta V=1.9$ kv, superposed on curve *A*; for this value the calculated curve is in satisfactory agreement with the

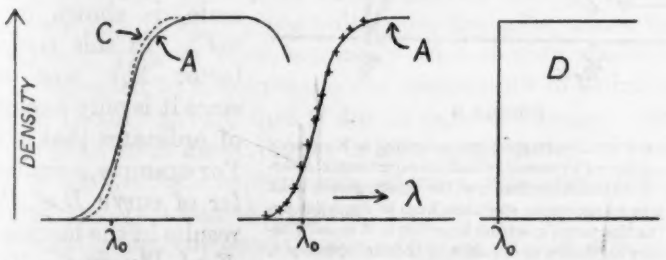

FIGURE 5.—*Corrections for slit width, in determining the structure of the high-frequency limit*

The ordinates here are photographic density, not X-ray energy

measured curve. 1.3 kv out of this 1.9 kv is due to the loss of speed of the cathode rays in penetrating the gold foil. The remaining 0.6 kv is very close to what would have been estimated as due to the variation of voltage (32.0 ± 0.3 kv) on account of the unsteadiness of the source of power. The position of λ_0 of the figures was selected on the supposition that the continuous spectrum limit of *A* was symmetrical about the wave length corresponding to $(32-1.3/2)$ kv.

It should, perhaps, be pointed out that the above method for calculating the shape of the limit involves the assumptions that the thin foil is of uniform thickness, that the cathode rays are not deflected appreciably in penetrating the foil, and that the variations in voltage are of a particular variety. However, serious departures from any of these conditions would have made themselves evident in the shape of the curve *A*; the only consistent irregularities in the curve seem to be accounted for rather by a halation effect. The gold foils used appeared quite uniform when viewed by transmitted light,

much more so than did beaten foils of silver or aluminum. Tests on the deflections of cathode rays in the foil indicated that most of the rays were deflected through angles less than 20°. These deflections contribute somewhat to the length of path in the foil, and consequently to the loss of speed of the cathode rays, but this error is in such a direction as to increase the probability that the end of the spectrum from an infinitely thin target would be in reality discontinuous.

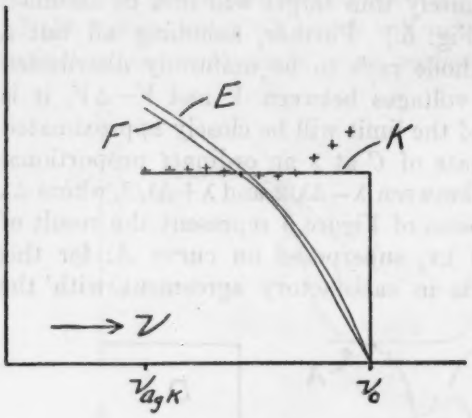

FIGURE 6

K, Thin target continuous spectrum according to Kramers's theory, confirmed by crosses, which are experimental observations. Note the discontinuity at the high-frequency limit
E, Thick target continuous spectrum, from an empirical formula. The thin target spectrum according to Wentzel's theory is somewhat similar to *E*, except for an infinite slope at ν_0.

For a comparison of thin with thick target spectra the thick target spectrum of Figure 4 was corrected for slit width by an extension of the above method. The fully corrected density curve, transferred to a frequency scale, is shown in Figure 6(*F*). In this transfer the factor λ^2/c was omitted, since it is only a comparison of ordinates that is needed. For example, a similar transfer of curve *D* of Figure 5 results in the horizontal line *K* of Figure 6. The true thick target spectral distribution (*E*, fig. 6) was calculated from the formula (2, 14).

$$(I_{\psi\nu})_{\psi=90°} = CZ\left[(\nu_0-\nu)+0.0027\,Z\nu_0\left(1-e^{-16\frac{\nu_0-\nu}{\nu}}\right)\right]$$

where C is a constant, Z is the atomic number of the material of the anticathode, and $(I_{\psi\nu})_{\psi=90°}$ is the intensity on a frequency scale at frequency ν which is radiated in the direction $\psi=90°$. Now, if *F* and *K* are both multiplied by such a factor (varying with frequency) that *F* is reduced to *E*, then *K* should be reduced to the true thin target energy distribution; the crosses indicate the result obtained in this manner. Absorption in the anticathode was negligible here.

Although the sharp increase of energy as ν approaches ν_0 may be anticipated on some grounds, the present work is not taken to confirm it, since the experimental uncertainties are especially large near ν_0 where the intensity of the thick target spectrum is low, and the empirical formula above is least certain.

The preceding experiments are regarded, however, as establishing the fact that the thin target spectrum has a finite discontinuity at

the high-frequency limit. Although the corrections have been carried out in detail only for X rays emitted perpendicular to the cathode stream ($\psi = 90°$), some experimental evidence at hand for angles up to 50° on either side of the perpendicular ($40° \leq \psi \leq 140°$) gives no indication that there is a decrease of sharpness of the discontinuity for other angles.

2. CONTINUOUS SPECTRUM ENERGY DISTRIBUTION

In the experiments just described the tube voltage was chosen, for reasons mentioned above, so that the difference between ν_0 and ν_{AgK} was small. Now, since it is frequencies greater than ν_{AgK} that best affect the photographic film, the region of the spectrum that is most readily measured, and consequently measurements of which are most certain, is the region from ν_{AgK} to ν_0. Thus the calculations of intensity for the preceding experiments were carried out only over this narrow range. When it is desired to measure a greater range of spectrum, adequate intensities with relatively short exposures can be best obtained by raising the voltage on the tube, which increases this frequency range. Now, especially with a wide spectrum, this might be expected to also increase the uncertainty of estimating the amount of density at ν_{AgK} that is due to general fogging. However, the silver absorption discontinuity is here again useful. It had been noticed in the previous experiments, where ν_0 was very close to ν_{AgK} (and consequently when the general fogging at ν_{AgK} was comparatively certain), that the density above the fog on the low-frequency side of the limit was approximately half the density above the fog on the high-frequency side. This relation should hold generally, provided either that the photographic films were uniform or that their absorption for the rays near ν_{AgK} was low; the latter, at least, proved to be the case. In this connection it was desirable to choose ν_0 somewhat less than $2\nu_{AgK}$, so that the second order reflection would not complicate the estimation of the fog density. This density was, in general, within experimental error; that is, within about 10 per cent of the density on the high frequency side of ν_{AgK}.

In order to make satisfactory comparison of the energy distributions for different values of ψ, several of the small Seeman spectrographs were constructed as nearly identical as possible, the crystals being cut from the same large calcite crystal, and special care being taken about the slit widths. These spectrographs were then placed at various positions inside the tube, m, n, f, h, r (fig. 1), a thin foil inserted, and an exposure made. The spectrographs were then reloaded, and the experiment repeated with m and h, and f and n interchanged. The experiment was performed a third time with a thick target of copper. The purpose of the interchange of spectrographs is to make the comparisons of the different directions for thin targets inde-

pendent of differences in the spectrographs, by averaging. It is to be noted that these comparisons, but not comparisons of thin with thick target spectra, are independent of nonuniformities in the thickness of the foils, since the spectrographs were all adjusted to the same height within the tube. Confidence in the latter comparison was gained, however, by repetition of the experiment with different foils.

Unfortunately, the experimental uncertainties were greatly magnified by the fact that the photographic films presented a mottled appearance, the cause for which has not yet been ascertained. The effect varied with the type of film used; for example, a certain kind of X-ray film in which a white material is coated with the emulsion was entirely useless. The irregularities were not appreciable in the

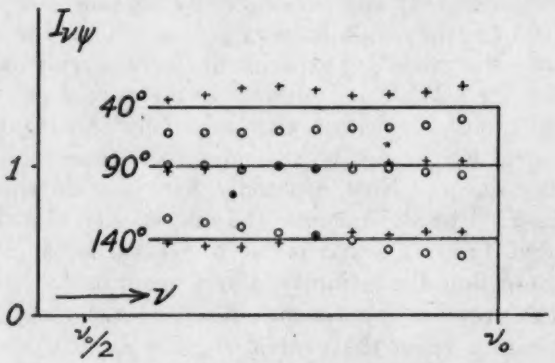

FIGURE 7.—*Thin target spectra in different directions*

The crosses are for gold targets, the circles for aluminum; the data for gold and for aluminum are on two different scales of intensities. The data for gold are more reliable. The experimental uncertainties are such as to make it questionable whether there is a variation with atomic number, as indicated

work described in the preceding section; this may have been due to the lower voltage used there or to greater intensities.

Continuous spectra from thin targets of gold and of aluminum, for $V=45$ kv, and various values of ψ, are shown in Figure 7. The thicknesses of the foils were 0.09 μ and 0.7 μ, respectively. The intensity scale for aluminum, data for which is represented by circles, is different from that for gold (crosses). The data for aluminum are less reliable on account of lower intensities; and data for $\psi=140°$ are less reliable for the same reason. The difference, for $\psi=40°$, between gold and aluminum is exaggerated by the fact that the two scales of intensity were chosen such as to make the ordinates for gold equal to those for aluminum for $\psi=90°$ rather than for some value of ψ between 40° and 90°. Accordingly, it is questionable, with the large experimental error, whether there is a variation with atomic number as indicated.

V. DISCUSSION

1. PASSAGE OF CATHODE RAYS THROUGH MATTER

Mention has been made of the uncertainties of applying the Thomson-Whiddington-Bohr law for cathode-ray penetration to the analysis of thick target spectra in terms of thin target spectra, on account of the Lenard "absorptions." There is no question, from the experiments of Whiddington (15), Terrill (16), Schonland (17), etc., that many of the cathode rays (those that are not deflected) obey this law in penetrating metal foils, but there is at hand no direct evidence about the cathode rays that have suffered deflections. Lenard (3) thought that these latter lost energy in large amounts by their contacts with atoms. It is certain, however, from experiments (18) with the cloud expansion chamber that in light gases, at least, practically all the cathode rays that have been deflected continue to approximately the same path length they would have attained had they not been deflected. (With the relatively few cathode rays that are observed to have suffered a large energy loss, this loss may be accounted for by the emission of an X ray.) The present experiments show that this is also the case with metals, and that radiationless stoppage of cathode rays, if existent at all, must be comparatively rare. The proof is that in the thin target spectra obtained here the energy in a given frequency range $d\nu$ is approximately independent of ν except at the high frequency limit, where there is a finite discontinuity, as Webster predicted (13) on the assumption that the Lenard process was nonexistent.

2. SYNTHESIS OF THICK TARGET SPECTRA

There is an important factor which has so far been neglected in the analysis of X rays from thick targets in terms of thin target spectra, namely, the deflections of the cathode rays in the target. A consideration of the effect of these deflections suggests a division of the X ray continuous spectrum into two parts—(A) a part due to cathode rays which have not been appreciably deflected and (B) a part due to the cathode rays which have become so much deflected as to approximate random directions. Strictly speaking, there is a third part due to cathode rays in the transition stage, but for present purposes this may be considered to consist, roughly, of two components, one of which is in class A and the other in class B. Considered as a class, the only cathode rays which have not been deflected are those which have also not yet lost much of their original speed;[8] thus part A of the

[8] In order that this statement may not appear to contradict the conclusion reached in the preceding section, it should be understood that the two processes considered here—that is, the small losses of speed, and the gradual deflections (diffusion)—may be considered as independent processes (5). But the net loss of speed and the net deflection of a cathode ray both increase with the number of atoms traversed, and this is what makes valid the statement made here.

spectrum has some of the characteristics of a thin target spectrum and should vary with direction (ψ) in the same way. On the other hand, part B of the spectrum should, by definition, not depend on ψ; it is due to cathode rays of relatively low speed.

In a previous paper (2) the author predicted that the X-ray continuous spectrum from a thin target should not show a horizontal distribution for values of ψ much different from 90°; this is not verified in the present experiments nor in some experiments by Duane (10) with his targets of mercury vapor. The predictions were based on an analysis of some data on X-ray isochromats, using the assumptions that the Thomson-Whiddington-Bohr law applied, and that the formula for unresolved intensity ($I_{\psi=90^\circ}=\kappa ZV^2$, where κ is a constant) varied with ψ in a manner suggested by a theoretical relation given by Sommerfeld (19). Since the first assumption is now known to be valid, the disagreement indicates that the second assumption, dealing with unresolved intensity, was not correct. Specifically, the fact that the observed thin target spectra are all approximately of the same form suggests that the unresolved intensity from a thick target does not vary markedly with ψ, or, in other words, that part B of the spectrum predominates.

A revision of the previous analysis on this basis leads to thick target spectrum distributions represented by the formula

$$J_{\psi,\nu}d\psi d\nu = CZ[(\nu_0-\nu)+x]\sin\psi d\psi d\nu$$

where $J_{\psi,\nu}d\psi d\nu$ is the energy between ν and $\nu+d\nu$ that is radiated in direction ψ within angular range $d\psi$, C is a constant, and x is a relatively unimportant term which probably varies with ψ, ν, V, and Z. The variation of x with ψ is similar to the corresponding variation of the thin target spectrum. This formula leads, by integration, to an expression for unresolved energy, of the form

$$J_\psi d\psi = KZ(V^2+p)\sin\psi d\psi$$

where $J_\psi=\int_0^{\nu_0}J_{\psi,\nu}d\nu$, K is a constant, and p is a relatively unimportant term similar to the x term above. It should be pointed out that, due to effects previously described (2), the absolute values of these terms x and p are not known, but their variation with ψ is established (2). They represent energy from part A of the spectrum.

For many purposes it is convenient to use the above formulæ in the form

$$I_{\psi,\nu}d\nu = CZ[(\nu_0-\nu)+x]d\nu$$

and

$$I_\psi = KZ(V^2+p)$$

where I is here a symbol for X-ray intensity (energy per unit solid angle); the subscripts mean the same as before. A graphical repre-

sentation of the spectral distributions for different values of ψ, obtained by the revision of the author's previous work, with a copper target, is shown qualitatively in Figure 8.

A simple way to view the spectral distributions is outlined in Figure 9, where the thick target spectrum is built up of successive thin target spectra (neglecting absorption in the anticathode). The thin targets are here chosen not of equal thickness, but of such thicknesses as to cause the cathode beam to lose energy in equal steps. It has been mentioned above that A is essentially a thin target spectrum, and it is readily seen that a variation of A with ψ after the

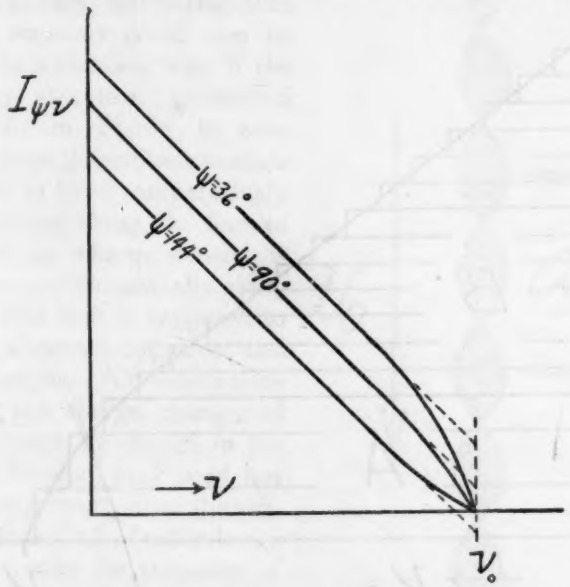

FIGURE 8.—*General character of the variation with direction of continuous spectra from thick targets, as shown by the present experiments with thin targets*

manner of Figure 7 will cause a variation with ψ of the thick target spectrum in the manner shown in Figure 8. It is interesting to notice that, even with thin target X rays the "hardness" of which does not vary with direction, thick target rays are obtained which are harder in the forward direction.

3. MECHANISM OF RADIATION

The theories of Kramers (20) and Wentzel (21) for continuous spectrum energy distribution from thin targets consider not $I_{\psi\nu}$ but only I_ν (that is $I_{\psi\nu}$ averaged over all values of ψ). The indication is that, since the present graphs of $I_{\psi\nu}$ are all approximately horizontal for a fairly wide range of ψ, and especially over the range that counts

most in the summation over ψ, it is reasonable to suppose that I_ψ is also approximately horizontal. This is in agreement with Kramers's theory but not with Wentzel's. Graphs of the predictions made by these theories are indicated in Figure 6. This same result was anticipated in some previous work by the author (2) and its bearing on the form of the "correspondence principle" discussed; accordingly it will not be elaborated on here.

The variation of intensity with ψ has usually been accounted for on the basis of a formula first derived by Sommerfeld (19) from classical electrodynamics, in which the variation is associated with the

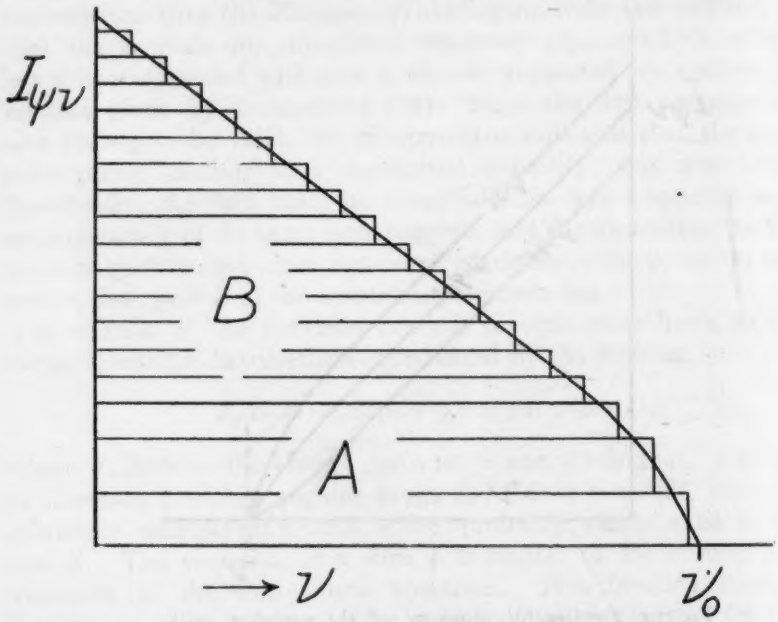

FIGURE 9.—*Synthesis of a thick target spectrum from successive thin target spectra*

rapid motion of the radiating cathode ray. Accepting this explanation, the type of variation with ψ shown in Figure 7 may be taken to indicate that the oscillating mechanism responsible for the X rays was in rapid motion at the instant of radiation. On the other hand, the fact that the high-frequency limit of the spectrum (ν_0) shows no measurable Doppler shift indicates just as emphatically that this mechanism was not in motion at the instant it was radiating. This discrepancy has long been known and appreciated (22); the present work merely makes possible a closer analysis of the anomaly.

The difficulty with the Doppler shift of frequency is provided for, formally at least, by the quantum theory, in which it is understood that the frequency of the end of the spectrum is determined only

by the energy of the cathode ray, and thus is independent of the direction of emission, except for an extremely small shift predicted from conservation of energy and momentum. The dependence of intensity on ψ is provided for by the "correspondence principle"; here the probability of emission of a quantum in a given direction may be expected to vary with direction in the same way as the classical spectrum, thus accounting, qualitatively at least, for the observed facts.

Now, it is very interesting that the above anomaly could also be explained in a classical way, if the cathode-ray structure illustrated schematically in Figure 10 were assumed. Here the cathode particle is supposed to have comparatively great extension along its line of motion, and its charge density is supposed to vary sinusoidally along its length; that is, it is supposed to consist of alternate negative and positive charges. (Considerations of stability, net charge, changes of potential energy by change in the charge distribution, etc., need not concern us at present, since the conception of this kind of cathode ray is advanced only for purposes of illustration; it may be pointed out, however, that by a slight modification of the continuous spectrum in a manner which would not be detected experimentally this cathode particle could be made to have a finite extension and a net negative charge.) Now if each portion of this cathode particle is suddenly stopped as it reaches a fixed point P, the radiation emitted will consist of a series of pulses and will have a single frequency (that is, no harmonics, since sinusoidal). Each pulse will have an intensity varying with direction in some manner such as described by Sommerfeld's theory; consequently the total radiated intensity will vary with direction in the same manner. The Doppler shift will be absent, since P is at rest. The

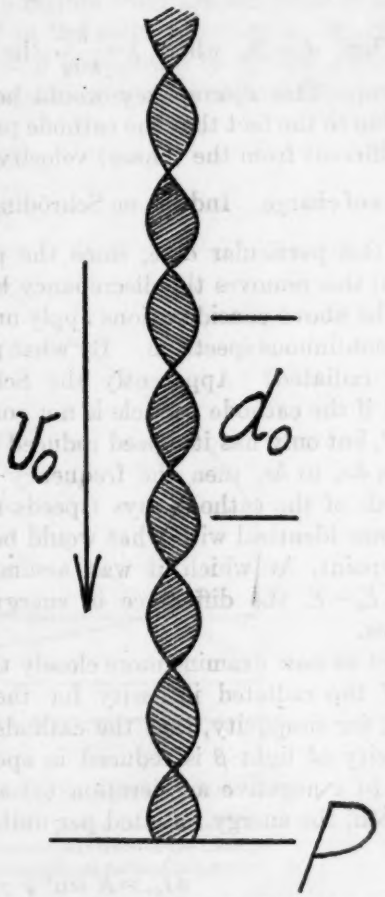

FIGURE 10.—*Schematic illustration of a "wave electron" which would explain in a classical way one of the long-standing anomalies of X-ray continuous spectra*

emitted frequency will be $\nu_0=\frac{v_0}{d_0}$. In order that the quantum condition $\nu_0=\frac{V_e}{h}$ hold, d_0 must be

$$\frac{v_0}{\nu_0}=\frac{hv_0}{h\nu_0}=\frac{hv_0}{\frac{1}{2}mv_0^2}=2\,\frac{h}{mv_0}$$

Thus, $d_0=2\lambda$, where $\lambda=\frac{h}{mv_0}$, the wave length of the De Broglie waves. This discrepancy would be interpreted in wave mechanics as due to the fact that the cathode particle velocity v_0 (group velocity) is different from the (phase) velocity (u_0) of the individual concentrations of charge. Indeed, on Schrödinger's theory, $u_0=\frac{E}{\sqrt{2m(E-U)}}=\frac{v_0}{2}$ for this particular case, since the potential energy (U) is assumed zero; this removes the discrepancy between d_0 and λ.

The above considerations apply only to the high-frequency limit of the continuous spectrum. By what process are frequencies lower than this radiated? Apparently the Schrödinger interpretation will be that if the cathode particle is not completely stopped by the obstacle at P, but only has its speed reduced from β_0 to β or its energy reduced from $h\nu_0$ to $h\nu$, then the frequency radiated is $\nu_r=\nu_0-\nu$. The final speeds of the cathode rays (speeds after the radiation process) then become identical with what would be expected on the older quantum viewpoint, in which it was assumed that the energy radiated is $h\nu=E_0-E$, the difference in energy between the initial and final states.

Let us now examine more closely the question of the dependence on ψ of the radiated intensity for the above conditions. Supposing, first, for simplicity, that the cathode ray moving with the fractional velocity of light β is reduced in speed by a very small amount $d\beta$ due to a negative acceleration (a) acting simply in the direction of motion, the energy radiated per unit solid angle will be (19)

$$dI_{\psi,\nu}=K\sin^2\psi\,\frac{a\,d\beta}{(1-\beta\cos\psi)^5}$$

where K is a constant independent of ψ, β, and a. The asymmetry (associated with unequal intensities for supplementary values of ψ) is seen to increase rapidly with increasing β; thus for a finite change in β, the space distribution is given by

$$I_{\psi,\nu}=K\sin^2\psi\int_{\beta}^{\beta_0}\frac{a\,d\beta}{(1-\beta\cos\psi)^5}$$

In general, a may be expected to be some function $a(\beta)$, since the cathode ray in its hyperbolic path about the nucleus will have an

acceleration which varies along this path. However, no reasonable choice of function $a(\beta)$ seems to lead in a satisfactory way to the simple experimental result (fig. 7) that the ratio of intensities for two given values of ψ is roughly independent of the frequency. Figure 11 illustrates some attempts to obtain agreement from the above formula—the dash-dot curve results from assuming (as Sommerfeld did) $a(\beta)$ constant, with β in the same direction as β_0; the dash curve is the same, except that β is opposite to β_0; the dotted curve assumes $a(\beta)$ such as to give a minimum ratio of intensities, for

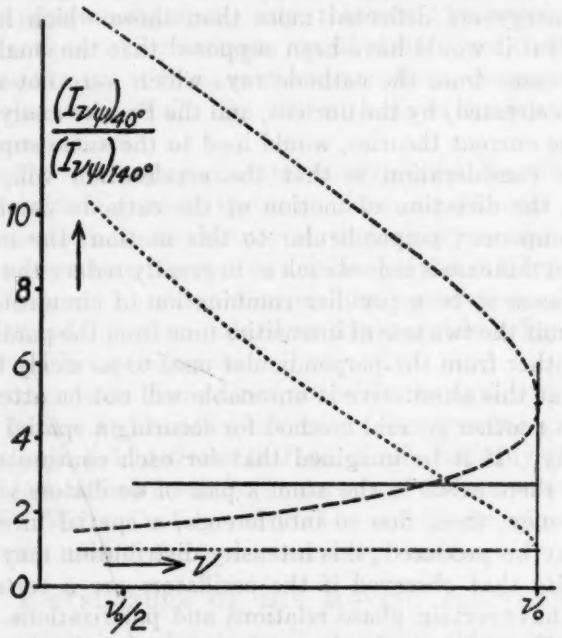

FIGURE 11.—*Ratio of intensities in different directions*

Full line, experimental observations. Broken lines, various attempts to account for the experimental observations on the assumption that continuous spectrum frequencies are radiated in spherical waves as single quanta

β in the same direction as β_0; the dash-dot-dot line is the same except that β and β_0 are in opposite directions. The unbroken line approximates the experimental results. It should be emphasized that the broken curves of Figure 11 are not particularly the ones to be compared with the experimental results; these curves merely represent limiting cases that were easy to calculate but which would give the clue as to the correct assumption to be made regarding $a(\beta)$. After careful consideration of various possibilities it was concluded that no choice of $a(\beta)$ could be made which would not be unsatisfactorily arbitrary and which would correspond with other known facts;

this includes the case in which $a(\beta)$ is, for part of the time at least, a positive acceleration in the direction of motion.

There remain several possibilities for explaining the above discrepancies. One is that the cathode particle will be deflected in its approach to the nucleus; these deflections will, in general, decrease the calculated ratios of Figure 11. But it is to be noted that to give correct experimental values these ratios would, in the more satisfactory cases represented in Figure 11, have to be decreased more in the low-frequency region than at high frequencies; this would indicate that the cathode rays which lose only a small fraction of their energy are deflected more than those which lose all their energy. But it would have been supposed that the smaller amounts of energy came from the cathode rays which were not so much deflected (accelerated) by the nucleus, and the Fourier analysis of orbits, used in the current theories, would lead to the same supposition.

Another consideration is that the acceleration will, in general, not be in the direction of motion of the cathode particle but will have a component perpendicular to this motion; the intensity distribution in this case is indeed such as to greatly reduce the asymmetry. It would seem to be a peculiar combination of circumstances which would permit the two sets of intensities (one from the parallel acceleration, the other from the perpendicular one) to so nicely balance, but a proof that this alternative is untenable will not be attempted here.

There is another general method for securing a spatial distribution of intensity. If it be imagined that for each continuous spectrum frequency there exists in the atom a pair of oscillators which radiate this frequency, then, due to interference, a spatial intensity distribution may be produced; this intensity distribution may be made to approximate that observed if the oscillators are a certain distance apart and have certain phase relations and polarizations. The oscillators would need to be in the atom rather than in the cathode ray to avoid Doppler effect. The difficulties with such a picture are, however, so great (for example, on account of the necessity of associating with an atom a continuous range of emitting oscillators instead of the discrete ones indicated by the emission spectrum of the atom, and the wide range of spacings and phases which would have to be postulated) that this possibility is given no weight in the present discussion.

Summarizing, it is believed to have been shown, with a fair degree of satisfaction, that either (1) the continuous radiation from thin targets is in large part composed of radiation due to acceleration of the cathode rays in a direction perpendicular to their line of motion (this is not necessarily opposed to a complete polarization at any one frequency; for example, the high-frequency limit, such as is indicated by the experiments of Ross (23)); (2) a cathode ray in interacting with

a nucleus to lose an amount of energy $h\nu$ does not radiate only the monochromatic frequency ν; or (3) the spatial intensity distribution is not such as to be accounted for by a relativity transformation, just as though radiation is not electromagnetic waves, but perhaps of the "photon" nature suggested by the experiments of Compton and Simon (24).

However, if the spectral distributions are really the same in all directions, as suggested by Figure 7, it is reasonable to seek a simple hypothesis to match this simple result. Such a hypothesis (strictly classical) might be that the accelerated cathode ray radiates the whole spectrum simultaneously; this would be associated with the existence in the moving cathode ray of either a continuous range of phase velocities (u) with u_0 as the upper limit, or (assuming $u = v_0$) a continuous range of d's (fig. 10) with d_0 as the lower limit, or a combination of these.

On account of the experimental uncertainties described above in connection with Figure 7, however, these experiments must be regarded somewhat in the nature of preliminary work; and a more detailed constructive discussion will be delayed until more accurate measurements are obtained to guide the speculation. The work is being continued by more refined methods and is being extended to other fields of X-ray emission.

These experiments were carried out while the author was a National Research Fellow at Cornell University. It gives me great pleasure to acknowledge indebtedness to Prof. F. K. Richtmyer for some of the basic ideas contributing to the success of the above work. I wish to thank Dr. W. D. Coolidge, of the General Electric Co., for some of the apparatus used in the preliminary experiments.

4. STRUCTURE OF THE MOVING ELECTRON[9]

The beautiful piece of work on X rays from thin targets, just published by Kulenkampff (25), leads me to an extension of the above ideas. Kulenkampff obtained the spatial intensity distribution, from $\psi = 22°$ to 150°, for several different frequencies in the continuous spectrum; these curves all appear to extrapolate to zero, or at least to comparatively small values of intensity, for the extreme angles 0° and 180°. This means that the component of the radiation emitted by the cathode ray due to its acceleration perpendicular to the original line of motion is comparatively small. Thus only two of the three possibilities mentioned above remain; that is, if X rays are electromagnetic waves, a cathode ray which has lost energy $h\nu$ will not, in general, have radiated frequency ν. Accordingly, it becomes desirable to examine in more detail the above postulate that the accelerated cathode ray radiates all frequencies simultaneously.

[9] This section was added Jan. 11, 1929.

As pointed out above, using the conceptions suggested by Figure 10, the radiation of a continuous band of frequencies with ν_0 as the upper limit might be accounted for by supposing either a continuous range of u's or a continuous range of d's; the latter seems to form the better basis for a physical picture. The explanation of continuous spectrum phenomena is thus relegated to the structure of the moving electron; we must next find the structure which would account for the observed results.

Let us first investigate what sort of electromagnetic "pulse" would account for the observed spectral distributions. The converse problem; that is, the analysis of a pulse into its Fourier components (Fourier integral, not series) is well known; in X rays it is familiar

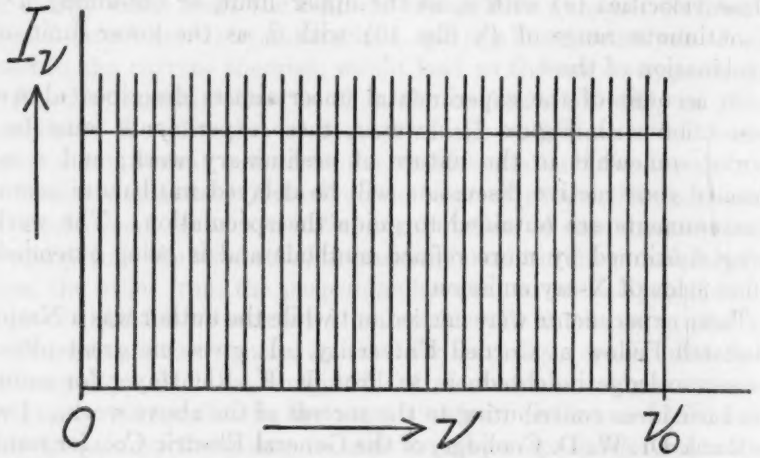

FIGURE 12.—*Manner in which a continuous spectrum may be approximated with a line spectrum*

especially from the attempts to account, on the basis of the old pulse theory, for the existence of a high-frequency limit in the X-ray continuous spectrum (26). In general, according to these attempts, a finite pulse must be thought of as composed of all frequencies between zero and infinity; and it would require a pulse with oscillations extending to infinity to account for an infinitely sharp high-frequency limit. The direct attack on the problem has been made by Kennard (27), who investigated the form of pulse that would account for an X-ray spectrum similar to the customary thick target spectrum, which has a discontinuity of slope at the high-frequency limit. For present purposes we must, of course, use the observed (fig. 7) thin target spectral distribution, which has a finite discontinuity in I_ν at the limit. Let us first approximate this continuous spectrum with a line spectrum in which the lines are so close together as not to be distinguishable from a continuous spectrum; if the lines are all of the same intensity and equally spaced on a frequency scale the "continuous spectrum" (compare fig. 12) will have the required horizontal

distribution. (It should be remembered that the thin target experiments have, so far, covered only the range $\nu_0/2$ to ν_0; however, there is no reason to believe, from the thick target work, that the extrapolation to zero frequency is essentially different from the one assumed here.) The frequencies of these lines are

$$\frac{\nu_0}{n}, \frac{2\nu_0}{n}, \frac{3\nu_0}{n}, \ldots \ldots \frac{k\nu_0}{n} \ldots \ldots \frac{n\nu_0}{n} (=\nu_0) \ldots \ldots (k=1, 2, 3 \ldots . n)$$

and the wave lengths are

$$\frac{n\lambda_0}{k} \ldots \ldots (k=1, 2, 3 \ldots . n)$$

where λ_0 corresponds to ν_0. The form of electromagnetic pulse (magnitude of electric vector as a function of distance along the radius vector r at a definite instant) is

$$\sum_{k=1}^{k=n} f(k) \cos \left(\frac{2\pi kr}{n\lambda_0} - p_k\right)$$

where p_k is a phase term and $f(k)$ is a factor connecting amplitude with intensity; this latter for wave trains sufficiently long will depend on their amplitude and not on their frequency, hence may be considered constant and for the present case where the lines are to be of equal intensity may be assumed unity. Placing the terms p_k each equal to zero, so as to make the pulse symmetrical, we have

$$\sum_{k=1}^{k=n} \cos \frac{2\pi kr}{n\lambda_0}$$

for the form of the pulse. Now, as n approaches infinity (that is, as our line spectrum approaches a truly continuous spectrum) the form of pulse is given by an integral

$$\int_{\frac{k}{n}=0}^{\frac{k}{n}=1} \cos \frac{2\pi kr}{n\lambda_0} d\left(\frac{k}{n}\right) = \frac{\lambda_0}{2\pi r} \sin \frac{2\pi r}{\lambda_0}$$

Then, remembering that the magnitude of the electric vector is proportional to the amount of charge being accelerated, other things being equal (compare fig. 10), the charge density (charge per unit length) along an electron in uniform motion becomes proportional to

$$\frac{d_0}{2\pi x} \sin \frac{2\pi x}{d_0}$$

where x is distance measured along the line of motion, with $x=0$ at the center of the electron. A graph of this function is shown in Figure 13.

The derived electron structure thus consists of alternate positive and negative pulses of charge; the "wave length" (that is, approximately, the distance between negative crests) being everywhere d_0 except at the center of the electron. The predominance of this spacing may be of importance in the explanation of effects similar to those recently investigated by Davisson and Germer. It is to be noted that the net charge on this electron (represented by the difference between area under the curve above the axis and that below) can be shown to be a finite determinate quantity. (A factor to keep this net charge constant, independent of speed, was neglected in the above formula.) The stability of this type of electron will not be considered here; it probably will be no more difficult to account for than it is to account for the stability of an electron consisting entirely of negative charge. An obvious difficulty still attaches to this electron, however, in that it extends to infinity in both directions; this infinite extension is associated with a continuous spectrum which has only

FIGURE 13.—*Charge density along a moving electron which would give in a classical manner the observed continuous spectra*

Negative charge above the axis, positive below

the frequencies specified in the above integral, with a perfectly sharp discontinuity at the limit. But experimentally, we can never make a perfect test of these conditions; it may well be that the limit is in reality spread out over a finite range of frequencies which is so small as not yet to have been detected by experiment, and that even at frequencies higher than the quantum limit there exists an amount of energy too small to have been noticed in experimental work to date. Thus the experiments can only indicate that, at a velocity corresponding to 40 kv, say, the electron is of the order of 15 Ångstroms long, as a minimum. In this connection it should be pointed out that, since the experimental and theoretical work (1, 2, 20) indicates that the thin target X-ray continuous spectrum intensity distribution is approximately horizontal on a frequency scale for all voltages, this would mean that the structure of the electron is essentially similar at all voltages. However, if this is strictly true, the electron in free space should expand greatly at very low velocities. On the other hand, if the length of the electron is to be kept within reasonable

limits by not allowing this expansion, the sharpness of the high-frequency limit must diffuse correspondingly; that is, we may expect for low velocities to observe a "structure" in this limit which would not be discovered at high velocities. That this structure has not yet been observed may be due to the fact that continuous spectra have not yet been observed for low enough electron velocities. There may be some experimental support for this viewpoint, however, in the work of E. O. Lawrence (28), who observed a fine structure in the curve representing the probability of formation of positive ions in mercury vapor as a function of electron speed for speeds near that required to produce ionization. This implies the assumption that it is frequencies contained in the moving electron which stimulate ionization.

Now, assuming this structure for the cathode ray, all known facts about X-ray continuous spectra appear to be accounted for qualitatively and in a classical manner. First of all, the anomalies of the present paper, of course, disappear, since it is on this work that the cathode particle structure is based. The dependence of spectral distribution on voltage has been discussed above in connection with this type of electron. It may be pointed out also that the space distribution of energy as a function of voltage which would be expected on the present theory is qualitatively in agreement with the thin target results of Kulenkampff (25), who found that the spatial asymmetry increased with increasing voltage for the high-frequency limit. Further, although the question has not been examined in detail, the total energy in the X-ray continuous spectrum seems to come out of the right order of magnitude, the inclusion of positive charge in the electron's structure being roughly couterbalanced by the greater length over which the charge is distributed. For example, this would not be the case if the electron's charge were distributed over a series of pulses which were entirely negative, since radiated energy is proportional to e^2 for a point charge, other things being equal.

Now, Kulenkampff found the most interesting fact that the spectral distribution is only to a first approximation independent of direction (ψ). Another way of saying the same thing is that the spatial intensity distribution is somewhat different for different frequencies in the spectrum. It is most important that this kind of variation is accounted for on the present theory, assuming that the acceleration of the cathode particle is due to its close approach to a nucleus; that is, that its acceleration is such as to be accounted for by its motion along a hyperbolic orbit. First of all, let us suppose, for simplicity, that the mass per unit length of the cathode ray is so adjusted that each part of the electron traverses the orbit in the same manner; the picture resembles that of pulling a light extensible cord through water.

(We neglect here the shearing forces between negative and positive "charge pulses" which would tend to disrupt the electron entirely; its resistance to this disruption must be connected with its internal structure which will not be examined here.) Now, if the acceleration were of extremely short duration, very short compared with $1/\nu_0$, the structure of the moving electron would be revealed exactly in the radiated spectrum, which would then have the same spectral distribution in all directions. But in the hyperbolic orbit this time of acceleration is, in general, appreciable; specifically, it is appreciable relative to $1/\nu_0$, but not so much so for $1/\nu_a$, where ν_a is a very low frequency compared with ν_0. The effect is to suppress the energy of frequency ν_0, but not that of frequency ν_a, in the radiated spec-

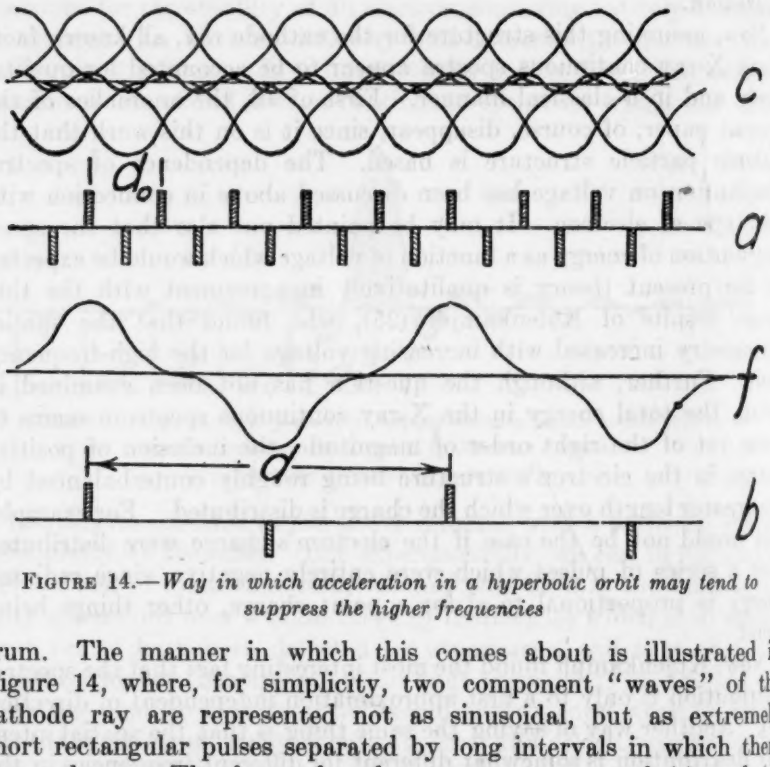

FIGURE 14.—*Way in which acceleration in a hyperbolic orbit may tend to suppress the higher frequencies*

trum. The manner in which this comes about is illustrated in Figure 14, where, for simplicity, two component "waves" of the cathode ray are represented not as sinusoidal, but as extremely short rectangular pulses separated by long intervals in which there is no charge. The form of each component curve of (*c*) and (*f*) represents, for a simple case, the electromagnetic pulse radiated by each small pulse of charge in traversing the hyperbolic orbit. It is readily seen that the effect is to suppress the oscillations, and consequently the energy, for the shorter *d*'s; it would not essentially change this conclusion if for (*a*) and (*b*) were substituted the actual sinusoidal curves. Thus, for hyperbolic orbits in which the cathode ray does not approach very close to the nucleus, the time of acceleration will be comparatively long, while for close approaches most of

the energy will be radiated in a shorter time; the radiated spectrum, therefore, depends on the type of orbit. But due to different speeds and different deflections, the spatial distribution of total radiated intensity will also vary with type of orbit. Consequently, the distribution of intensity in the radiated spectrum will depend on direction ψ, as Kulenkampff observed.

A further result of these ideas is that, in general, the radiated spectral distributions may be expected to vary somewhat with both the voltage and the atomic number of the anticathode material as well as with ψ. This suggests that the indicated difference (fig. 7) between the spectra for gold and aluminum may be real, although it is believed that these experiments are not precise enough to be sure of the point.

The use of hyperbolic orbits suggests a further analysis of the point in connection with the part of the radiation due to acceleration perpendicular to the initial direction of the cathode ray. It was sufficient for the argument given above that for $\psi = 40°$ and $140°$ the energy in this component (N) of the radiation should not be large compared with the energy in the component (M) due to acceleration along the original line of motion. But if the cathode ray is to describe a hyperbolic orbit, as here assumed, the component N should, in general, not be zero for any frequency, and Kulenkampff's curves [say $F(\psi, \nu, V)$] should, therefore, not extrapolate to zero for $\psi = 0°$ and $180°$. Now, if the radiation were really all of the type M, it would mean that F would, on the present theory, be given by an integral, as above:

$$\frac{F(\psi, \nu, V)}{\sin^2 \psi} = k \int_{\beta_1}^{\beta_0} a(\beta)\ (1 - \beta \cos \psi)^{-5}\ d\beta$$

taken over the range of variation of β. Considered as a function of ψ, the integral on the right must, regardless of the form of $a(\beta)$, continually decrease as ψ varies from 0 to π; thus the quantity on the left must do likewise. I have divided by $\sin^2 \psi$ Kulenkampff's F for different values of ν and V and plotted the results in Figures 15 and 16. The fact that none of these curves decreases continuously from $\psi = 0$ to $\psi = \pi$ indicates that in all of them there is an appreciable component N. Thus the continuous spectrum will be expected to be incompletely polarized throughout the range here considered; this is satisfactory from the standpoint of the present theory of hyperbolic orbits.

It should be pointed out that the high-frequency limit of the spectrum does not change for the various hyperbolic orbits even though the speed of the cathode particle along the orbit is in general, greater than v_0. This means that the emitted frequencies depend only on the energy of the cathode ray before it encounters the atomic field. This circumstance is also easily understood on the present

conceptions: As the front end of the cathode particle penetrates the field of the nucleus it is accelerated so that an elongation of this end of the particle occurs, but on strictly mechanical ideas, the distance between crests in the moving electron will be proportional to the velocity at every point; thus the frequency radiated, being $\frac{v}{d}$, will be unmodified. It is to be remarked that the relation $d_o = \frac{2h}{mv}$ does not hold along the entire orbit. Another viewpoint that leads to the same result as above is that, since the cathode particle is very long compared with the diameter of the space strongly influenced by the field of the atom, only a small part of the cathode particle, that which

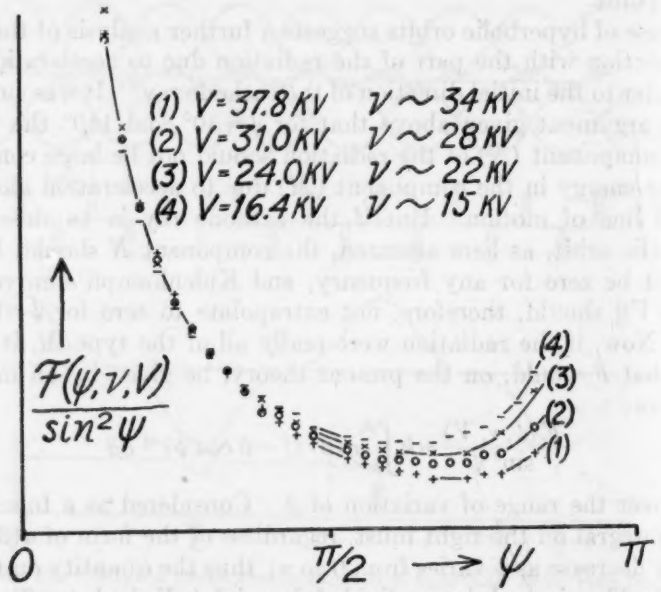

FIGURE 15.—*Calculations from Kulenkampff's data which indicate that the thin target X-ray continuous spectrum is incompletely polarized throughout the range yet observed*

is in the vicinity of the nucleus, will have its velocity changed. The frequency at which the pulses of charge are fed into the strong field, however, is determined by the condition of the part of the cathode particle which is as yet uninfluenced by the field of the atom, and this is the frequency which is radiated. In the electrostatic field between anode and cathode, the cathode particle, being in its entirety at a comparatively uniform potential, will adjust its length to its velocity. This recalls the concept used by Schrödinger that ordinary mechanics breaks down for systems of atomic dimensions.

Let us now imagine this electron in a repeating orbit, say, a circular one. On account of its great length, the electron may be supposed

in general, to be curled many times around the orbit, something like a coil of rope. Very roughly speaking, it may be supposed that, independent of what forces bind the separate coils together, the positive charge of one turn will tend to superpose on the negative charge of the preceding turn; if, then, the circumference of the orbit ($2\pi r$) is a multiple (n) of $d_0\left(=\frac{2h}{mv}\right)$, we have $mvr=\frac{nh}{\pi}$, in which the angular momentum is quantized ("stationary states"). Further, it is seen, roughly, that there is a tendency to nullify variations in charge density around the orbit; when these variations disappear no varying

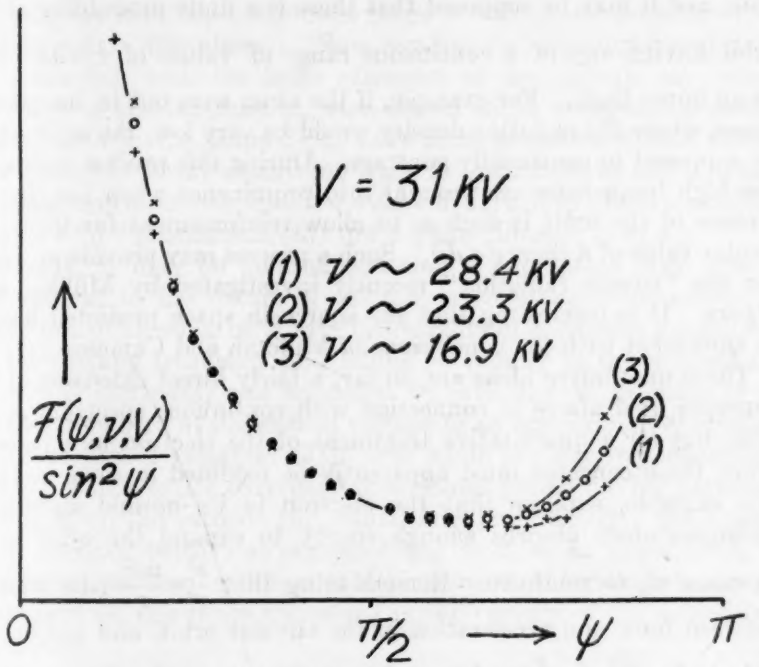

FIGURE 16.—*Calculations similar to Figure 15*

fields will be set up due to the orbital motion, and the particular stationary state will be radiationless—that is, the "normal state." A more accurate use of the ideas previously stated may be obtained, however, by returning directly to the original conception of the moving electron as containing a continuous range of d's with d_0 as a minimum. For example, if $2\pi r=d_0$ it is obvious from this viewpoint that of all component d's only d_0 can superpose constructively (that is, negative crest of one turn superposing on negative crest of preceding turn). More generally, if $2\pi r\geq d_0$, it will be found that reinforcement always occurs for one or more values of d (corresponding to one or more negative crests in the circumference), and if $2\pi r<d_0$ reinforcement never occurs.

Thus, the only condition in which the orbit is radiationless is when $2\pi r < d_0$. Strictly speaking, however, a small amount of radiation (and absorption) should occur even in this condition, due to the finite length of the electron. For, as has been pointed out above, if the electron is to be of finite length, in general, some energy at frequencies higher than corresponds to d_0 must be present. Just what these frequencies are and what prominence they have is, of course, a matter to be decided by experiment. Now, if the electron were to absorb just as much energy as it radiated, the orbit would remain of exactly the same radius. But, in general, this will not be true, and it may be supposed that there is a finite probability of the orbit having any of a continuous range of values of r with $r \doteq \frac{d_0}{2\pi}$ as an upper limit. For example, if the atom were out in interstellar space, where the radiation density would be very low, the orbit might be supposed to continually contract. During this process various of the high frequencies are brought into prominence when the circumference of the orbit is such as to allow reinforcement for their particular value of d (here $d < d_0$). Such a process may provide an origin for the "cosmic radiation" recently investigated by Millikan and others. It is interesting that the source in space predicted here is in agreement with the conclusions of Millikan and Cameron (29).

These qualitative ideas are, so far, a fairly direct extension of the concepts used above in connection with continuous spectrum radiation; but for a quantitative treatment of the electron in a periodic orbit, these concepts must apparently be modified in some manner. For example, suppose that the electron in its normal state in a hydrogen atom absorbs enough energy to expand the orbit so as to cause d_0 to reinforce. Remembering that $\frac{e^2}{r^2} = \frac{mv^2}{r}$ (the relation between force and acceleration in the circular orbit, and putting, as before, $d_0 = \frac{2h}{mv}$, $\nu = \frac{v}{d_0}$ and $2\pi r = d_0$, we obtain

$$\nu = \frac{R}{4}$$

where R is the Rydberg constant; this is different from the Lyman series limit (the K critical absorption discontinuity) by a factor of 4. Such a discrepancy is not surprising, however, as the conditions governing the cathode ray in free space are scarcely expected to be applicable at once to an electron curled many times around an orbit. Rather the aperiodic conditions must be regarded as a special case of more general laws yet to be formulated; no attempt will be made here to formulate these laws.

The above coincidence (except for the factor of 4) of the critical absorption frequency with the electron frequency corresponding to d_0 suggests a picture of the sometimes-postulated trigger action connected with the photoelectric effect: Assuming the orbital electron to have stored up internally the amount of energy necessary to enable it to get outside the field of the atom, the electromagnetic frequency which would disengage it would be that frequency which would displace one end of the electron, pulse by pulse, from its orbit; this is the frequency associated with d_0. An extension of this idea leads one to associate the continuous absorption on the high-frequency side of the limit with the continuous range of values of r possible in the normal state. (See above.) Now, recalling the ideas introduced above in connection with the finite extension of the cathode ray (where values of d shorter than d_0 were shown to be possible), if certain values for d in the range $d<d_0$ have more prominence than others, this picture of X-ray absorption leads to predictions of fine structure in absorption discontinuities (for d close to d_0) and to effects resembling Barkla's "J" phenomena (30) (for d quite different from d_0).

Finally, it may be pointed out that a conception may now be obtained as to the nature of the difference between the curves for excitation of an atom by X rays (probability of excitation a maximum at the limiting frequency and falling off rapidly as the incident frequency is increased) and excitation by cathode rays (probability increases from zero at the critical voltage to an approximately constant value at higher voltages) (31). For while the electromagnetic frequency would excite only particular atoms (those having particular values of r), the cathode ray, containing prominently a great range of frequencies (with that corresponding to d_0 as an upper limit, for the prominent ones) will be capable, in general, of exciting atoms with a range of r's, this range increasing as the velocity of the cathode ray increases.

Many difficulties must be overcome in the above theory (for example, with regard to the stability, in strong fields, of the proposed electron, and the storing up of energy in orbits) before the above descriptions can be regarded as actual pictures. Consequently, until these difficulties have been examined in more detail this section can claim to provide no more than a schematic picture of an electron, which seems to be adaptable to an explanation of many of the effects associated with the quantum theory.

VI. BIBLIOGRAPHY

1. Webster and Hennings, Phys. Rev., **21,** p. 312; 1923.
2. W. Nicholas, Phys. Rev., **29,** p. 619; 1927.
3. P. Lenard, Ann. der Physik, **80,** p. 1; 1926.
4. H. Kulenkampff, Ann. der Physik, **80,** p. 261; 1926.
5. W. Bothe, Handbuch der Physik, **24,** p. 1.
6. W. D. Coolidge, J. Frank. Inst., **199,** p. 628; 1925.
7. Physique des Rayons X, p. 45; Paris, 1921.
8. X Rays and Electrons, p. 256.
9. W. Duane, P. N. A. S., **13,** p. 662; 1927.
10. W. Duane, P. N. A. S., **14,** p. 450; 1928.
11. Bergen Davis, Phys. Rev., **11,** p. 433; 1918.
12. Glocker and Traub, Phys. Zeits., **22,** p. 345; 1921.
13. D. L. Webster, Phys. Rev., **9,** p. 220; 1917.
14. D. L. Webster, Radiology; April, 1924.
15. Whiddington, Proc. Roy. Soc., **86,** p. 360; 1912; **89,** p. 559; 1914.
16. H. M. Terrill, Phys. Rev., **22,** p. 101; 1923.
17. B. F. J. Schonland, Proc. Roy. Soc., **104,** p. 235; 1923; **108,** p. 187; 1925.
18. C. T. R. Wilson, Proc. Roy. Soc., **104,** p. 192; 1923.
19. See Atombau and Spektrallinien, 4th ed., p. **37,** or X Rays and Electrons, p. 44.
20. H. A. Kramers, Phil. Mag., **46,** p. 869; 1923.
21. G. Wentzel, Z. f. Phys., **27,** p. 257; 1924.
22. See D. L. Webster, N. R. C. Bulletin, **1,** p. 427; 1920, and A. H. Compton, "X Rays and Electrons," Chapter II.
23. P. A. Ross, J. Opt. Soc. Am. and Rev. Sci. Int **16,** p. 375; 1928.
24. A. H. Compton and A. W. Simon, Phys, Rev., **26,** p. 289; 1925.
25. H. Kulenkampff, Ann. der Physik, **87,** p. 597; 1928.
26. D. L. Webster, Phys. Rev., **6,** p. 56: 1915.
27. E. H. Kennard, Phys. Zeits., **24,** p. 372; 1923.
28. E. O. Lawrence, Phys. Rev., **28,** p. 947; 1926, and **29,** p. 609; 1927.
29. Millikan and Cameron, Phys. Rev., **32,** p. 533; 1928.
30. See A. H. Compton, X Rays and Electrons, p. 188.
31. K. T. Compton and C. C. van Voorhis, Phys. Rev., **26,** p. 436, and **27,** p. 724; 1926. Webster, Clark, Yeatman, and Hansen, P. N. A. S., **14,** p. 679; 1928.

WASHINGTON, January 11, 1929.

A MULTIPLE-STRAND TEST FOR YARNS [1]

By Charles W. Schoffstall and H. A. Hamm

ABSTRACT

The essential features of the multiple-strand test method for determining stress-strain relationships of yarns are as follows: The yarn is wound from its original form of put-up onto a specimen holder under uniform tension in such a way that the strands are placed parallel and do not overlap. The specimen holder containing the yarn is then placed in the jaws of an automatic stress-strain recording tester of the inclination-balance type. The speed of the pulling jaw is recommended to be 12 inches per minute. The distance between jaws is recommended to be 4 inches. The number of strands may be varied but should be calculated to a basis of 100 strands. In cases of various sizes of the same type of yarn further simplification of results on a strength-count basis is recommended.

CONTENTS

	Page
I. Introduction	871
1. Single-strand test	872
2. Skein test	873
3. Proposed A. S. T. M. test	874
II. Apparatus and testing procedure	875
1. Apparatus	875
2. Testing procedure	876
3. Discussion of apparatus and method	876
III. Test results	877
1. Influence of the number of strands	877
2. Comparison of A. S. T. M. (proposed) method and multiple-strand method	878
3. Influence of the variables of the multiple-strand method on strength results	879
4. Results of tests on different kinds of yarn	883
IV. Summary	884
1. Essential features of method	884
2. Advantages of the method	884
V. Acknowledgment	885

I. INTRODUCTION

The need for adequate methods of obtaining the stress-strain relationships of yarns is well recognized in the textile industry. This is especially true for rayon, because variations in the stretch characteristics affect both the appearance and quality of the final product.

[1] A preliminary report on this method was published in the Textile World, Sept. 24, 1927, p. 97, including a comparison with the method outlined tentatively by the rayon subcommittee of D-13 of the American Society for Testing Materials.

The "shiners" which occur at times in the rayon fabric and the puzzling striped effects which are sometimes found in knitted rayon tubing have been attributed to the application of uneven tension to the rayon yarn at some point of the manufacturing process, which distorted the yarn when the load was sufficient to stretch it beyond the elastic limit.

Two general methods have been used for determining the breaking strength of yarns—the single-strand test and the skein test.[2]

The single-strand test consists in stretching a single strand of prescribed length at a prescribed rate of elongation until it breaks. In the skein test a skein, previously wound on a yarn reel, is transferred to the drums of a testing machine and loaded as in the single-strand test. The testing machine in each case records the maximum load applied.

1. SINGLE-STRAND TEST

Several types of apparatus have been devised which will record the stress-strain data on textile yarns and fibers. The Schopper machines in use in this country give the ultimate stretch but do not record the stress-strain relationship. Scott testers for cords and twines have automatic devices for recording stress-strain data, but these machines are not sufficiently sensitive for single yarn or fiber tests. Both of these machines are of the pendulum inclination balance type.

Midgely [3] states that "the pendulum balance is extremely simple in principle and is peculiarly adaptable for the design of simple, accurate, easily calibrated machines which for facility of manipulation are greatly superior to all other types. The sensitiveness of the machine is not a constant quantity, however, and rapidly increases when the angle of inclination of the pendulum to the vertical becomes large, and for this reason the motion of the pendulum should be limited."

Some inherent errors due to inertia effects are present and cause some waviness of the actual curve drawn by the recording device. Shorter and Hall [4] discuss this point and set forth a theory of the motion, with a mathematical analysis indicating that the angular velocity of the pendulum, instead of having a steady value, actually oscillates about this value. This results in "a series of periodic momentary stoppages of the pendulum such as are actually observed."

Several experimental machines have been devised for specific research projects. Barratt [5] subjected cotton fibers to a smooth loading by an electromagnetic apparatus and obtained data on

[2] The skein test is sometimes termed the hank test, or the lea test.

[3] Midgely, The Machine Commonly Used in the Cotton Industry for the Testing of Materials, J. Text. Inst., T189, **14**, No. 7; July, 1923.

[4] Shorter, S. A., and Hall, W. J., The Dynamical Theory of the Pendulum Yarn-Testing Machine, J. Text. Inst., T501, **14**; 1923.

[5] Barratt, T., Measurements of Breaking Stresses, Extensibilities, and Elasticities of Single Fibers of Cotton, etc., J. Text. Inst., T17, **13**, No. 1; January, 1922.

extension at break and breaking strength. New [6] used a spring balance and applied tension by running water into a pan attached to the yarn. A mechanical recording system was incorporated which recorded the stress-strain curve.

Matthew [7] applied a load through a lever system by water running at a constant rate into a vessel suspended from the end of a lever. An automatic recording system with pen and drum was provided. Shorter and Hall [8] describe a spring-balance type of machine which reduces the effects of inertia and friction to a minimum, so that the stress-strain relationships which hold during rapid changes can be investigated. In this machine all motion-compounding devices are eliminated. "The top end of the yarn is attached to the spring and the bottom end to the stretching mechanism. The pen is attached to the spring and partakes of its vertical motion. The paper is attached to the carriage which, by means of a simple mechanism, is made to move horizontally at a rate equal to that of the vertical motion of the lower end of the yarn * * *".

These machines are typical of those described in the literature. For a further and more detailed study the surveys and discussion of Midgely and Pierce [9] [10] [11] [12] are suggested.

2. SKEIN TEST

The skein test has been used quite extensively in cotton mills and wool mills. The voluminous data [13] compiled by the Draper Co. over a period since 1886 were based on results obtained using this method.

Many changes have been suggested for improving the skein test. In the basic test a skein of 120 yards is first prepared by winding the yarn onto a reel of 1½ yards perimeter to form a skein of 80 strands. The skein is then placed around the drums of a tester, and a pull sufficient to break it is gradually applied; the machine records the maximum force transmitted during the test.

Friction, nonuniform distribution of tension, and variations in the stretch of the individual yarns appreciably influence skein tests, so that the test does not give the average of a large number of single strands. Nevertheless Hall [14] states, "* * * Although the

[6] New, G. F., The Stress-Strain Curves of Various Yarns, J. Text. Inst., T52, **13**, No. 2; February, 1922.
[7] Matthew, J. A., The Elastic Properties of Yarns, J. Text. Inst., T45, **13**, No. 2; February, 1922.
[8] Shorter, S. A., and Hall, W. J., A New Autographic Testing Machine for Yarns and Fibers, J. Text. Inst., T495; December, 1923.
[9] See footnote 3.
[10] Midgely, E., and Pierce, T. F., Tensile Tests of Cotton—(I) A Survey of Current Tests; (II) The Ballistic Test for Work of Rupture; (III) The Rate of Loading; Shirley Inst. Memoirs, 5; 1926.
[11] Pierce, T. F., Tensile Tests of Cotton—(IV) The Dynamics of Some Testing Instruments; (V) The "Weakest Link" Theorems on the Strength of Long and of Composite Specimens; Shirley Inst. Memoirs, 5; 1926.
[12] Pierce, T. F., The Mechanical Testing of Cotton Materials—(A) The Measurement of the Mechanical Properties of Cotton Materials, J. Text. Inst., T161, **14**; No. 7; July, 1923.
[13] Textile Texts, 4th ed., 1917, Draper Corporation, Hopedale, Mass.
[14] Hall, W. J., An Experiment Examination of the Hank Test and a Comparison with the Single-Thread Tensile Test for Woolen and Worsted Yarns, J. Text. Inst., T223, **16**; 1925.

strength of the single thread can not be deduced from the results of the hank (lea) test, yet the hank test will grade a series of yarns in approximately the same quantitative order as the single-thread test. Since most tests are comparative rather than absolute, the hank test is thus proved to be of considerable value, particularly when it is remembered that generally single-thread testing is unreliable on account of the insignificant amount of material tested, and impractical for general use if enough tests are carried out to give truly representative results * * *."

Hall refers very briefly to a test which has some similarity to the multiple-strand test procedure herein described in that he wound the yarn on a frame and clamped both ends in the machine. No details were given regarding the winding nor were any stress-strain data given. He states, "The hank test gives an appreciable greater value for the breaking load than the multiple single-thread test clamped at both ends, but less than that calculated from the ordinary single-thread test." Lack of details of the procedure precludes any discussion of this conclusion in relation to the test described herein or the results obtained.

A distinct disadvantage of the skein test from many standpoints is the fact that accurate stress-strain data can not be obtained.

3. PROPOSED A. S. T. M. TEST

The rayon subcommittee of D–13 of the American Society for Testing Materials has recommended in their proposed specification[15] for rayon a modification of the skein test for measuring strength and stretch.[16] This is a step in the direction of eliminating the inherent difficulties of the skein test. This method requires the breaking of a segment of a skein prepared as in the skein test. The procedure is as follows:

"The initial distance between jaws shall be 10 cm (4 inches). The skein to be tested shall first be clamped in the upper jaws spread out evenly so that the ends are parallel, forming a ribbon approximately three-eighths to three-fourths inch in width. The rayon shall then be drawn down through the lower jaws and spread out to make a band of equal width, pulled just taut and clamped."

For routine work in which an accuracy no greater than 10 per cent is required the above test is apparently satisfactory. However, for research work in which small differences in the stress-strain curves are to be studied the precision is not sufficient. Much of the inaccuracy is due to the personal equation involved, first, in the way in which the individual strands are placed in the jaws of the tester; and second,

[15] Tentative Specifications for Tolerances and Test Methods for Rayon, serial designation D238-27T; revised, 1927; A. S. T. M.

[16] Edwards, W. F., Value of the Serigraph Test, Textile World, Dec. 23 and 30, 1922; also, Universal Tensile Tests for Yarns, Textile World, p. 2355; Apr. 3, 1926.

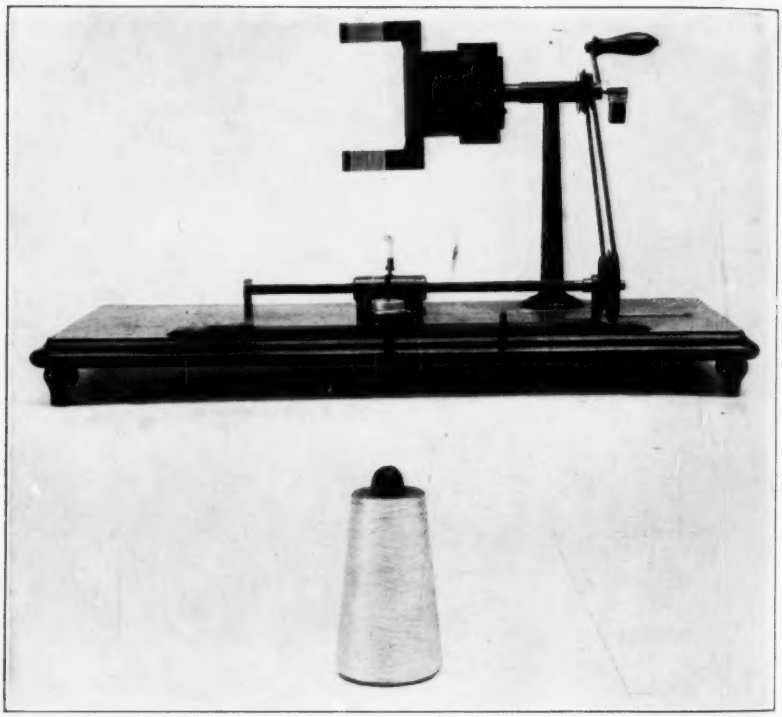

FIGURE 1.—*General view of apparatus for winding the yarn on the specimen holder (multiple-strand method)*

A card winder for evenness tests is adapted. The yarn is led through the tensioning device. A clamp to which is attached the specimen holder takes the place of the usual card. A revolution counter is attached.

in the inequality of the tension of the individual strands as they are fastened between the jaws of the tester. The proposal of Prof. G. B. Haven [17] to fasten the specimen at each end with a gummed label or sticker, so that the yarns will not slip during handling, is an improvement in this respect.

II. APPARATUS AND TESTING PROCEDURE

The apparatus and testing procedure used in the multiple-strand test are described below.

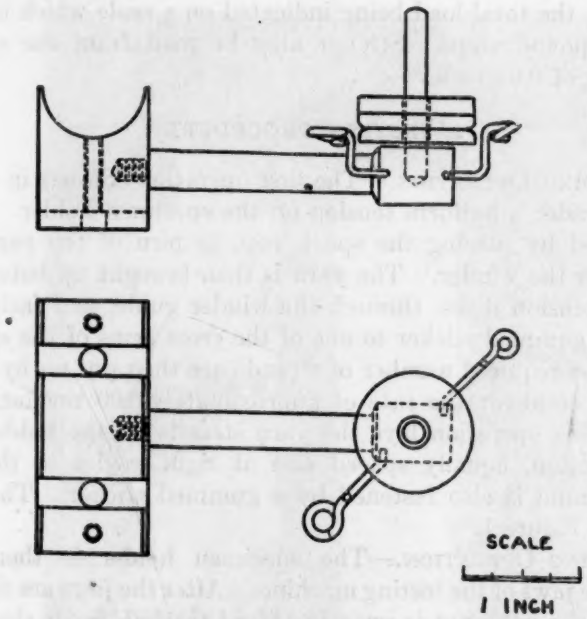

FIGURE 2.—*Tension device used in winding the specimen in the multiple-strand method*

The disks are aluminum about 3.5 g each. The remainder is brass (or any suitable metal).

1. APPARATUS

(*a*) YARN WINDER.—The winder is an adaptation of a card winder used for inspection of yarn evenness. (Fig. 1.) It is equipped with a tension device attached to the usual driving-screw carrier mechanism, and a ratchet counter for indicating the number of strands.

(*b*) TENSION DEVICE.—The tension device (fig. 2) consists essentially of three highly polished aluminum disks arranged so that they are free to revolve and a holder with eyelets for guiding the yarn

[17] Massachusetts Institute of Technology.

through the disk arrangement. Each disk weighs approximately 3.5 g.

(*c*) SPECIMEN HOLDER.—This consists of two arms and a clamp for holding them (figs. 1 and 3). The arms are clamped in proper position by using as guides several small pins which project from the clamp and fit into holes in the arms. The wing nut and bolt are used to secure the arms in position during the winding operation.

(*d*) BREAKING-STRENGTH MACHINE.—The machine used for breaking the specimens is an automatic recording Scott power tester of the inclination-balance type with capacities of 0 to 55 pounds and 0 to 110 pounds, the total load being indicated on a scale which is graduated in ½-pound steps. Stretch may be read from the curve to an accuracy of 0.02 inch.

2. TESTING PROCEDURE

(*a*) WINDING OPERATION.—The first operation consists in winding the yarns under a uniform tension on the specimen holder. This is accomplished by placing the spool, cop, or pirn of the yarn to be tested under the winder. The yarn is then brought up between the two lower tension disks, through the winder guide, and fastened by means of a gummed sticker to one of the cross arms of the specimen holder. The required number of strands are then put on by turning the winder crank at the rate of approximately 100 revolutions per minute. This operation lays the yarn strands on the holder under uniform tension, equally spaced and at right angles to the arms. The last strand is also fastened by a gummed sticker. The set-up is shown in Figure 1.

(*b*) TESTING OPERATION.—The specimen holder is then transferred to the jaws of the testing machine. After the jaws are tightened (see fig. 3) the wing nut is unscrewed and the holder for the arms is removed (see fig. 4). The specimen is then broken in the usual manner.

3. DISCUSSION OF APPARATUS AND METHOD

Several changes were made in the winding apparatus, the most important of which was the addition of a tension device attached to the part holding the eyelet. It was found, by trial, that two polished aluminum disks, rotating on a third, each weighing approximately 3.5 g, produced satisfactory tension for the several types of yarn under consideration; that is, this appeared to the eye to be the minimum weight which would lay the yarn on the rod straight and unkinked. This device is similar to those sometimes used in yarn-winding machines. The tension was found to be 8 g for a 150-denier rayon yarn moving at 80 feet per minute through the disk tension device. These disks and the upright on which they are placed must be kept

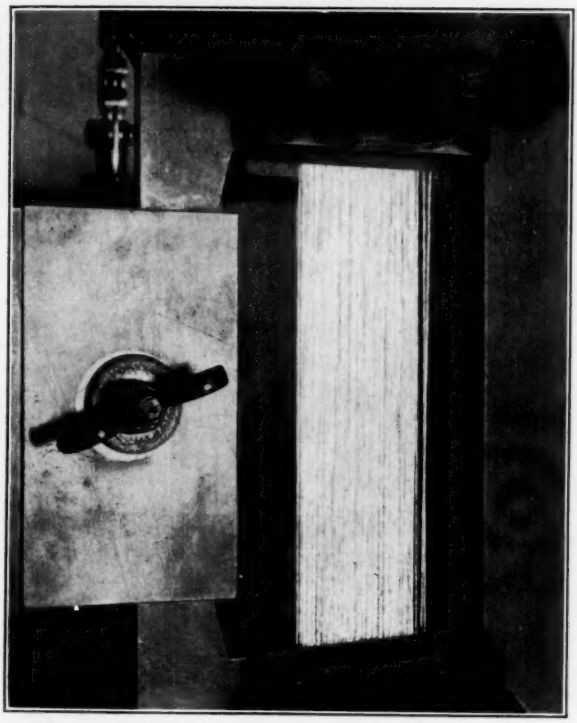

FIGURE 3.—*Specimen holder inserted in the jaws of the machine with clamp still attached*

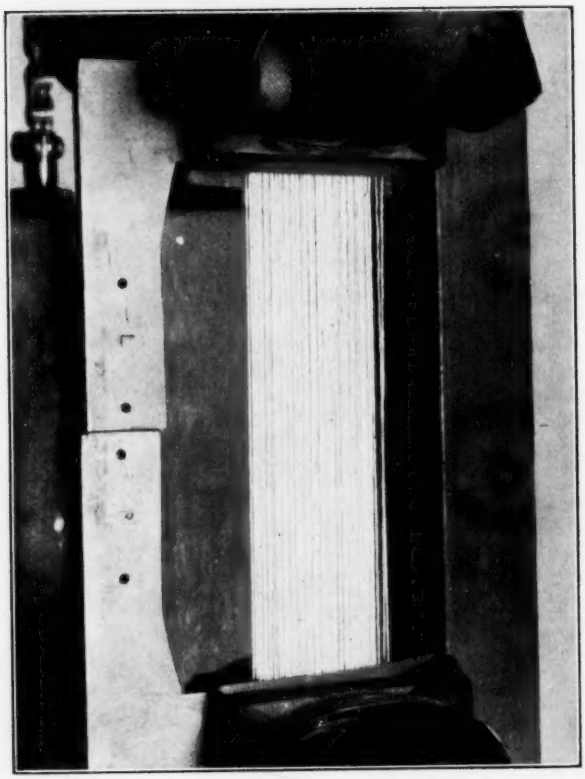

FIGURE 4.—*Specimen holder in the jaws of the machine with clamp removed*

smooth and polished. This is especially important for silk or rayon, because roughened places may cut or break the filaments.

The testing procedure for the multiple-strand test has three major advantages over previous attempts to supplant or improve the skein test. These are (1) minimum handling of the yarn (2) uniform tension on the strands of the test specimen, and (3) no overlapping of the strands.

III. TEST RESULTS

1. INFLUENCE OF THE NUMBER OF STRANDS

From each of four different types of rayon (obtained in February, 1927), specimens wound to contain 20, 40, 60, 80, and 100 strands [18]

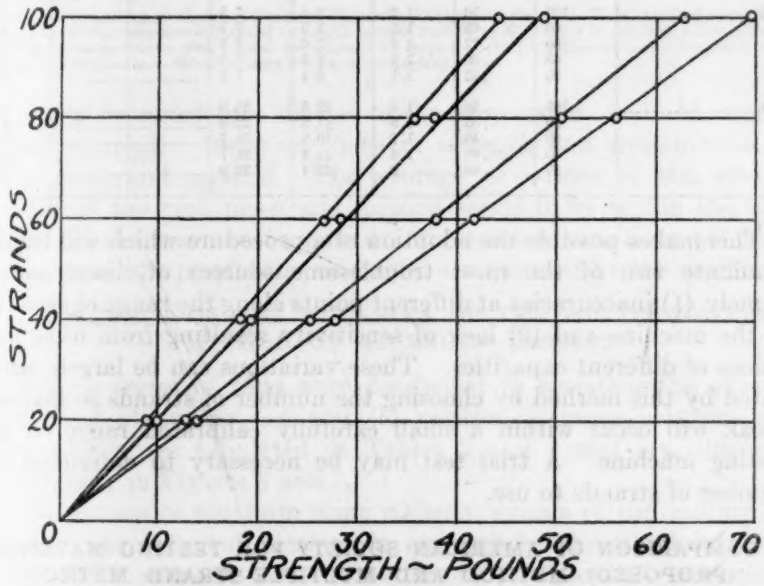

FIGURE 5.—*The effect of number of strands in the specimen on the strength using the multiple-strand method*

Four types of rayon yarns were used in this test. Note the excellent straight-line relationship indicating a direct proportionality between number of strands and strength with this method.

were tested. The results calculated on a basis of 100 strands are given in Table 1.

The results are given in graphical form in Figure 5. It will be noted that the total breaking load is closely proportional to the number of strands and that comparable results in per cent of stretch are obtained regardless of the number of strands used in the specimen. The agreement of the results when computed to a basis of 100 strands is especially good.

[18] "Strand" is used in this paper to mean a part of the specimen extending from one arm of the specimen holder to the other and should not be confused with the words "filament" or "ply."

TABLE 1.—*Influence of the number of strands on the breaking strength*

[All results calculated on 100-strand basis]

Sample	Number of strands	Stretch at—						Breaking strength
		10 pounds	20 pounds	30 pounds	40 pounds	50 pounds	60 pounds	
		Per cent	*Per cent*	*Per cent*	*Per cent*	*Per cent*	*Per cent*	*Pounds*
V-1	100	0.42	1.4	1.8	7.7	11.4	15.1	69.8
	80	.46	1.4	1.9	7.7	11.6	15.1	70.0
	60	.53	1.4	2.0	7.9	11.8	15.8	69.7
	40	.46	1.2	1.8	7.7	11.4	15.3	69.6
	20	.46	.93	1.9	7.6	11.2	14.5	70.0
N-2	100	.70	1.2	2.3	6.1	8.9	12.0	62.3
	80	.46	1.2	2.1	6.2	8.7	12.0	63.1
	60	.53	1.2	1.9	6.0	8.9	12.4	63.3
	40	.46	1.2	1.9	6.0	8.9	11.9	63.3
	20	.77	1.2	2.5	6.5	8.8	11.6	63.3
C-3	100	.70	1.2	3.6	7.5	----	----	48.8
	80	.60	1.2	3.0	7.5	----	----	47.1
	60	.77	1.3	3.0	7.5	----	----	47.2
	40	.60	1.2	2.6	7.5	----	----	48.3
	20	.53	1.1	3.4	7.3	----	----	50.0
A-4	100	.56	1.5	12.5	23.0	----	----	44.1
	80	.53	1.5	11.5	22.8	----	----	44.8
	60	.46	1.7	10.8	21.7	----	----	44.7
	40	.46	1.6	11.4	21.7	----	----	45.8
	20	.46	.9	13.1	22.9	----	----	45.0

This makes possible the adoption of a procedure which will largely eliminate two of the most troublesome sources of discrepancies, namely (1) inaccuracies at different points along the range of capacity of the machine and (2) lack of sensitivity resulting from using machines of different capacities. These variations can be largely eliminated by this method by choosing the number of strands so that the break will occur within a small carefully calibrated range on the testing machine. A trial test may be necessary to determine the number of strands to use.

2. COMPARISON OF AMERICAN SOCIETY FOR TESTING MATERIALS (PROPOSED) METHOD AND MULTIPLE-STRAND METHOD

A series of tests were made on four different types of rayon using the proposed method of the rayon subcommittee of the A. S. T. M. A specimen of rayon yarn from a particular cone was tested according to the multiple-strand method; the next length was tested using the A. S. T. M. method and so on. Since the A. S. T. M. method proposes a speed of pulling jaw of 6 inches per minute and most of the work on the multiple-strand method was done at 12 inches per minute, both these speeds were included for comparison. An analysis of the results is given in Table 2.

TABLE 2.—*Comparison of results on rayon using the proposed A. S. T. M. and the multiple-strand methods*

[All results are on a 100-strand basis]

Test method	Number of tests	Number of strands per test	Speed of pulling jaw	Maximum deviation strength	Maximum deviation stretch	Maximum deviation in load at 0.1 inch stretch
				Pounds	*Per cent*	*Pounds*
A. S. T. M.	40	80	6	3.3	0.09	3.0
M. S.	40	80	6	.6	.06	1.5
A. S. T. M.	40	100	6	2.1	.10	3.5
Do	100	100	12	2.3	.09	4.0
M. S.	100	80	12	.3	.06	1.6
A. S. T. M.	180			2.5	.09	3.7
M. S.	140			.4	.06	1.6

NOTE.—The mean deviation of the strength results obtained by the A. S. T. M. method using 12-inch speed of pulling jaws was 0.6 pound (strength ranged from 43 to 59 pounds in 100 tests using 100-strand specimens) as compared with a mean deviation of 0.1 pound for the multiple-strand test (strength ranged from 37 to 47 pounds in 100 tests using 80-strand specimens).

It will be noted that the use of the proposed A. S. T. M. method leads to greater deviations both in strength and stretch than the multiple-strand method. The average deviations in the strength results of the multiple-strand method seems to be within the sensitivity of the machine (½ pound); the stretch variations are about three times the possible experimental error caused by the machine.

3. INFLUENCE OF THE VARIABLES OF THE MULTIPLE-STRAND METHOD ON STRENGTH RESULTS

Several series of tests were conducted to ascertain the effect of (*a*) speed of pulling jaw and (*b*) various distances between jaws. The results are tabulated in Tables 3 and 4 and are illustrated graphically in Figures 6 and 7.

The results of the tests using different speeds of the pulling jaw showed the expected increase in strength as the speed increased. The chief interest in these results lies in the 6 and 12 inch speeds. There has been some discussion as to whether or not a 6-inch speed should be used for stress-strain testing. As noted previously, the proposed A. S. T. M. method for rayon specifies 6 inches. However, the most common speed used in textile testing with this type of machine is 12 inches per minute.[19] Probably for this reason the gearing of the machine is such that it operates best at about 12 inches per minute, although other speeds may be obtained by changes in the pulleys or by placing a rheostat in the power line. Judging from the results obtained in this study, there seems to be little justification for the change to 6 inches, and in the interest of standardization in laboratories testing all types of yarns and fabrics the 12-inch speed is to be preferred.

[19] Federal Specification Board specification No. 345a; A. S. T. M. test methods Nos. D39-27, D180-27, D203-25, D122-27, D179-27.

TABLE 3.—*Breaking strength of yarns broken at different distance between jaws* [1]

Sample No.	Kind	Breaking strength at distance between jaws				
		1 inch	2 inch	3 inch	4 inch	6 inch
		Pounds	*Pounds*	*Pounds*	*Pounds*	*Pounds*
1	Rayon	60	60	58	58	56
2	Rayon	56	56	56	54	52
3	Rayon	45	44	43	43	41
4	Rayon	37	36	35	35	34
5	Rayon	39	38	37	37	36
6	Rayon	37	36	36	35	34
7	Rayon	46	45	44	44	43
8	Rayon	39	39	39	38	.....
9	Rayon	40	40	40	39	40
10	Worsted	20	18	16	15	14
11	Cotton	41	40	37	35	34
12	Silk	60	58	54	52	50
13	Mercerized cotton	64	59	57	55	53

[1] Multiple-strand method; speed of machine 12 inches per minute; 80-strand specimens.

TABLE 4.—*Breaking strength of yarns broken at different speeds of pulling jaw* [1]

Sample No.	Kind	Breaking strength at speeds per minute				
		1 inch	2 inch	6 inch	12 inch	20 inch
		Pounds	*Pounds*	*Pounds*	*Pounds*	*Pounds*
1	Rayon	124	131	141	149	152
2	Rayon	111	121	135	139	144
3	Rayon	90	94	101	105	110
4	Rayon	75	80	85	85	90
5	Rayon	85	91	102	110	115
6	Rayon	74	81	91	94	96
7	Rayon	90	95	103	109	112
8	Rayon	76	81	88	93	96
9	Rayon	73	83	92	95	98
10	Worsted	30	35	36	38	42
11	Cotton	81	80	85	86	90
12	Silk	118	125	132	147	151
13	Mercerized cotton	138	138	139	142	145

[1] Multiple-strand method; distance between jaws was 4 inches; 200-strand specimens were used; capacity of machine was 300 pounds.

Considering the curves (fig. 7) for different distances between jaws, it is clear that the percentage stretch and the breaking strength decrease as the distance between jaws increases, probably due to the increase in the time of break, which is equivalent to decreasing the rate of elongation. A pulling speed of 12 inches per minute on a 6-inch specimen represents a rate of elongation of 2 inches per inch of specimen per minute (assuming that the pendulum jaw is stationary). The same speed on a 1-inch specimen represents a rate of elongation of 12 inches per inch per minute, or six times as great.

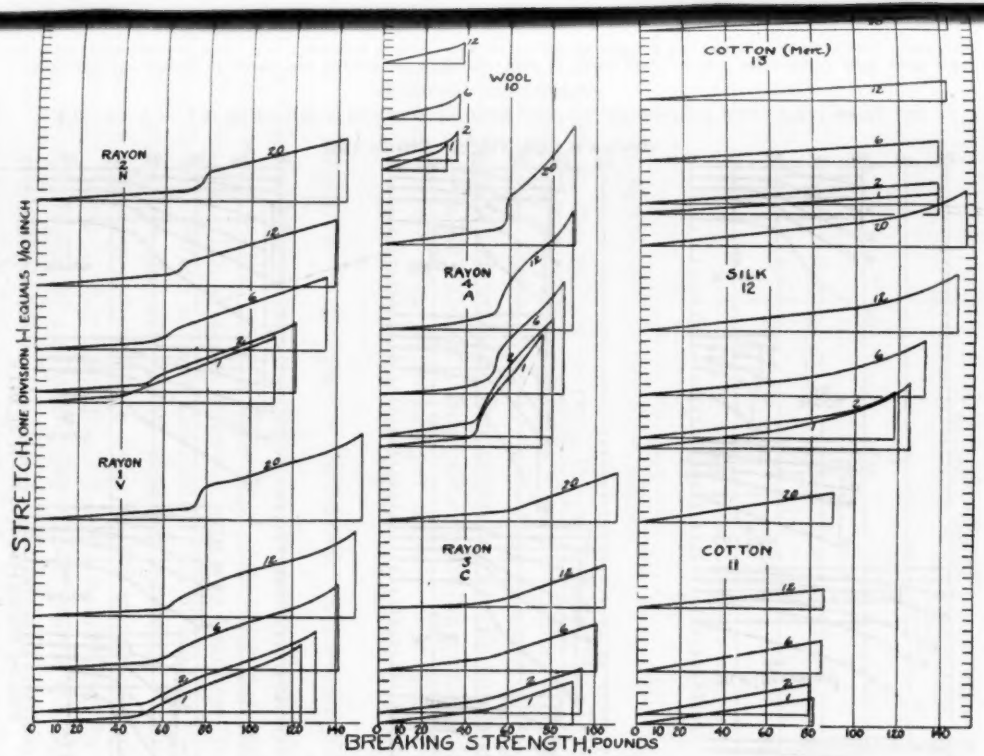

FIGURE 6.—*The influence of speed of pulling jaw on the strength and stretch using the multiple-strand method*

Although the groups of curves are typical for different types of yarns, they are not comparable with each other because of differences in size. The Figures 1, 2, 6, 12, and 20 on the curves indicate the speed of the pulling jaw. The zero-stretch or base line is drawn for each curve.

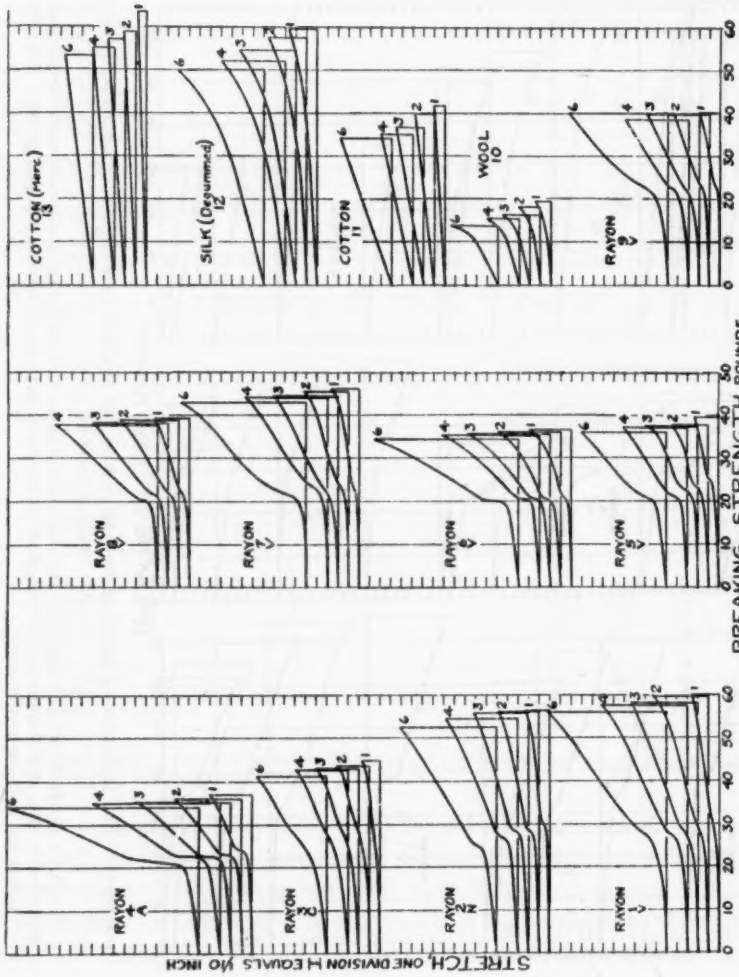

FIGURE 7.—*The influence of distance between jaws on the strength and stretch using the multiple-strand method*

Although the groups of curves are typical for different types of yarns they are not comparable with each other because of differences in size. The Figures 1, 2, 3, 4, and 6 on the curves indicate the distance between jaws. The zero-stretch base line is drawn for each curve.

TABLE 5.—*Comparison of results obtained with different test conditions*

[Calculated to 100-strand basis]

No.	Conditions	
	2 inches between jaws, 12 inches per minute, 80-strand specimen	4 inches between jaws, 20 inches per minute, 200-strand specimen
1	75	76
2	70	72
3	55	55
4	45	45
5	47.5	57.5
6	45	48
7	56.3	56
8	48.7	48
9	50	49
10	22.5	21
11	50	45
12	72.3	75.5
13	72.7	72.5

NOTE.—Sample No. 5 was noticeably variable in its structure.

A check on the method covering the proportionality of the number of strands and the pulling speed is shown in Table 5, in which the strength results obtained at 12 inches per minute, with 2 inches between jaws for 80 strands, is compared with the results shown in the last column of Table 4. Both sets of results are calculated to a 100-strand basis. The 20 inches per minute on a 4-inch specimen are roughly equal to 12 inches per minute on a 2-inch specimen.

4. RESULTS OF TESTS ON DIFFERENT KINDS OF YARN

In order to demonstrate the universal character of this test method for all types of textile yarns, a number of tests were made on various kinds of yarns. The distance between jaws was 4 inches; the number of strands was varied so that the results fell within the range of 30 to 70 pounds on the 110-pound capacity machine. Table 6 summarizes the results reduced to a basis of 100 strands by simple calculations. Some further simplification of the results may be desirable from the standpoint of any particular class of yarn. In the column headed "strength-count factor," a suggested unit basis for rayon and silk is indicated which is obtained by dividing the strength per 100 strands by the size, respectively. The remaining data in this column are not comparable because calculations are made on a different basis. The results have little significance in themselves, because the samples were chosen more or less at random and only for the purpose of showing the application of the method to all types of yarns. The strength results are averages of 10 breaks.

TABLE 6.—*Breaking strength and stretch (multiple-strand method) of various kinds of yarns*

Sample No.	Kind	Description	Count [1]	Count system	Number of strands	Breaking strength	Breaking strength 100-strand	Strength-count factor	Stretch at breaking
						Pounds			*Per cent*
1	Rayon		150	Denier	100	69.8	69.8	0.44	20.9
2	do		154	do	100	62.8	62.8	.41	14.0
3	do		135	do	100	48.9	48.9	.36	11.4
4	do		156	do	100	44.1	44.1	.28	29.5
5	do		153	do	100	51.3	51.3	.36	15.1
6	do		150	do	100	43.4	43.4	.29	23.2
8	do		149	do	100	43.4	45.4	.30	22.1
10	Wool	Fr. worsted	52.6	Worsted	160	30.3	19.0	.36	3.7
11	Cotton	Unbleached	34	Cotton	100	44.3	44.3	1.3	7.1
12	Silk	Degum	135	Denier	40	40.0	100.0	.74	11.1
13	Cotton	Mercerized	60/2	Cotton	60	44.3	73.3	1.1	4.3
14	do	do	15	do	40	51.8	129.5	8.6	7.1

[1] Denier (legal) system, the size is the weight of a 450 m skein in deniers (0.05 g); cotton system, the size is the number of 840-yard hanks in 1 pound (avoirdupois); worsted system, the size is the number of 560-yard hanks in 1 pound (avoirdupois).

IV. SUMMARY

1. ESSENTIAL FEATURES OF METHOD

The essential features of the multiple-strand test method for determining stress-strain relationships of yarns are as follows: The yarn is wound from its original form of put-up onto a specimen holder under uniform tension in such a way that the strands are placed parallel and do not overlap. The specimen holder containing the yarn is then placed in the jaws of an automatic stress-strain recording tester of the inclination-balance type. The speed of the pulling jaw is recommended to be 12 inches per minute. The distance between jaws is recommended to be 4 inches. The number of strands may be varied but should be calculated to a basis of 100 strands. In case of various sizes of the same type of yarn a further simplification of results on a strength-count basis is recommended.

2. ADVANTAGES OF THE METHOD

The advantages of the multiple-strand test method may be summarized as follows:

(*a*) The apparatus required is simple. It utilizes two machines which are generally available in most laboratories and plants, namely, an inclination-balance tester and an evenness tester. The changes necessary on the evenness counter are the addition of the tension device and ratchet counter. The only other device needed is a specimen holder which may be made easily. The procedure is easy to carry out, requiring only the care and technique of the usual laboratory operator.

(*b*) The average deviation of the strength results obtained, especially on rayon, are within the recording accuracy of the machine. The stretch deviations are about three times the possible experimental error caused by the machine. These are in both cases better than the proposed A. S. T. M. method for rayon, which is the nearest comparable method.

(*c*) The handling of the specimen has been reduced to a minimum. The necessary handling is mechanical and not personal.

(*d*) Each strand of the specimen is under uniform tension, and there is no overlapping of the strands.

(*e*) A smaller amount of the sample is wasted than in the skein test or the proposed A. S. T. M. test for rayon.

(*f*) Probably the chief advantage is based on the results which show that the breaking strength is directly proportional to the number of strands of the specimen. This permits the selection of the number of strands for any particular sample which will bring the result within a small range on the testing machine. (A trial test may be necessary to select this.) This procedure will avoid two of the most troublesome sources of variation in results, namely, inaccuracies at different portions along the range of the machine and differences in sensitivity of machines of different capacities.

(*g*) The results may be readily converted either to a unit basis of 100 strands or to a strength-count basis.

V. ACKNOWLEDGMENT

Acknowledgment is made to A. M. Tenney, chairman of the rayon subcommittee of the A. S. T. M.; Dr. E. E. Chandler, consulting physicist of the Department of Agriculture; and David C. Scott, for helpful suggestions in connection with the development of this project. Acknowledgment is also made to W. T. Schreiber and R. E. Stevens, of the bureau staff, for help in obtaining the data and to a number of rayon manufacturers for samples.

WASHINGTON, December 19, 1928.

THERMAL EXPANSION OF TANTALUM

By Peter Hidnert

ABSTRACT

This paper gives data on the linear thermal expansion of three samples of worked and annealed tantalum over various temperature ranges between −190° and +500° C. A summary of available data by previous observers on the thermal expansion of tantalum is included.

Worked tantalum was found to expand practically the same as annealed tantalum. The following equation is given as the most probable second-degree equation for the expansion of tantalum between 20° and 500° C.:

$$L_t = L_o [1 + (6.59t + 0.00008t^2) 10^{-6}]$$

The coefficient of expansion of tantalum increases slightly with temperature. From 20° to 100° C. the average coefficient of expansion is 6.6×10^{-6} per degree centigrade. Table 6 gives additional coefficients of expansion for various temperature ranges.

CONTENTS

	Page
I. Introduction	887
II. Materials investigated and uses of tantalum	888
III. Apparatus	890
IV. Results	890
V. Summary	894

I. INTRODUCTION

Tantalum was discovered by Ekeberg, of Sweden, in 1802. He assigned the name tantalum, because "when placed in the midst of acids it is incapable of taking any of them up and saturating itself with them."

The earliest available value for the linear thermal expansion of tantalum between 0° and 50° C. was obtained by the Normal-Aichungskommission, of Germany. Later Disch and Worthing published some data on the linear thermal expansion of tantalum. Disch determined the expansion of a sample of tantalum over several temperature ranges between −78° and +400° C. and Worthing reported results of one set of observations from 300° to 2,700° K. A summary of these results is given in Table 1.

The present paper gives results of 15 sets of observations. One sample of worked tantalum and two samples of annealed tantalum were used in this investigation. Expansion determinations were made over various temperature ranges between −190° and +500° C.

The author wishes to express his appreciation for the cooperation by the Fansteel Products Co., North Chicago, Ill. This company furnished the samples of tantalum and information about the preparation. Acknowledgment is due to H. W. Bearce and W. Souder, of the Bureau of Standards, for valuable suggestions and to H. S. Krider, of the Bureau of Standards, for assistance in the investigation.

TABLE 1.—*Summary of expansion data on tantalum by previous observers*

Observer	Date	Material	Temperature or temperature range	Coefficient of linear expansion per degree centigrade	Expansion equation
			°C.	× 10^{-6}	
Normal-Aichungs-kommission.[1]	(?)	Tantalum	0 to 50	7.9	
Disch [2]	1921	do.[3]	−78 to 0	[4] 5.9	$L_t=L_o\,[1+(6.46\ t+0.00090\ t^2)\ 10^{-6}]$, where L_t is the length at any temperature t between 0° and 400° C. and L_o the length at 0° C.
			0 to 100	[4] 6.6	
			0 to 200	[4] 6.6	
			0 to 300	[4] 6.7	
			0 to 400	[4] 6.8	
Worthing [5]	1926	Tantalum wire	27	[6] 6.6	$\frac{\triangle L}{L}=6.60\times10^{-6}\ (T-300)+8.2\times10^{-11}\ (T-300)^2$, where L is the length at 300° K. and T is any temperature between 300° and 2,700° K.
			27 to 1,400	[6] 7.3	
			27 to 2,400	[6] 7.8	

[1] Reported by von Bolton, Zeitschrift für Elektrochemie, **11**, p. 45; 1905. Other publications (von Bolton and Feuerlein, Electrotechnische Zeitschrift, **26**, p. 105; 1905; and Escard, Revue Générale des Sciences, **24**, p. 47; 1913) state that the coefficient of expansion 7.9×10^{-6} applies for the temperature range 0° to 60° C. or 0° to 100° C.

[2] Disch, Zeitschrift für Physik, **5**, p. 173; 1921. Disch states that his equation satisfies the observations to an accuracy of ± 0.01 mm/m.

[3] From Glühlampenwerk der Siemens und Halske A.-G., in Charlottenburg, Germany.

[4] Computed from data given by observer.

[5] Worthing, Phys. Rev., **28**, p. 190; 1926.

[6] Computed from expansion equation.

II. MATERIALS INVESTIGATED AND USES OF TANTALUM

Three samples of tantalum were investigated. The following information relating to these samples was furnished by the company that supplied the material:

Sample 1235 is practically chemically pure tantalum and has been worked to a considerable extent since its last anneal or heat treatment in a vacuum.

Samples 1236 and 1237 represent the metal in practically a state of complete anneal. The last heat treatment consisted in heating the material very close to its melting point in a vacuum furnace and maintaining the vacuum for some time in order to degas the metal as completely as possible. Very careful test of this metal would probably show that it still contains small amounts of hydrogen. Chemically, this is about as pure as it is possible to make the metal commercially. The only impurities which are probably present will be traces of iron, manganese, and possibly carbon, although the amount of any of these will be very small. This material after the final heat treatment was rolled lengthwise only enough to smooth up the metal and obtain as nearly uniform thickness as possible. Samples 1236 and 1237 will probably be considerably softer [1] than sample 1235.

[1] W. T. Sweeney, of this bureau, determined the hardness of two of these samples by means of the Vickers pyramid hardness testing machine made by Vickers (Ltd.), of London, England. A load of 30 kg was used. The hardness numbers for samples 1237 and 1235 were found to be 146 and 202, respectively.

Table 2 gives the chemical composition and the density of the samples.

TABLE 2.—*Chemical composition and density of tantalum*

Sample	Treatment	Chemical analyses [1]							Density [2] in g/cm³ at 23° C.
		Tantalum [3]	Manganese	Iron	Carbon	Molybdenum	Silicon	Columbium	
		Per cent	*Per cent*	*Per cent*	*Per cent*	*Per cent*	*Per cent*	*Per cent*	
1235	Worked	99.9+	0.019	0.01	<0.005	<0.001	[4]	[5]	16.57
1236	Annealed	99.9+	.014	.004	<.005	<.001	[4]	[5]	16.53
1237 [6]	Annealed								16.56

[1] Determined by R. M. Fowler, of this bureau.
[2] Determined by E. L. Peffer, of this bureau (after the expansion tests).
[3] Ignition of the metal to the oxide, Ta_2O_5, indicated a tantalum content greater than 99.9 per cent.
[4] Not detected.
[5] Not detected—if present, less than 0.10 per cent.
[6] Cut from same bar as sample 1236.

The following résumé by Fansteel Products Co.[2] includes uses to which tantalum has been put and uses which its properties suggest:

In considering the applications to which this metal is adapted the main points to be considered are its high melting point, its resistance to chemical corrosion, its tendency to absorb gases when heated, and the fact that it oxidizes when heated in air to a red heat. Among the uses for tantalum may be mentioned the following:

Dental instruments and dental spatulas.
Surgical tools.
Pen points.
Filament wire for incandescent lamps or thermionic tubes.
Plates and support wires for thermionic tubes.
Hypodermic needles.
Cathodes for use in electrochemical analysis.
Analytical weights, laboratory dishes, spatulas, stirrers, and other devices in which a perfectly acid-proof metal would be more suitable than porcelain or glass.
Parts of scientific instruments.
Acid-proof pumps and parts of commercial chemical equipment.
Electrolytic valves for the manufacture of rectifiers for obtaining direct current from alternating current course, as in battery chargers, electrolysis apparatus and radio.

For additional information about the preparation of tantalum, its physical and chemical properties, and its uses, the reader should refer to the papers mentioned in the footnote [3] below and to the note at the end of this paper.

[2] Eng. and Min. J., **116**, p. 816; 1923.

[3] W. von Bolton, Das Tantal, Seine Darstellung und Seine Eigenschaften, Zeitschrift für Elektrochemie, **11**, p. 45; 1905. W. von Bolton and Feuerlein, Die Tantallampe, eine neue Glühlampe der Firma Siemens und Halske A.-G., Elektrotechnische Zeitschrift, **26**, p. 105; 1905. Smith, Observations on Columbium and Tantalum, The Chem. News, **92**, p. 209; 1905. Siemens, Tantalum and Its Industrial Applications, The Chem. News, **100**, p. 223; 1909; or The Chem. Engineer, **10**, p. 207; 1909; or Engineering, **87**, p. 601; 1909. Escard, Le Tantale et Ses Applications Industrielles, Revue Générale des Sciences, **24**, p. 47; 1913. Balke, The Story of the Production and Uses of Ductile Tantalum, Chem. and Met. Eng., **27**, p. 1271; 1922; or Annual Report of the Smithsonian Institution, p. 233; 1923.

III. APPARATUS

Two types of thermal expansion equipment were used in this research, namely, (*a*) precision comparator and (*b*) fused-quartz tube. The first type was described in 1926 [4] and the second in 1928.[5] All sets of observations except several at low temperatures were made by means of the precision comparator.

IV. RESULTS

The linear thermal expansion of three samples of tantalum were investigated over various temperature ranges between −190° and +500° C. During the investigation it was found that tantalum

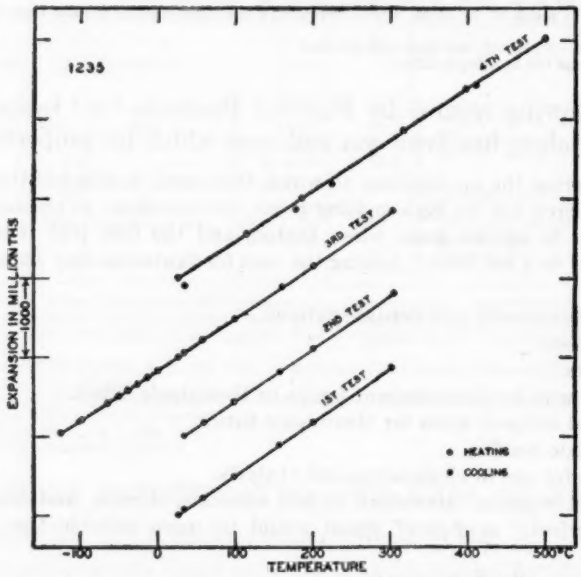

FIGURE 1.—*Linear thermal expansion of worked tantalum from −125° to +500° C.*

(See fig. 2 for additional tests)

oxidized in air at approximately 600° C. The maximum temperature of the expansion tests, therefore, was maintained below this temperature.

The results obtained on worked and annealed tantalum are shown in Figures 1 to 4, inclusive. The curves in these figures are plotted from different origins to display the individual characteristics of each curve. If drawn from the same origin, the curves would be so close together as to be confusing. The coefficients of expansion [6] which were obtained from the expansion curves are given in Tables 3 and 4.

[4] Souder and Hidnert, B. S. Sci. Papers, 21 (No. 524), p. 1; 1926.
[5] Hidnert and Sweeney, B. S. Jour. Research, 1 (No. 29), p. 771; 1928.
[6] All coefficients of expansion given in this paper were derived from the observations on heating.

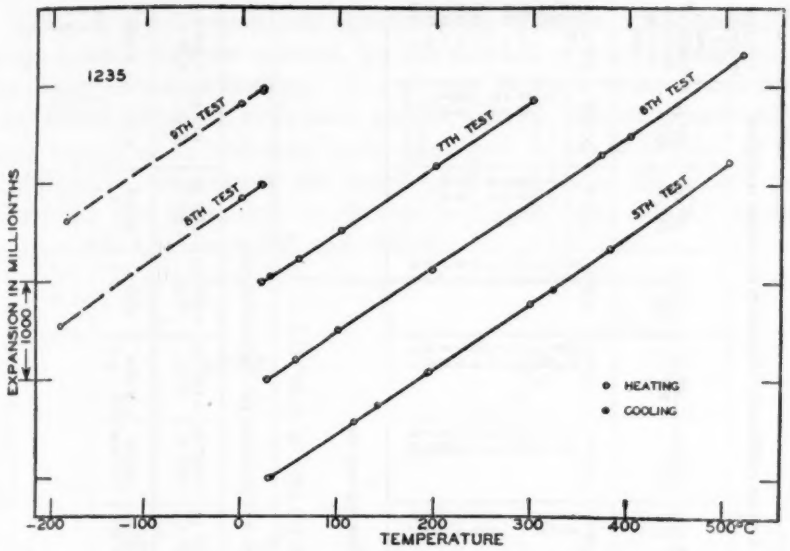

FIGURE 2.—*Linear thermal expansion of worked tantalum from −190° to +500° C.*

(See fig. 1 for previous tests)

The last column in Table 3 shows the differences in length before and after the expansion tests. The plus (+) sign indicates an increase in length and the minus (−) sign a decrease in length.

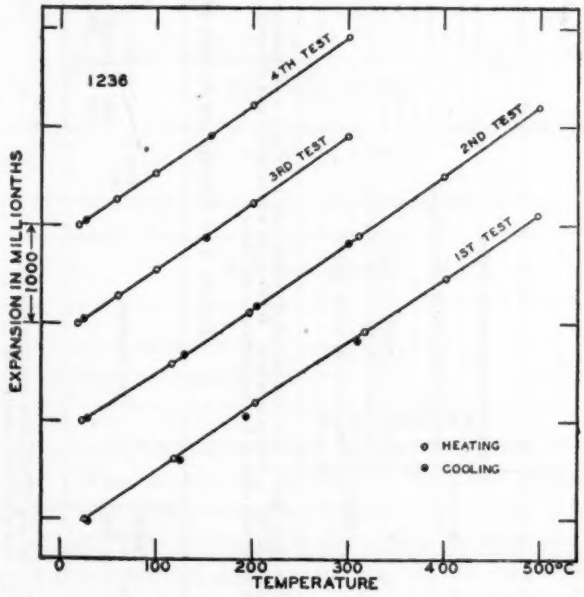

FIGURE 3.—*Linear thermal expansion of annealed tantalum from 20° to 500° C.*

TABLE 3.—*Average coefficients of expansion (20° to 500° C.) and length changes of tantalum*

Sample	Tantalum content	Test method	Test No.	Average coefficients of expansion per degree centigrade						Change in length due to heat treatment received during test
				20° to 60° C.	20° to 100° C.	20° to 200° C.	20° to 300° C.	20° to 400° C.	20° to 500° C.	
				×10⁻⁶	×10⁻⁶	×10⁻⁶	×10⁻⁶	×10⁻⁶	×10⁻⁶	*Per cent*
Worked: 1235	*Per cent* 99.9+	Precision comparator (bath)	1	6.8	6.7	6.8	6.8			+0.003
		do	2	6.5	6.6	6.6	6.7			.000
		do	[1] 3	6.6	6.5	6.5	6.6			.000
		Precision comparator (air furnace)	4		6.2	6.3	6.4	6.4	6.4	−.015
		do	5		6.4	6.5	6.6	6.6	6.8	−.001
		do	[2] 6	6.6	6.7	6.6	6.7	6.6	6.7	
		Precision comparator (bath)	[2] 7	6.2	6.3	6.6	6.6			.000
Annealed: 1236	99.9+	Precision comparator (air furnace)	1		6.6	6.7	6.6	6.5	6.6	−.004
		do	2		6.2	6.4	6.6	6.6	6.7	−.001
		Precision comparator (bath)	3	6.8	6.7	6.8	6.8			+.001
		do	4	6.6	6.6	6.7	6.8			.000

[1] Before these results were obtained observations were made at low temperatures. (See Table 4.)
[2] Heated to 700° C. during this test. White oxide was removed and the ends of sample were repolished before the next test.
[3] For additional tests at low temperatures see Table 4.

TABLE 4.—*Average coefficients of expansion of tantalum (−190° to +20° C.)*

Sample	Tantalum content	Test method	Test No.	Average coefficients of expansion per degree centigrade									
				−125° to −100° C.	−100° to −50° C.	−50° to 0° C.	0° to +20° C.	−125° to +20° C.	−100° to +20° C.	−125° to 0° C.	−100° to 0° C.	−50° to +20° C.	−190° to 0° C.	−190° to +20° C.
				×10⁻⁶	×10⁻⁶	×10⁻⁶	×10⁻⁶	×10⁻⁶	×10⁻⁶	×10⁻⁶	×10⁻⁶	×10⁻⁶	×10⁻⁶	×10⁻⁶
Worked: 1235	*Per cent* 99.9+	Precision comparator (bath)	[1] 3	6.1	6.2	6.4	6.8	6.3	6.4	6.2	6.2	6.5		
		Fused-quartz tube [2]	[3] 8				6.9						6.9	6.9
Annealed: 1237	99.9+	do	9				6.8						6.6	6.6
		do	1				6.0						5.8	5.9
		do	2				6.6				[4] 6.0		5.9	5.9

[1] See Table 3 for additional data obtained during this test.
[2] This method is not as accurate as the precision comparator.
[3] For previous tests at high temperatures see Table 3.
[4] Between −80° and 0° C.

Table 5 gives expansion equations for samples 1235 and 1236. These equations were derived, by the method of least squares, from the observations on heating. For sample 1235 the observations from tests 1 to 7, inclusive, were used, and for sample 1236 the observations from tests 1 to 4, inclusive, were employed in the derivation of the equations. L represents the length of the metal at 20° C. and $\triangle L$ represents the expansion or change in length from 20° C. to any temperature t between 20° and 500° C.

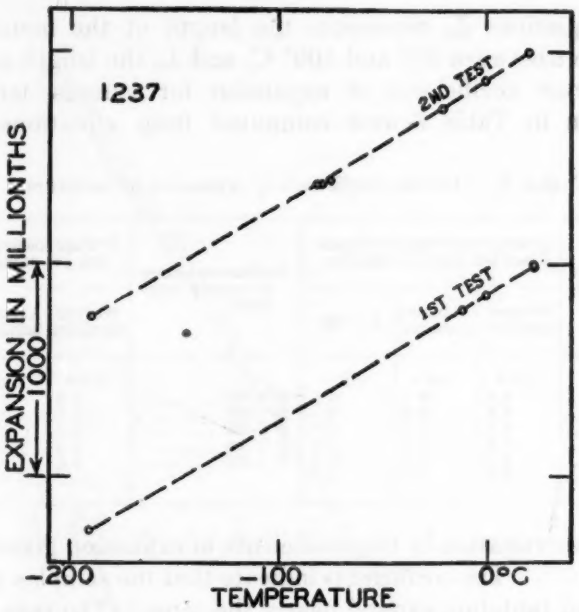

FIGURE 4.—*Linear thermal expansion of annealed tantalum from −190° to +20° C.*

TABLE 5.—*Expansion equations of tantalum*

Sample	Expansion equation	Probable error of $\triangle L$
Worked: 1235	$\triangle L = L\,[6.53\,(t-20)+0.00023\,(t-20)^2]\,10^{-6}$	$\pm 0.000023L$
Annealed: 1236	$\triangle L = L\,[6.66\,(t-20)-0.00007\,(t-20)^2]\,10^{-6}$	$\pm .000016L$

The expansion curves represented by the equations in Table 5 are nearly linear. The maximum deviation between these curves for worked and annealed tantalum is 14 millionths of the original length and occurs at 237° C. Since this deviation is approximately equal to the probable error of each equation, it is concluded that the samples of worked and annealed tantalum expand the same.

The equations of Table 5 may be transformed into the following:

Worked tantalum:

$$L_t = L_o\,[1 + (6.52\,t + 0.00023\,t^2)\,10^{-6}] \quad (1)$$

Annealed tantalum:

$$L_t = L_o\,[1 + (6.66\,t - 0.00007\,t^2)\,10^{-6}] \quad (2)$$

Average of equations (1) and (2):

$$L_t = L_o\,[1 + (6.59\,t + 0.00008\,t^2)\,10^{-6}] \quad (3)$$

In these equations L_t represents the length of the metal at any temperature t between 20° and 500° C. and L_o the length at 0° C.

The average coefficients of expansion for various temperature ranges given in Table 6 were computed from equations (1), (2), and (3).

TABLE 6.—*Average coefficients of expansion of tantalum*

Temperature range in degrees centigrade	Average coefficients of expansion per degree centigrade			Temperature range in degrees centigrade	Average coefficients of expansion per degree centigrade		
	Worked tantalum	Annealed tantalum	Average		Worked tantalum	Annealed tantalum	Average
	$\times 10^{-6}$	$\times 10^{-6}$	$\times 10^{-6}$		$\times 10^{-6}$	$\times 10^{-6}$	$\times 10^{-6}$
20 to 60	6.5	6.7	6.6	20 to 100	6.5	6.7	6.6
60 to 100	6.6	6.6	6.6	20 to 200	6.6	6.6	6.6
100 to 200	6.6	6.6	6.6	20 to 300	6.6	6.6	6.6
200 to 300	6.6	6.6	6.6	20 to 400	6.6	6.6	6.6
300 to 400	6.7	6.6	6.6	20 to 500	6.6	6.6	6.6
400 to 500	6.7	6.6	6.7				

The largest variation in the coefficients of expansion given in Table 6 is 0.2×10^{-6}. The coefficients indicate that the samples of worked and annealed tantalum expand nearly the same. The rate of expansion of tantalum changes slightly with temperature.

Figure 5 shows a comparison of the average expansion curve obtained in the present investigation on tantalum, with data from previous observers. The curve was derived from equation (3) and the data at low temperatures. Most of the values of previous observers lie above the curve.

V. SUMMARY

This paper gives data on the linear thermal expansion of three samples of worked and annealed tantalum over various temperature ranges between −190° and +500° C.

Two types of expansion apparatus were used in this investigation. A summary of available data by previous observers on the thermal expansion of tantalum is included.

Worked tantalum was found to expand practically the same as annealed tantalum. The following equation is given as the most

FIGURE 5.—*Comparison of the average expansion curve obtained in the present investigation on tantalum with data from previous observers*

probable second-degree equation for the expansion of tantalum between 20° and 500° C.:

$$L_t = L_o\,[1 + (6.59\,t + 0.00008\,t^2)\,10^{-6}]$$

The coefficient of expansion of tantalum increases slightly with temperature. From 20° to 100° C. the average coefficient of expansion is 6.6×10^{-6} per degree centigrade. Table 6 gives additional coefficients of expansion for various temperature ranges.

NOTE.—After the manuscript was submitted to the printer, C. W. Balke, chemical director, of Fansteel Products Co., informed the author that tantalum has found a very definite place [7] in the manufacture of spinnerets used in the manufacture of artificial silk, particularly by the viscose process. In this connection tantalum is replacing platinum and gold-platinum alloys. Because of the very attractive interference colors which can be produced on tantalum by electrolytic oxidation, there is at present considerable interest in its use for various articles of jewelry, particularly woven mesh wrist-watch straps, beads, spectacle frames, etc. It seems quite probable that tantalum will be commercially used along some of these lines.

WASHINGTON, December, 1928.

[7] For other uses of tantalum see p. 889.

SOUNDPROOFING OF AIRPLANE CABINS

V. L. Chrisler and W. F. Snyder

ABSTRACT

The present article contains a report of the work done in determining the structure which will give the maximum amount of sound insulation in an airplane cabin for a minimum weight.

Various small structures were tested at frequencies varying from 150 to 1,120 cycles per second to determine the best structure available within the allowable limit of weight.

A test flight was made in a treated cabin to determine how satisfactory the structure was under operating conditions. It was found that the noise in the cabin was about the same as in a railway coach in motion.

CONTENTS

	Page
I. Introduction	897
II. Method of measurement	898
III. Method of expressing results (sensation units)	899
IV. Discussion of results	900
V. Tests in airplanes in flight	903
VI. Description of panels	906
VII. Conclusions	908

I. INTRODUCTION

This paper is the first report of an investigation which is being carried out by the Bureau of Standards for the Aeronautics Branch of the Department of Commerce for the purpose of developing, if possible, practicable methods for reducing noise in the cabins of airplanes. It is, of course, desirable to reduce the noise as much as possible at its source, and more efficient exhaust mufflers may be developed which will contribute to this end. It may also be possible to reduce somewhat the noise of the propeller. At present, however, the soundproofing of the cabin seems to afford the most promising line of attack.

This problem is not a simple one. The noise of an airplane in flight has been found [1] to be of a very complex character, containing sounds of both high and low frequency. Other work on sound transmission shows that many materials are much better sound insulators at high frequencies than at low ones. The noise of an airplane engine

[1] The Problem of Noise in Civil Aircraft and the Possibilities of its Elimination, W. S. Tucker, A. M. I. E. E.; January, 1928.

is to a large extent composed of sounds of low frequency, in the region of 200 cycles per second. Tucker calls attention to the fact that in multimotored planes low-pitched beat notes may be produced when two engines are running at slightly different speeds.

In addition to the difficulty of insulating against noises of such a character the question of weight must be considered. In this respect the limitations are severe. It is also to be recognized that the engine and cabin are both attached to the same frame. This allows vibrations from the engine to be transmitted by solid conduction directly into the cabin.

Taking all these facts into consideration, it seems that the most practicable way to obtain a reasonable degree of quiet without excessive weight is to build the cabin walls in layers. Such a structure when composed of light materials may give rise to a considerable amount of back reflection at each surface of discontinuity, thus producing on the whole a greater opacity to sound than would a homogeneous wall of the same weight.

For the determination of the best materials to be used in such a construction a large number of transmission tests were made on common materials, heavy and light—the lightest being a sheet of wrapping paper. In these experiments the transmission was measured at three different frequency bands, 150–220, 400–470, and 1,000–1,120 cycles per second. It was felt that the lowest band would represent fairly well the fundamental frequencies that characterize the noise from the engine exhaust, while the highest band would correspond approximately to overtones or other high-pitched noises that may occur with any considerable intensity.

II. METHOD OF MEASUREMENT

The method used in measuring the sound transmission of the various materials and their combinations was that described in a previous publication.[2] In all these measurements the test panels were placed in the horizontal opening between the upper and lower rooms in the sound chamber building. It was found advisable to reduce this opening to fit the size of the sheets of material tested as cross supports were thus avoided. This reduction was effected by the use of 8-inch concrete blocks. The size of the opening used was 21½ by 40 inches. The samples were placed on top of this opening and sealed around the edges to prevent sound leakage.

All the materials tested had relatively high values of sound transmission, in comparison with which any transmission through the concrete blocks was negligible.

[2] B. S. Sci. Paper No. 526, Transmission and Absorption of Sound by Some Building Materials.

III. METHOD OF EXPRESSING RESULTS (SENSATION UNITS)

All results given in this paper and in the previous publication above referred to [3] have been obtained by use of the telephone receiver as a detector and measurer of sound energy. The indications of this instrument are given on what is called the physical scale, which measures the energy of the sound wave. But the instrument most universally used for detecting sound and estimating its intensity is the human ear, and unfortunately the ear does not respond according

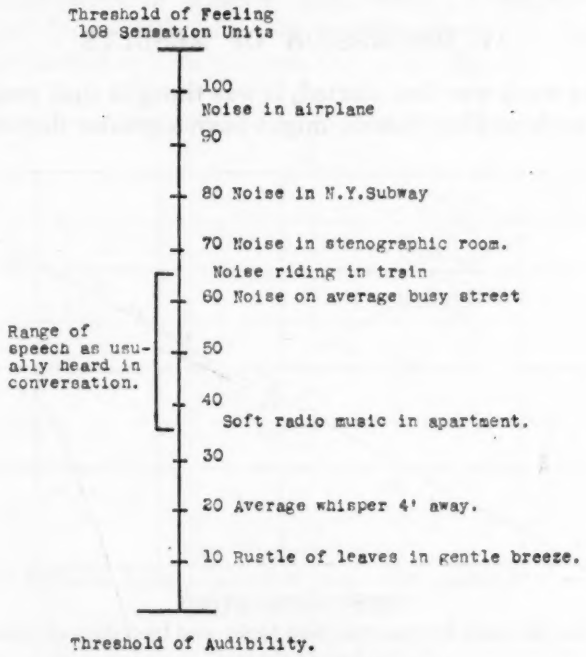

FIGURE 1.—*Ear sensation scale*

to the physical scale. As the intensity of a sound increases steadily on the physical scale the response of the ear fails to keep pace with it. There appears to be in the ear a regulating or protective mechanism whose nature is not clearly understood, which, like the well-known mechanism of the eye, protects that organ against excessive stimulation. Experience shows that the response of the ear is proportional to the logarithm of the physical intensity; that is, energies proportional to 10, 100, and 1,000 would produce in the ear effects proportional to 1, 2, and 3, respectively. This logarithmic scale has been termed the ear scale.

A slight modification of this scale has been employed for some time by telephone engineers,[4] and is used on all audiometers made

[3] See footnote 2.

[4] Fletcher, Bell Telephone Laboratories, Reprint B-152-1, J. Frank. Inst.; September, 1923.

by the Western Electric Co. This scale merely multiplies the numbers of the ear scale by 10, the unit of this new scale being that fractional change in intensity which is approximately the smallest that the average ear can detect. For this reason it is called a sensation unit. In the example given above, intensities corresponding to 1, 2, and 3 on the ear scale would be represented by 10, 20, and 30 sensation units.

Wallace Waterfall[5] has suggested a way of illustrating the values of sensation units in familiar terms. We may call it an ear sensation scale. (Fig. 1.)

IV. DISCUSSION OF RESULTS

When the work was first started, it was thought that possibly some materials, such as fiber boards, might have a greater degree of sound

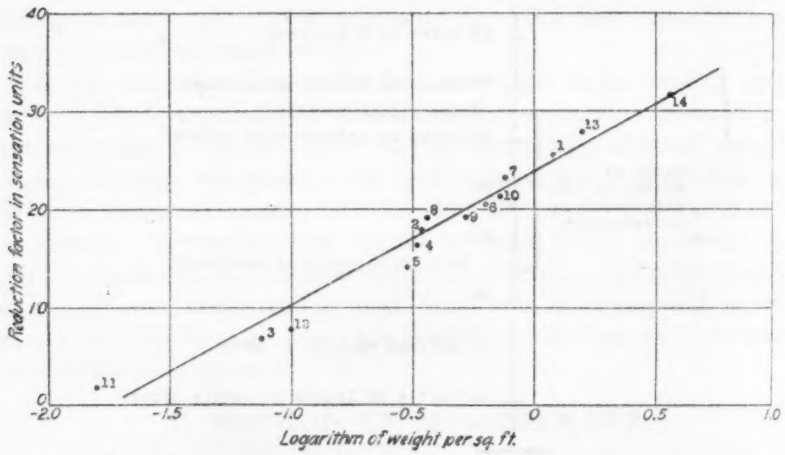

FIGURE 2.—*Relation between reduction factor and logarithm of panel weight (single sheets)*

insulation than a sheet of metal of the same weight. When the results were plotted—the reduction factors in sensation units against the logarithm of the weight per square foot—a straight line was obtained (fig. 2), the points in every case following close enough to the line to be within experimental error. This indicated that weight was the predominating factor rather than the nature of the material.

The next attempt was to use two sheets of material with an air space between them. Two sheets of aluminum with a 1¾-inch air space between them gave an average reduction factor of 14.6 sensation units, while a single sheet of the same aluminum gave 17.9. When this result was first obtained it was thought to be due to some error in measurement, but a repetition gave the same result. Sheets

[5] Engineering News Record, p. 60; Jan. 10, 1929.

of fiber board and of glass were tested in the same way. With these materials the presence of an air space showed a slight decrease in transmission compared with that of a single sheet, but, at least at low frequencies, the advantage gained was not enough to compensate for the increased weight.

It appears that two thin sheets of metal may be so flexible that the air between them may act as a mechanical tie, causing the two sheets to vibrate together and thus transmit sound. With more rigid materials, such as glass, this effect is less noticeable and a slight improvement in opacity may result. The point for this combination (panel 20) falls just a little above the straight line which was drawn for homogeneous materials (fig. 3). Had the air

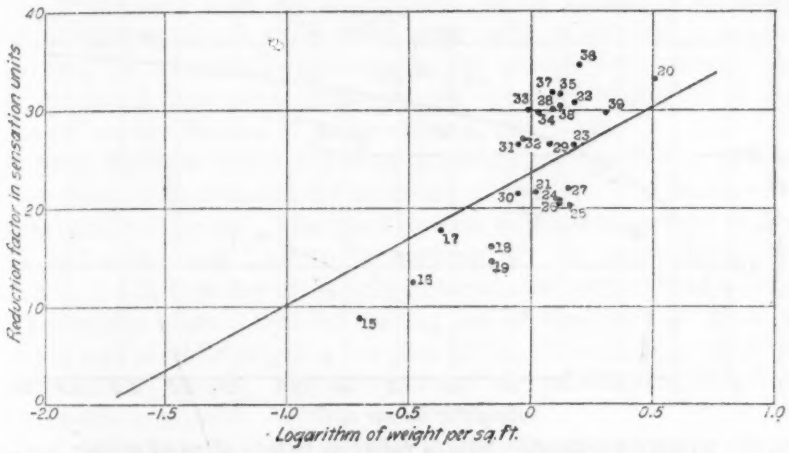

FIGURE 3.—*Relation between reduction factor and logarithm of panel weight (composite structures)*

space been very effective the point would have been found much higher. For two sheets of one-half inch Insulite (panel 22) there is quite an improvement, the point coming considerably above the line.

Insulite is not as stiff as glass, and, therefore, by the previous reasoning should not have given a lower transmission. Insulite, however, possesses a quality not found in glass or metal, which may account for this difference. This is its greater absorptive power for sound, which may be from 15 to 20 per cent as compared with from 1 to 3 per cent for glass and metal. In the case of fiber-board sheets separated by an air space the absorption occurring at each back reflection prevents the sound from building up in the air space to an intensity sufficient to penetrate the second sheet to the same extent as with less absorbent materials.

If this is correct, the introduction of absorbing material between two sheets of thin metal, such as aluminum, should decrease the

transmission of the combination. Panel 36 was thus constructed and, as may be seen in Figure 3, its reduction factor came out about eight sensation units greater than might have been expected on the basis of weight alone. In building construction it has been found [6] that no appreciable improvement is obtained by introducing sound-absorbing materials between two masonry walls or between two solid plaster partitions separated by a small distance. It is remarkable that this same rule does not seem to apply to very light structures.

There is considerable freedom of choice in the filling material. Balsam wool, cotton, and hair felt were tried with similar results.

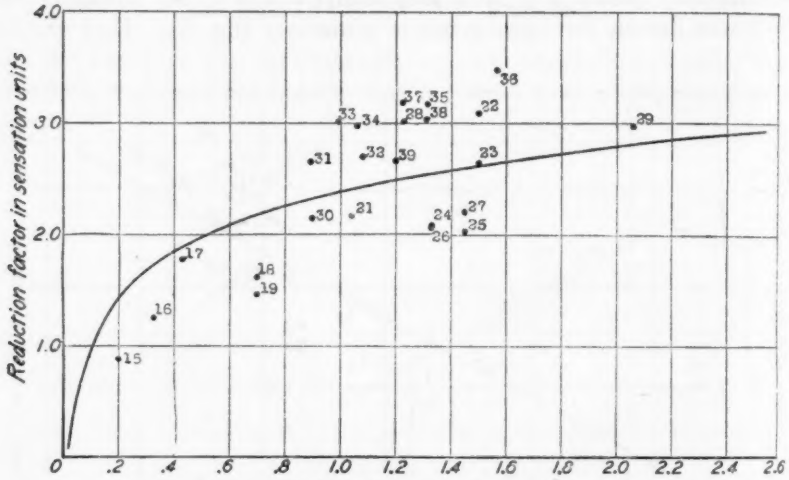

FIGURE 4.—*Relation between reduction factor and panel weight*

Such an arrangement gives a reduction factor which is as great as might be expected from a homogeneous material of twice the weight.

Panel 38 was built with two layers of balsam wool separated by a very thin sheet of aluminum with the idea of obtaining still better results. Measurement, however, showed no improvement over panel 28, which did not contain the central sheet of aluminum. The same plan was tried in panel 39, which contained alternate layers of cotton and wrapping paper, but without satisfactory results.

A combination of sheet aluminum, absorbent material, and fiber board (panel 33) was found to give a reduction factor equivalent to that of a homogeneous partition of about three times its weight.

Figure 3 shows graphically the results obtained by various combinations of materials. The straight line, representing the values that might have been expected if the weight were the only factor to be considered, furnishes a basis of comparison. This figure gives, in general, a somewhat distorted representation, being plotted to the

[6] B. S. Sci. Paper No. 552; Paul Sabine, The Armour Engineer; May, 1926.

logarithm of the weight in order to obtain the straight line. In Figure 4 the same data have been replotted, using the weight per square foot as the abscissa. From Figure 3 it might be inferred that panel 36 is the best combination, but Figure 4 shows that this panel is nearly twice as heavy as panel 33, while its reduction factor is only five sensation units greater. Considering weight, panel 33 gives the best results of all combinations tested.

To test this further, a larger panel, No. 40, of the same structure as panel 33, was built on a light wooden frame. On test its reduction factor was found to be 36, as compared with 30 for the smaller panel.

V. TESTS IN AIRPLANES IN FLIGHT

The preliminary tests above described having indicated the possibility of constructing a panel sufficiently light to be used in an airplane and yet of considerable opacity to sound, arrangements for tests in actual flight were made by the courtesy of the Army Air Corps and of the Bureau of Aeronautics of the Navy.

In these flights a Western Electric audiometer, type 2–A, was used as a measuring instrument for intensity of sound. This instrument has certain limitations. The most intense airplane noises are of low pitch and rather too loud to be matched by the audiometer. In addition, the audiometer gives only notes of one frequency at a time, not a complex noise. But by making use of the masking effect of noises it was possbile to get a fair idea of the reduction factor of the different cabins tested. The agreement of several different observers on this point was good.

Tests were made in the cabin of a Fokker trimotored plane placed at our disposal by the Army Air Corps. The cabin of this plane was a framework covered on the outside with airplane fabric and on the inside with plywood. The reduction factor was about 10 sensation units.

A Ford trimotored plane, furnished by the Navy, had a cabin covered on the outside with corrugated duralumin. A thin layer of kapok in burlap covers was attached to the inside of this metal sheet. Over this kapok was a layer of some composition resembling leather in appearance. The windows were of plate glass approximately one-eighth inch thick. The reduction factor for this cabin was about 20 sensation units.

From audiometer measurements the average close-up intensity of the noise of an airplane in flight is about 95 sensation units. If a cabin could be built with a reduction factor of 35 units, the intensity of the noise within the cabin (60 units) would be about that in a railway coach in motion. Panel 40, of reduction factor 36, gave promise of furnishing this result.

Before modifying an airplane cabin in this way three model cabins were built for laboratory test, each about the actual size of the cabin of a 4-passenger Fairchild plane.

Cabin No. 1 was covered with a thickness of airplane fabric, doped and varnished as in ordinary practice. Cabin No. 2 was covered both outside and inside with 3-ply plywood, leaving an air space of 1¾ inches between the two layers. Cabin No. 3 (fig. 5) was covered on the outside with 0.02-inch duralumin, and on the inside with one-fourth inch Insulite. The space between was filled with a fibrous material known as Dry Zero blanket. This is a natural fiber which is stated to have the unusual property of having the end of each tubular fiber closed.

An additional layer of 2-inch Dry Zero blanket was placed over the Insulite, and the inside was finished by a protective coating of perforated sheet aluminum. The object of this is not materially to decrease the transmission, but to absorb such sound as may be transmitted into the cabin. It can be shown theoretically [7] that if there is no absorption in a closed space the intensity in this space after a steady state is reached is the same as the intensity outside the inclosure, no matter how good a sound insulator the walls may be.

For this reason it is advisable to line the interior of the cabin with some very absorbent material to prevent the sound that does pass through from building up to a disagreeable intensity. Any material which has a relatively high absorption at the lower frequencies will serve this purpose. Unfortunately, few materials are good absorbers at low frequencies. Taking weight into consideration, Dry Zero blanket was the best absorber that was found. It has, therefore, been used in all of these tests.

The weight, in pounds per square foot of each construction (exclusive of the wooden frame), was approximately as follows:

	Pounds
Cabin No. 1	0. 1
Cabin No. 2	1. 04
Cabin No. 3	1. 24

The cabins were then placed in the reverberation room where a comparatively loud sound of varying frequency could be produced. Audiometer tests were made at four different frequency bands. The results, expressed in sensation units, are given in Table 1.

TABLE 1.—*Reduction factor in sensation units for frequencies (cycles per second)*

Cabin	150–187	250–285	500–547	1,000–1,070	Mean
1	1	5	5	5	4
2	15	15	18	23	18
3	30	28	28	35	30

[7] See footnote 2, p. 898.

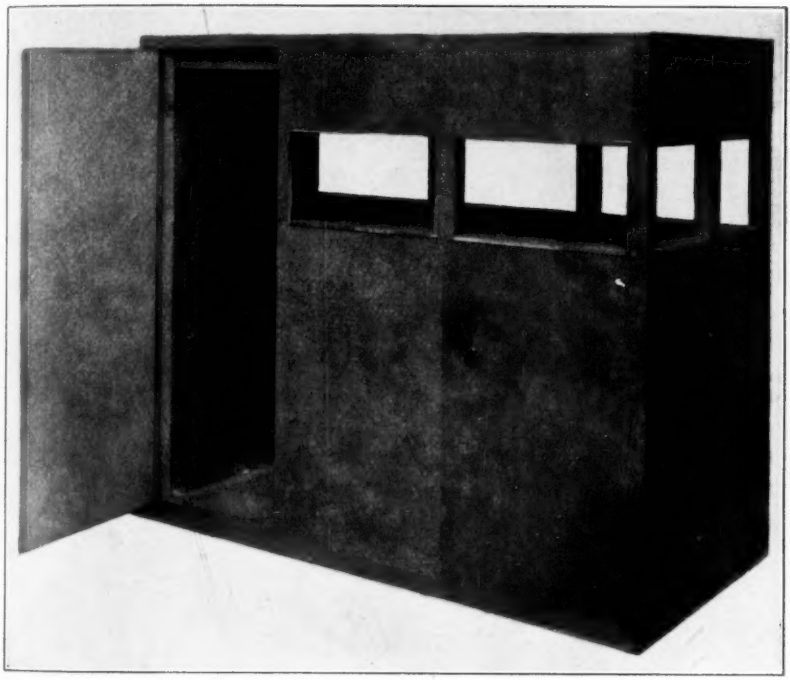

FIGURE 5.—*Experimental test cabin No. 3*

The results obtained with cabin No. 3 were regarded as sufficiently encouraging to warrant the modifying of an actual airplane cabin for experimental test. Permission was obtained from the Navy Department to make a temporary installation in the cabin of the Ford plane, in which one of the previous flight tests were made.

For purposes of comparison it was decided to divide the cabin into two parts, modifying one half and leaving the other in its original state.

The interior finish of the forward part of the cabin was removed, and a 2-inch layer of Dry Zero blanket placed next to the outer metal covering. Over this was fastened a layer of fiber board one fourth inch thick. Over the fiber board was placed another 2-inch layer of Dry Zero blanket, and the inside was finished with perforated sheet aluminum. The windows, being of rather thin glass, would have interfered with the tests, and were also covered. To give results equivalent to the rest of the structure the glass should have been one-fourth inch thick.

The measurements in flight were made by three observers. The average reduction factor of the treated portion of the cabin was 18 sensation units greater than in the unaltered part. As mentioned above, the unaltered cabin had a reduction factor of 20 units as compared with outside measurements. It thus appears that the treatment applied to the cabin gave a reduction factor of 38.

Observations were made as to the ease with which conversation could be carried on while the plane was in flight. In the unaltered part of the cabin it was necessary to raise the voice and frequently to repeat a sentence. In the treated portion one could talk in an ordinary tone and be understood by another as far away as the size of the cabin allowed, and it was seldom necessary to repeat.

It was the judgment of the observers that most of the residual noise in the cabin came through the floor, which had received no treatment. It is probable that the floor also could be protected against sound if this were done at the time the plane was built.

TABLE 2

Panel No.	Reduction factor in sensation units at frequency bands of—				Weight per square foot	Log of weight per square foot
	150–220	400–470	1,000–1,120	Average		
					Pounds	
1	24.5	25.7	26.6	25.5	1.2	0.08
2	16.1	17.3	20.3	17.9	.35	−.46
3	5.5	6.6	8.3	6.8	.075	−1.12
4	16.6	16.4	16.1	16.4	.33	−.48
5	9.6	15.8	16.9	14.1	.30	−.52
6	17.1	20.3	24.0	20.5	.63	−.20
7	21.4	23.3	25.0	23.2	.75	−.12
8	20.9	16.3	20.3	19.2	.36	−.44
9	17.5	18.7	21.8	19.3	.52	−.28
10	18.6	20.8	24.5	21.3	.73	−.14
11	1.6	1.8	2.3	1.9	.017	−1.80
12	5.3	6.7	11.2	7.7	.10	−1.00
13	24.7	27.0	32.9	27.9	1.6	.20
14	28.7	32.0	34.2	31.6	3.65	.56
15	7.4	9.5	9.5	8.8	.20	−.70
16	9.8	11.2	16.4	12.5	.33	−.48
17	14.8	16.7	22.0	17.8	.43	−.37
18	14.5	15.1	18.6	16.1	.70	−.16
19	13.2	15.5	15.0	14.6	.70	−.16
20	29.1	27.5	42.8	33.1	3.2	.505
21	19.9	18.8	26.5	21.7	1.04	.02
22	26.2	29.0	37.6	30.9	1.50	.18
23	24.0	25.8	29.7	26.5	1.50	.18
24	19.7	21.3	21.6	20.9	1.33	.12
25	19.6	21.6	20.1	20.4	1.45	.16
26	18.8	16.2	27.0	20.7	1.33	.12
27	19.3	17.4	29.2	22.0	1.45	.16
28	20.8	27.6	41.8	30.1	1.23	.09
29	26.8	23.1	39.8	29.9	2.06	.31
30	17.6	15.1	31.8	21.5	.90	−.05
31	22.5	23.2	33.7	26.5	.89	−.05
32	24.3	24.0	32.7	27.0	1.08	.03
33	26.7	25.9	37.6	30.1	.97	−.01
34	27.0	27.5	34.9	29.8	1.06	.03
35	20.3	30.9	43.9	31.7	1.31	.12
36	31.4	32.2	40.6	34.7	1.57	.20
37	29.1	26.9	39.4	31.8	1.23	.09
38	20.7	26.9	43.7	30.4	1.31	.12
39	26.0	24.5	29.4	26.6	1.20	.08
40	28.6	35.6	45.0	36.4	.97	−.01

VI. DESCRIPTION OF PANELS

Unless otherwise specified the materials were fastened to a wood frame made out of 1¾ by 1¾ inch stock. The outside dimensions of the panels were 25 by 43½ inches.

Panel No.

1. Single sheet of galvanized iron 0.03 inch thick.
2. Single sheet of aluminum 0.025 inch thick.
3. Single sheet of aluminum 0.006 inch thick.
4. Single sheet of duralumin 0.020 inch thick.
5. Single sheet of aluminum-coated duralumin.
6. Single sheet of standard Celotex building board 7/16 inch thick.
7. Single sheet of Insulite ½ inch thick.
8. Single sheet of Insulite ¼ inch thick.
9. Single sheet of plywood ⅛ inch thick.
10. Single sheet of plywood ¼ inch thick.

11. Single sheet of wrapping paper 0.006 inch thick.
12. Single sheet of airplane fabric, doped five times, varnished two times.
13. Single sheet of double-strength glass ⅛ inch thick.
14. Single sheet of plate glass ¼ inch thick.
15. Single sheet of ½ inch balsam wool, paper on both sides.
16. Single sheet of 1 inch balsam wool, paper on both sides.
17. Single sheet of Insulite 5/16 inch thick.
18. Two sheets 0.025-inch aluminum separated by ½-inch air space.
19. Two sheets 0.025-inch aluminum separated by 1¾-inch air space.
20. Two sheets double-strength glass separated by ½-inch air space.
21. Two sheets ⅛-inch plywood separated by 1¾-inch air space.
22. Two sheets ½-inch Insulite separated by 1¾-inch air space.
23. Two sheets ½-inch Insulite placed together.
24. Single sheet 0.025-inch aluminum, one sheet 7/16-inch Celotex, second sheet aluminum.
25. Single sheet 0.025-inch aluminum, one sheet ½-inch Insulite, second sheet aluminum.
26. Single sheet 0.025-inch aluminum, ⅝-inch air space, one sheet 7/16-inch Celotex, ⅝-inch air space, second sheet aluminum.
27. Single sheet 0.025-inch aluminum, ⅝-inch air space, one sheet ½-inch Insulite, ⅝-inch air space, second sheet aluminum.
28. Single sheet aluminum, ½-inch layer balsam wool covered on both sides with paper, 1-inch layer balsam wool covered on both sides with paper, second sheet aluminum.
29. Single sheet 0.025-inch aluminum, 2 layers 1-inch hair felt, second sheet aluminum.
30. Single sheet 0.025-inch aluminum, ½-inch layer balsam wool covered on both sides with paper, second sheet aluminum.
31. Single sheet 0.025-inch aluminum, one layer 2-inch Dry Zero blanket, second sheet aluminum.
32. Single sheet 0.025-inch aluminum, 2 layers 2-inch Dry Zero blanket, second sheet aluminum.
33. Single sheet 0.025-inch aluminum, one layer 2-inch Dry Zero blanket, one sheet 5/16-inch Insulite.
34. Single sheet 0.025-inch aluminum, one layer 2-inch Dry Zero blanket, one sheet ⅛-inch plywood.
35. Single sheet 0.025-inch aluminum, ½-inch layer balsam wool covered on both sides with paper, 1-inch layer balsam wool covered on both sides with paper, 5/16-inch sheet Insulite.
36. Single sheet ⅛-inch plywood, ½-inch layer balsam wool covered on both sides with paper, 1-inch layer balsam wool covered on both sides with paper, ⅛-inch sheet plywood.
37. Single sheet ⅛-inch plywood, one layer 2-inch Dry Zero blanket, second sheet ⅛-inch plywood.
38. Single sheet 0.025-inch aluminum, ½-inch layer balsam wool with paper on both sides, single sheet 0.006-inch aluminum, 1-inch layer balsam wool with paper on both sides, sheet of 0.025-inch aluminum.
39. Single sheet 0.025-inch aluminum, four layers cotton approximately ½ inch thick separated by sheets of wrapping paper, second sheet of aluminum.
40. This was a large panel 70 by 84 inches made of 1¾ by 1¾ inch stock. There were crosspieces running the shorter way approximately 16 inches apart. Sheets of aluminum 0.025 inch thick were fastened on one side of this frame. Two-inch Dry Zero blanket was cut up and placed in the spaces between the framework. The opposite side was covered with sheets of 5/16-inch Insulite.

VII. CONCLUSIONS

Though airplane noises are intense and there is a limit to the additional weight that a plane may carry, it has been found that by a comparatively moderate increase in weight the sound intensity in an airplane cabin can be reduced to a degree where conversation can easily be maintained.

It should also be noted that the structure used was found to be an excellent heat insulator, and should make the cabin comfortable from the standpoint of temperature in even the coldest weather or at high altitudes.

Sound insulation installed during the construction of the plane, with care as to details, should give even better results than those obtained in the experiments described.

WASHINGTON, January 22, 1929.

PRISM REFRACTOMETRY AND CERTAIN GONIOMETRICAL REQUIREMENTS FOR PRECISION

By L. W. Tilton

ABSTRACT

A surprisingly small gain in the accuracy of absolute measurements of index of refraction has been made since the experiments of Fraunhofer. The classical method of minimum deviation is fundamentally important and for solid or liquid media the most sensitive of absolute methods.

To obtain an accuracy of ± 1 unit in the sixth decimal place of index by this method, angles must be measured to fractions of a second and it would seem imperative to use a fully calibrated circle. Frequently, however, correction curves are based on comparatively few of the numerous graduations on a circle and relate only to the periodic errors of low frequency. In such cases it is still necessary, therefore, to resort to repetition on various parts of the circle in order to eliminate accidental errors and those of high frequency. On the other hand, with four or more equidistant microscopes and the proper advancing of the circle between observations, both accidental and periodic errors may be eliminated simultaneously and it becomes possible, even on uncalibrated circles of fairly high grade, to attain an accuracy approaching the order required.

Important steps in using any circle are (1) the slight displacements of the microscopes from their equidistant locations in such manner that the average readings are free from periodic errors of the degree subdivisions, and (2) frequent determinations of the error of the "runs" of the micrometers under the exact conditions of use. By these means the special error-free use of an uncalibrated circle is satisfactorily extended, so that it covers not merely a few cases of little more than theoretical interest but also many of the most important angle measurements required in minimum-deviation refractometry.

To minimize the effects of torsional strains in the male and female members of a conical bearing it is advisable to adhere strictly to uniform manipulative procedures in carefully planned observational programs.

CONTENTS

		Page
I.	Introduction	910
II.	Critical review of sixth decimal prism refractometry	912
III.	Concerning methods	916
IV.	Tolerances in angular measurements	920
V.	Use of multiple microscopes in minimizing circle errors	924
	1. Special use of an uncalibrated circle	924
	2. Elimination of degree-subdivision errors	927
VI.	Micrometer errors	928
VII.	Nonconstant residual mechanical strains in the instrument	929

I. INTRODUCTION

Recent progress relating to the effects of heat history on the optical properties of glass [1] has resulted in the application of heat treatment to effect the removal of certain heterogeneities in glass.[2] Consequently, it now seems that optical-glass manufacturers can, by the elimination of temperature gradients in annealing furnaces, secure a greater degree of homogeneity within each melt than was formerly thought possible. Furthermore, an adequate control of annealing temperatures, together with the use of "annealing equilibrium coefficients of index of refraction," may even reduce appreciably the range of variation in the optical quality of annealed glass from melt to melt of the same type. Every advance in the uniformity of the properties of optical glass is of great importance because it furthers standardization in the manufacture of optical systems, and complete standardization is one of the chief requirements for American leadership in any industry.

Increased uniformity of refractive media results at once in a demand for more numerous and more accurate determinations of the index of refraction and of the partial dispersions than have been warranted in the past. Even at the present time optical-glass catalogues are customarily issued with indices to five decimals, and at least one firm makes some use of the sixth for some of the partial dispersions. Consequently, it is evident that a careful consideration of the conditions necessary for accuracy in the measurement of indices to six places of decimals is important.

This survey of requirements was in fact occasioned by the necessity of developing improved equipment for measurements on transparent media submitted to this bureau by commercial organizations which have already experienced the need of increased accuracy in index measurements. Such measurements were also required in providing adequate standards of index for the testing of commercial refractometers, some of which are now made to permit readings to the fifth decimal place and are used [3] in chemical analysis and in other work, both scientific and technical.

Before proceeding with the design of new or improved auxiliary apparatus, it seems desirable to investigate all the requirements for sixth decimal place accuracy in prism refractometry. Obviously, it is useless to proceed far toward satisfying any one requirement without giving consideration to all, and such a review must be made with

[1] A. Q. Tool, L. W. Tilton, and E. E. Hill, Meeting Opt. Soc. Am., Ithaca, N. Y., 1925; Abstract in J. Opt. Soc. Am. and Rev. Sci. Inst., **12**, pp. 490–491; 1926.

[2] L. W. Tilton, A. N. Finn, and A. Q. Tool, B. S. Sci. Papers (No. 572), **22**, pp. 719–736; 1927–28. See also J. Amer. Ceramic Soc., **2**, pp. 292–295; 1928.

[3] See, for example, D. A. Coleman and H. C. Fellows, United States Department of Agriculture Bulletin No. 1471, pp. 25–26; March, 1927; C. F. Hottes and W. A. Huelsen, Science, **65**, p. 576; 1927; Frank Urban and V. W. Meloche, J. Am. Chem. Soc., **50**, pp. 3003–3009; 1928.

sufficient detail and comprehensiveness to serve as a basis for the efficient direction of the effort to be expended in seeking higher accuracy.

An examination of the literature discloses comparatively few measurements of indices of solids for which any precision in the sixth decimal has been claimed, and, indeed, doubt has been expressed [4] concerning the extent to which all of the difficulties have been overcome in any one set of measurements. In view of this uncertainty, and also on account of the paucity of recent attempts at accurate refractometry with the spectrometer, it has been thought desirable to present, somewhat in detail, the course followed in this investigation.

The requirements which need discussion may be classified as pertaining to either (1) goniometry or (2) the knowledge and control of the conditions which affect the velocity of light in various media. The present paper, being introductory in character, deals only with a portion of the first of these categories, and it refers particularly to minimum-deviation spectrometry of the visible spectrum because the experimental work in progress in this refractometric laboratory is limited chiefly to that field.

The notation used is explained in the text, but for further convenience of reference the definitions of the various characters are summarized here as follows:

$A \equiv$ the refracting angle of a prism;

$A_a \equiv$ the refracting angle of a prism for use in the autocollimating method;

$a \equiv$ the temperature coefficient of relative index per 1° C.;

$\alpha \equiv$ the angular displacement of one microscope from its customary position diametrically opposite a second miscroscope;

$D \equiv$ the angle of minimum deviation produced by a prism;

$D_a \equiv$ the (essentially positive) angle of deviation of incident or emergent light at the refracting face of a prism when using the autocollimating method;

$d \equiv$ the number of subdivisions per degree of arc on a spectrometer circle;

$E \equiv$ the angle of refraction at the emergent face of a prism;

$e \equiv$ the angular eccentricity of a spectrometer circle;

$F \equiv$ the angle between emergent rays in the Féry-Martens autocollimating method and in the grazing incidence method;

$m \equiv$ the number of angularly equidistant microscopes for use in making readings on a spectrometer circle;

$N \equiv$ the number of degree subdivision scale graduations in one complete high-frequency error period;

[4] L. C. Martin, Opt. Measuring Instruments, p. 129 (London); 1924.

$n \equiv$ the relative index of refraction of a medium;
$n_o \equiv$ the relative index of refraction of a medium at 0° C.;
$n_D \equiv$ the relative index of refraction of a medium for sodium light, wave length, 5,893 A;
$r \equiv$ the number of repetitions of a given angular measurement in an observational program;
$T_A \equiv$ the tolerance, in measuring refractive angle, which corresponds to an error of $\pm 1 \times 10^{-6}$ in the measurement of refractive index;
$T_{2D} \equiv$ the tolerance, in measuring (double) deviation, which corresponds to an error of $\pm 1 \times 10^{-6}$ in the measurement of refractive index;
$t \equiv$ the temperature in degrees C.;
$x \equiv$ the minimum number of complete traverses on a circle or on its equivalent "perfect arc" which permit the elimination of scale-graduation errors in the measurement of a given angle by a method of repetitions.

II. CRITICAL REVIEW OF SIXTH DECIMAL PRISM REFRACTOMETRY

Fraunhofer [5] measured and published indices of refraction to the sixth decimal place, and a precision in index to this degree has figured prominently in several investigations [6] concerning objectives made from his glasses. The original index tables by Dutirou [7] also contained six decimals, and some indices of Merz [8] glasses have been published to the same order of precision. Aside from questions of instrumental and manipulative errors, however, the general inadequate reference to working conditions [9] makes it unlikely that even the fifth decimal place is accurate in any of this early work. An inspection of Fraunhofer's indices for the flint melt No. 23 (n_D = 1.633666), for which results were obtained with prisms of 60° and 45°, confirms this view. Comparing values for the solar lines B, C, D, E, F, G, and H, the differences in the indices of these prisms in units of the sixth decimal place are +32, +18, +1, −49, −24, −1, and +6, respectively. Although this series shows the presence of a large systematic error in the fifth decimal, it suggests, nevertheless, a

[5] Joseph von Fraunhofer, Denkschriften d. K. Akad. Wissenschaften zu München, **5**, pp. 193-226; 1817; also Joseph von Fraunhofer's Gesammelte Schriften, p. 30 (München); 1888.

[6] For references, see S. Czapski u. O. Eppenstein, Grundzüge der Theorie der Optischen Instrumente, p. 565 (Leipzig); 1924.

[7] L'abbé Dutirou, Annales de Chimie et de Physique (3), **28**, pp. 176-210; 1850, measured 18 glasses for each of 7 Fraunhofer lines, but the corrected values for the indices, pp. 501-502 of the same volume, are in every case reduced to five decimal places.

[8] Sigmund Merz, Zeitschrift f. Instrumentenkunde, **2**, pp. 176-180; 1882.

[9] Dutirou records temperatures for all data, and Fraunhofer does also for some observations, but air pressures are lacking in all cases.

remarkably high degree of precision for measurements made over 100 years ago.

Two noteworthy series of measurements of this kind, published half a century ago, seem quite worthy of serious consideration as examples of accurate spectrometry. The first, by Hastings,[10] gives relative indices and temperature coefficients of five glasses for 10 or 11 wave lengths in the visible spectrum, the data being given for a temperature of 20° C. and an air pressure of 30 inches of mercury. The measurements were made by the method of minimum deviation, using a spectrometer with a circle of known periodic errors and provided with two microscopes reading directly to two seconds of arc. This work was very favorably mentioned by Müller[11] who a few years later was publishing his own more extensive results of the same character, the second of the two noteworthy series above mentioned. Müller gives full observational data on five glasses for from 7 to 12 wave lengths at room temperatures ranging from −6 to +28° C. Two spectrometers were employed, the microscopes reading directly to 5 seconds on one and to 2 seconds on the other, and correction formulas were used for the periodic errors of scale and screws. The results were corrected to a standard air pressure of 760 mm, and the indices, n_o for 0° C., together with temperature coefficients, a, were determined for each wave length by least squares solutions of the equations, $n = n_o + at$. The probable errors of the results so adjusted were confined to the sixth decimal place, excepting for one line at the extreme violet end of the visible spectrum. The majority of the individual observations depart from the computed values by less than one unit of the fifth decimal place. Some confirmation of the precision of this work is also to be found in the highly satisfactory results which Hartmann[12] obtained when using these indices in a test of his dispersion formula.

The importance of air-pressure corrections is amply demonstrated by Hastings and by Müller in these precise measurements, but it seems to have escaped the notice of some later workers in this and related fields. Several years later the older measurements by Hopkinson[13] were mentioned by Taylor[14] as being perhaps the most accurate and reliable determinations of index of glass. Yet the results referred to, although given to six decimals, were obtained on a spectrometer with verniers reading to 10 seconds, and no mention was made of pressure or even of temperature. In the sixth decimal place data by Dufet[15] no pressures are given, and the last place is admittedly

[10] C. S. Hastings, Am. J. Sci., **15**, pp. 269–275; 1878.
[11] G. Müller, Publicationen des Astrophysikalischen Observatoriums zu Potsdam, **4**, pp. 149–216; 1885.
[12] J. Hartmann, Publicationen des Astrophysikalischen Observatoriums zu Potsdam, **12**, appendix, pp. 1–16; 1902.
[13] J. Hopkinson, Proc. Royal Soc., London, **26**, pp. 290–297; 1877.
[14] H. Dennis Taylor, Monthly Notices, Royal Astron. Soc., **54**, p. 69; 1893.
[15] H. Dufet, J. de Physique (3), **1**, pp. 163–177; 1892.

of little value. Conroy [16] worked on the index of water to six decimals but recorded no pressures, and since he worked at temperatures different from those of the room there is, furthermore, some question as to the temperature of the reference medium. Paschen [17] also, in connection with dispersion investigations on rock salt, sylvite, and fluorite, has published relative indices to the sixth decimal without an accompanying statement concerning air pressures.

Gifford's early work [18] on 27 glasses, for which sixth decimal indices were published for many wave lengths, including 13 in the visible region, is often referred to and used for purposes requiring exact values for the dispersion of glasses. But, aside from the lack of pressure observations, only one microscope was used on the circle. Furthermore, an unsymmetrical use of apertures may have resulted from the practice of translating the prism to vary the intensity of the slit image specularly reflected from the polished third side of the prism. Any one of these three factors could have caused errors affecting the fifth decimal place.

Pressure effects have received attention more recently in England. Gifford,[19] publishing indices for seven additional glasses, mentions an attempt to measure the effect; Guild [20] wrote a note on the subject; and Gifford [21] then published, for seven more glasses, indices corrected to standard conditions of 15° C. and 760 mm pressure. These last data by Gifford, and those previously given by Hastings and by Müller, and to which reference has already been made, constitute practically [22] all the published indices of optical glass for which both temperature and pressure conditions are precisely stated. The list may be extended to cover all goniometrically determined indices of solid media, it is thought, by the addition of references to Hastings'[23] indices of iceland spar to six decimal places, to the seventh place indices of quartz by Macé de Lépinay,[24] to Langley's [25] bolometrically determined indices of rock salt and of fluorite, to the sixth decimal place measurements on fluorite and on quartz made at the Reichsanstalt by Schönrock,[26] and also to the latter's seventh [27] decimal work

[16] Sir John Conroy, Proc. Royal Soc., London, **58,** pp. 228–234; 1895.

[17] F. Paschen, Annalen d. Physik, **26,** pp. 127, 134; 1908; **41,** pp. 670–672; 1913.

[18] J. W. Gifford, Proc. Royal Soc., London, **87,** pp. 189–193; 1912.

[19] J. W. Gifford, Proc. Royal Soc., London, **91,** pp. 319–321; 1915.

[20] J. Guild, Trans. Opt. Soc., London, **22,** pp. 153–155; 1920. See also Proc. Phys. Soc., London, **36,** p. 188; 1918.

[21] J. W. Gifford, Proc. Royal Soc., London, **100,** pp. 621–626; 1921–22.

[22] Some index data, measured by the writer, have been published, chiefly in a paper by L. W. Tilton, A. N. Finn, and A. Q. Tool, loc. cit.

[23] Charles S. Hastings, Am. J. Sci., **35,** pp. 60–73; 1888.

[24] J. Macé de Lépinay, Annales de Chimie et de Physique, (7), **5,** pp. 216–231; 1895; (7), **11,** pp. 112–116; 1897.

[25] S. P. Langley, Annals of the Astrophys. Observatory of the Smithsonian Institution, **1,** pp. 219–237; 1900.

[26] O. Schönrock, Zeitschrift f. Instrumentenkunde, **30,** pp. 185–186; 1910; **33,** p. 161; 1913; **34,** pp. 191–192; 1914.

[27] O. Schönrock, Zeitschrift f. Instrumentenkunde, **40,** pp. 93–96; 1920; **41,** pp. 103–105; 1921; **48,** pp. 275–276; 1928.

on the same materials at specified temperature, pressure, and humidity. It may be added that absolute indices of quartz for definite temperatures have been determined interferometrically by Macé de Lépinay and Buisson [28] to the seventh decimal place and also by Pérard [29] to the seventh and eighth places.

With reference to decimal places beyond the sixth, it should be mentioned that Macé de Lépinay's seventh place results, obtained by the use of a spectrometer, seemed precise to about one unit of the sixth but were later adjudged [30] too low in absolute value by five or more such units when compared with the interferometric measurements just referred to as made by Macé de Lépinay and Buisson. The opinion that the limits of accuracy in prism refractometry are reached at something scarcely to be called certainty in the fifth decimal place seems somewhat disturbing, especially if, as reported, it was held by one with Macé de Lépinay's experience. The explanation that this discrepancy between the results from the two methods is due to the extreme difficulty in obtaining accurate collimation with the spectrometer, appears untenable to the writer in view of the liberal tolerances which are permissible in collimation when making measurements of minimum deviation.[31] It is, in fact, considered as probable that the real cause was an unsuspected but avoidable systematic error in deviation measurements which, for example, could have occurred to approximately the extent in question through a variation in certain mechanical strains such as those mentioned in Section VII of this paper.

At and near the center of the visible spectrum, Schönrock's seventh decimal indices of flourite and quartz prisms, when compared with the computed values by the adjusted dispersion formulas, seem almost consistent to the nearest sixth decimal place. An intercomparison of Pérard's interferometrically obtained values for the 10 and 20 mm quartz end standards reveals inconsistencies in the sixth decimal, but the indices for the 50 and 100 mm standards seem consistent to within a few units of the seventh decimal. Only Schönrock and Pérard seem to have taken account of water vapor in the air, the variations in which, if neglected, completely vitiate the seventh decimal place of index and may affect the sixth place slightly. Pérard mentions the lack of carbon dioxide determinations which, in laboratory air, are quite important in the eighth place.

---

[28] J. Macé de Lépinay and H. Buisson, Annales de Chimie et de Physique, (8), **2**, pp. 78–108; 1904.

[29] Albert Pérard, J. de Physique (6) **3**, pp. 252–260; 1922; (6), **8**, pp. 344–352; 1927.

[30] J. Macé de Lépinay and H, Buisson, loc. cit., p. 108. See also Traveau et Memoirs, Bureau International des Poids et Mesures, 10 (Determination du Volume du Kilogramme d'Eau, Lépinay et al), pp. 9–10; 1910.

[31] Defective prism-angle measurement is practically eliminated as a contributory source of error in Macé de Lépinay's indices, because he averaged results involving adjusted values for all three refractive angles. The subject of collimation receives quantitative treatment in a forthcoming paper relating to prism quality and adjustment.

III. CONCERNING METHODS

The prism methods of measuring indices of refraction are the oldest and are fundamentally important. The interferometric methods are commonly used when dealing with gases, but they require in practice, for work on solids and liquids, previously determined index values of fairly high accuracy to permit a determination of the order of interference by the method of coincidences. Pérard, for his initial data, made use of the published indices of quartz to which he fitted a dispersion formula; and Peters,[32] using an interferometric method in measuring the index of glass at high temperatures, required preliminary spectrometric values of index correct within two units of the fourth decimal place, and of dispersion correct within two units of the fifth decimal place. Furthermore, these interferometric methods require two or more complete determinations on samples of progressively increasing thickness, to reach an accuracy of one unit of the sixth decimal place, and these successive samples must be constant in index to a degree not always found in the case of glass. Consequently, it is obviously desirable to increase the accuracy of spectrometer measurements of index and limit the use of the interferometer in such work to those cases where the use of the former instrument is unsuitable or inadequate. Improved quality in index determinations by the spectrometer is also of importance in lessening the labor involved in the application of interferometry to such special cases.

Guild [33] names, as the two methods of major importance in the precise refractometry of prisms, the classical minimum-deviation method of Newton-Fraunhofer and the grazing incidence (critical angle) method of Euler-Kohlrausch. He shows, in general, that the former possesses advantages in sensitivity. Relative ease of computation also favors the classical method, according to which the index, n, is given in terms of refracting angle, A, and angle of minimum deviation, D, by the formula

$$n = \frac{\sin \frac{A+D}{2}}{\sin A/2} \tag{1}$$

of Newton, as compared with the second method, for which there is the corresponding expression

$$n^2 = 1 + \left(\frac{\cos A - \sin E}{\sin A}\right)^2 \tag{2}$$

of Kohlrausch, where E is the angle made by the emergent ray with reference to the face normal, positive if toward the refracting edge

[32] C. G. Peters, B. S. Sci. Papers (No. 521), **20**, p. 640; 1926.

[33] J. Guild, Proc., Phys. Soc., London, **33**, p. 186; 1921; or Nat. Phys. Laboratory, Collected Researches, **17**, p. 9; 1922.

of the prism. Moreover, the character of the settings in minimum-deviation measurements compares favorably with the asymmetrical conditions necessary in critical-angle refractometry. Thus it is, perhaps, somewhat significant that all of the above-mentioned attempts at precise prism refractometry were carried out by the Newton-Fraunhofer method.

It should be mentioned, however, that for media in the form of prisms having low values for their refracting angles (less than approximately 65° at index 1.3 and 30° at 1.9), the tolerances in deviation measurements by the grazing incidence method are actually larger than those for the minimum deviation method. Furthermore, if one determines the (positive) angle, F, between the emergent rays from both faces of a refracting angle, the $-\sin E$ of equation (2) may be replaced by $+\cos\left(\frac{F-A}{2}\right)$ and then, by taking the partial derivative of n with respect to A for each form of the equation in turn, it is found that the tolerances in measuring refractive angle are not as unfavorable in this "double" variation of the grazing incidence method as in the above-mentioned case discussed by Guild.

In commercial refractometry, the methods of predominant importance are those of measuring a sample in contact with a medium of known higher index. A special case was used by Wollaston, but the names of Abbe and of Pulfrich are more often associated with some of the important variations. These methods offer interesting possibilities of obtaining great sensitiveness on special instruments of carefully determined constants, as is shown by discussions such as those of Guild,[34] Simeon,[35] Smith,[36] and Schultz,[37] but they do not lead to absolute or fundamental measurements and so have no place in the present discussion.

Variations of Abbe's autocollimating method of prism refractometry are finding some favor for precise work and his method should be compared with that of minimum deviation. The index is obtained by the equation

$$n=\frac{\sin E}{\sin A_a} \tag{3}$$

of Descartes, where E, although observed directly, may be expressed as A_a+D_a, the subscript, a, referring to the autocollimating method as distinguished from that of minimum deviation, and the refractional deviation, D_a, being considered in this case as an essentially positive angle equal in absolute value to the change in direction of the

[34] J. Guild, Proc., Phys. Soc., London, **30,** pp. 157–189; 1918; or Nat. Phys. Laboratory, Collected Researches, **14,** pp. 273–296; 1920.

[35] Frederick Simeon, Proc., Phys. Soc., London, **30,** pp. 190–203; 1918.

[36] T. Smith, Nat. Phys. Laboratory, Collected Researches, **14,** pp. 297–300; 1920.

[37] H. Schultz, Zeitschrift f. Technische Physik. **3,** pp. 90–93; 1922; Zeitschrift f. Instrumentenkunde, **48,** pp. 26–30; 1928.

incident or emergent light at the refracting face of the prism. For any prism of $A_a°$ which can be used in Abbe's method it is possible to use one of the same medium having an angle $A=2A_a°$ in the method of Fraunhofer, and it is customary to use in the autocollimating method a prism of 30° with one face silvered. When the incident and emergent rays coincide in Abbe's method, the conditions which exist are then very closely related to those which obtain for the minimum-deviation setting of a 60° prism in the classical method. In fact, a comparison, assuming $A=2A_a$, shows that $E=A/2+D/2$.

Abbe's method automatically eliminates error due to prism table orientation. It offers those advantages in design relating to compactness of instrument and to a lightness of weight of all moving parts, the latter being particularly desirable since it reduces torsional and other mechanical errors. (See Sec. VII.) At the same time a telescope of large aperture may be used without resorting to an unfavorable aperture ratio. Furthermore, the use of a tangent screw for differential measurements renders such a spectrometer especially efficient for temperature coefficient and dispersion determinations.[33] This type of instrument also has certain very important merits in connection with a solution of the problems of temperature control; and, finally, the simplicity of the computations and the smallness of the required sample may be mentioned.

With respect to permissible errors in angular measurements, however, the Abbe method is decidedly inferior to that of minimum deviation, as is shown by taking the partial derivatives of n, as defined by equations (1) and (3), with respect to A, D, A_a, and E. This procedure with equation (1) yields equations (4) and (5) of the following group; and, similarly, the respectively corresponding expressions (6) and (7) are obtained from equation (3).

$$\frac{\partial n}{\partial A}=-\frac{\sin D/2}{2\sin^2 A/2} \tag{4}$$

$$\frac{\partial n}{\partial D}=+\frac{n}{2\tan\frac{(A+D)}{2}} \tag{5}$$

$$\frac{\partial n}{\partial A_a}=-\frac{\sin E\cos A_a}{\sin^2 A_a} \tag{6}$$

$$\frac{\partial n}{\partial E}=+\frac{n}{\tan E} \tag{7}$$

Thus the tolerances in the measurement of refracting angles are $2\sin E\cos A_a\operatorname{cosec} D/2$ times as great in the minimum-deviation method as in that of autocollimation.

[33] This appears to have been first pointed out by C. A. von Steinheil (Sitzungsberichte d. Münchener Akademie, **I**, pp. 47-51; 1863). For an example of its extensive use, see C. Pulfrich, Annalen d. Physik, **45**, pp. 613-619; 1892.

The value of this ratio varies widely for various indices and refracting angles but always equals or exceeds 2, a limit which corresponds to the condition of grazing incidence and emergence. When A is selected from the series of its most favorable values (see line $A=2$ arc tan n^{-1} in fig. 1) this ratio in favor of the minimum-deviation method is $2n^2/(n^2-1)$, which for indices of 1.3, 1.5, 1.7, and 1.9 yields numerical values of 4.9, 3.6, 3.1, and 2.8, respectively.

Similarly, a comparison of equations (5) and (7) shows that a constant ratio of 2 exists between the tolerances for determinations of D and E. Moreover, since in making the observations for D it is customary to eliminate the direct or zero reading and measure $2D$ by observing the angle between right and left hand deviations, the sensitivity of the classical method as practiced is in this particular four times that of Abbe.[39] This serious handicap is in part offset by the increased sensitivity afforded by the autocollimating spectrometer in effecting coincidence of slit image and fiducial reference mark, the angular error of pointing as read on the circle corresponding in this case to only one-half the apparent error in the field of view.

Of the considerations which have been mentioned as relating to methods of prism refractometry, those of sensitivity and temperature control are the most important. The former has usually received more attention because the errors of circle division are frequently viewed as the limiting factors in index measurement; consequently, the minimum-deviation method has usually been chosen whenever the temperature-control problem can be satisfactorily handled.

A constant-temperature room is the solution often adopted for temperature control, but it is very inadequate for work on liquids and seldom provides for work over a desirable range of temperature. Nevertheless, this plan provides uniformity of working conditions for the whole apparatus, it does not complicate the problems of instrument design, and it offers no interference with the usual procedure of operation. A satisfactory constant-temperature prism chamber or housing offers, on the other hand, a solution of the temperature-control problem which contrasts sharply with that of the constant-temperature

[39] Nonsilvering, or half silvering, of the 30° faces of the Abbe prism permits the use of the Féry-Martens autocollimating method (C. Féry, Compt. Rend., **119**, pp. 402-404; 1894; F. F. Martens, Verh. d. Deutschen Phys. Gesellschaft, **3**, p. 14; 1901) in which one measures A_a and the supplement, F, of $(2E-A_a)$, so that the equation for the index should be written as $n=\dfrac{\cos\left(\frac{F-A_a}{2}\right)}{\sin A_a}$. Under these conditions the partial derivatives are found to be $\dfrac{\partial n}{\partial A_a}=-\dfrac{\sin D_a+\sin E\cos A_a}{2\sin^2 A_a}$, and $\dfrac{\partial n}{\partial F}=-\dfrac{n}{2\tan E}$; and when compared with equations (4) and (5) the resulting tolerance ratios in favor of the minimum-deviation method are not so large as those given above. For refracting angles the value in this case is $(1+\sin E\cos A_a \operatorname{cosec} D/2)$. Although, like the previous similar expression, this always equals or exceeds 2, it reduces to $(2n^2-1)/(n^2-1)$ with optimum values of A, and thus gives for indices of 1.3, 1.5, 1.7, and 1.9 the ratio values 3.4, 2.8, 2.5, and 2.4, respectively. In deviation measurements the advantages of this variation of the autocollimating method are more marked and the ratio of tolerances in measuring $2D$ to those in determining F is only 2 instead of the ratio of 4 which exists between the maximum permissible errors in $2D$ and the similar errors in E. But the loss of intensity is a serious matter for many of the spectral lines which it is desirable to use.

room when both of these proposals are compared along all the lines just mentioned. It is, therefore, evident that the best program should include both housing and room control.

A temperature-control housing for a minimum-deviation spectrometer must provide two windows, adjustable through wide limits in azimuth, with respect to the prism table and to each other. Furthermore, suitable jacketing means considerable weight to be sustained by the prism table, since the housing must rotate with the prism. Because of these and other difficulties, few minimum-deviation housings have been attempted. On the other hand, for Abbe's autocollimating method, satisfactory housings are relatively simple. They require but one window, and it is fixed with respect to the housing; their weight is sustained by supports which are entirely independent of the instrument; and their construction has been standardized for commercial production.[40] Furthermore, within a housing of this kind, a mirror suitably mounted with respect to the prism table[41] may take the place of a collimator and enable the autocollimating spectrometer to perform to a certain extent like an instrument of the more usual, or minimum-deviation, type.

For all index work with bright line sources, the mirror arrangement mentioned seems to combine in a favorable way the full sensitivity of the Fraunhofer method with many of the advantages of that of Abbe. This applies particularly to deviation measurements where, as compared with the classical method, the precision of pointings is doubled and the error corresponding to that of prism table orientation is halved. Accordingly, these considerations give a clear indication of one course to be followed whenever the construction of an entirely new spectrometer for precise work is contemplated. The instrument at hand in this laboratory was, however, of the minimum-deviation type, and certain exigencies required a more immediate solution which, if possible, should include provision for an adequate temperature-control housing sufficiently flexible in use to handle at minimum deviation the wide range of samples on which index measurements are required at this bureau.

IV. TOLERANCES IN ANGULAR MEASUREMENTS

Strictly speaking, accurate sixth decimal place indices are obtained only when the errors are confined to less than five units of the seventh place; but in this and in certain subsequent papers treating of the

[40] Zeitschrift f. Instrumentenkunde, **9**, p. 362; 1889.

[41] This is one of the valuable suggestions concerning autocollimation which were made by C. A. von Steinheil (loc. cit.) soon after J. Duboscq had built a half-prism spectroscope (using a 30° prism silvered on one side) and O. von Littrow (Sitzungsberichte d. Wiener Akademie, **47**, pp. 26–32; 1863) had independently applied the principle of autocollimation to his multiple prism spectroscope. A mirror device of this kind is used on the Goerz autocollimating spectrometer as designed by F. Weidert. The feature receives detailed mention in a description of this instrument in a circular privately issued by the C. P. Goerz Co.

requirements for accuracy in measuring refractive indices the tolerance, T, to be considered in referring to any measurement will be that corresponding to an error of plus or minus one unit of the sixth decimal place of index.

From equations (4) and (5) the tolerances in the goniometric measurements for minimum-deviation prism refractometry may be written as

$$T_A = \pm 0.4125 \frac{\sin^2 A/2}{\sin D/2} \text{ seconds,} \tag{8}$$

and

$$T_{2D} = \pm 0.8251 \frac{\tan \frac{A+D}{2}}{n} \text{ seconds.} \tag{9}$$

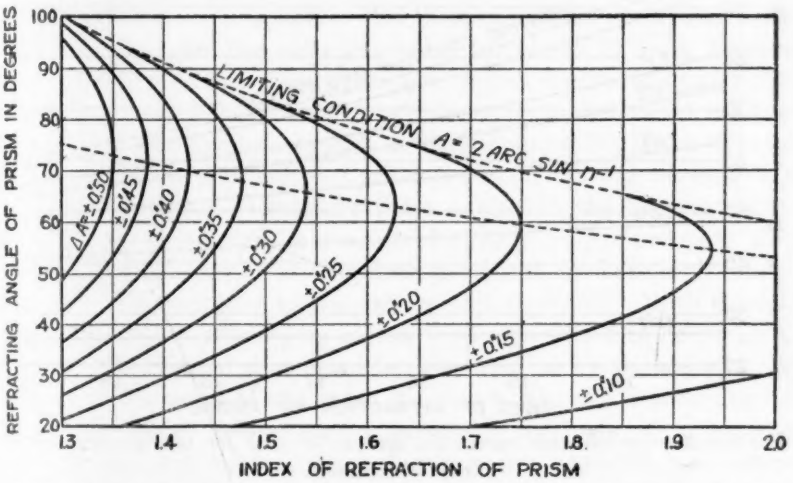

FIGURE 1.—*Iso-tolerance curves (in seconds of arc) for the measurement of prism angle*

For an accuracy of $\pm 1 \times 10^{-6}$ in a determination of refractive index by the method of minimum deviation, it is necessary that the refracting angle of a prism be measured within the limits of error, ΔA, which are expressed by these curves. Values of the most favorable prism angle, $A = 2$ arc tan n^{-1}, for work on media of a given index, are indicated by the undesignated dotted line. The latter shows not only the general merit of using 60° prisms, but also under what conditions it is advisable to depart from that usual value for the refracting angle.

From equations (8) and (9) curves have been computed which are very useful in choosing favorable working conditions for certain specific problems and, also, in making small corrections to previously computed data. These curves have been reproduced in Figures 1 and 2 for reference and for showing at a glance the wide variation in the values of the tolerances T_A and T_{2D}, respectively, for the various combinations of A and n which it may be necessary or desirable to use.

Concerning the choice of A in particular instances, it may be readily shown that the value of the refracting angle for the limiting

condition of grazing incidence and emergence in minimum-deviation refractometry is $A=2$ arc sin n^{-1}, and from equation (1) it follows that the corresponding limit of deviation is $D=2$ arc cos n^{-1}. Moreover, by taking partial derivatives with respect to A of the tolerance T_A, expressed in terms of A and n, the condition for most favorable tolerance in prism-angle measurement is found to be $A=2$ arc tan n^{-1}. Corresponding to this condition, the deviation is expressible as $D=2$ arc cos $2n(n^2+1)^{-1}$. This special value of A reduces equation (9) to $T_{2D}=\pm 0.825$ seconds, showing that for all media a given error in deviation measurement corresponds to the same unit error in index provided the prism angle has this specified optimum value.

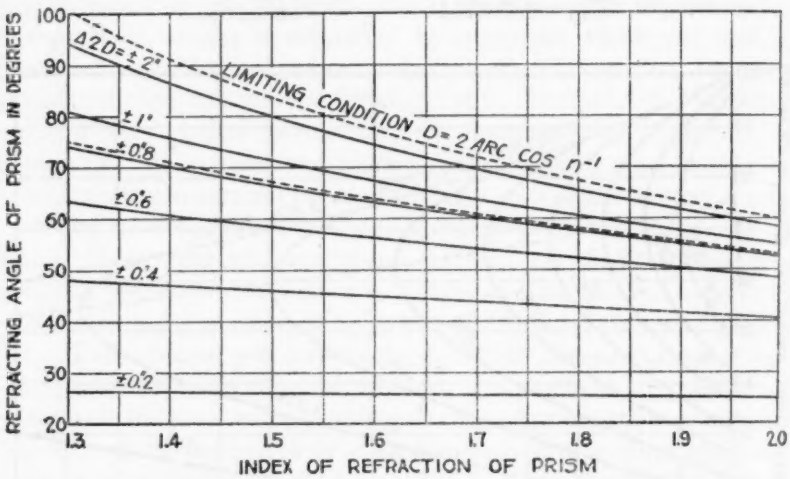

FIGURE 2.—*Iso-tolerance curves (in seconds of arc) for the measurement of double deviation*

For an accuracy of $\pm 1\times 10^{-6}$ in a determination of refractive index by the method of minimum deviation, it is necessary that the angle of double deviation be measured within the limits of error, $\Delta 2D$, which are expressed by these curves. The line of limiting condition, $D=2$ arc cos n^{-1}, is identical with the limiting condition, $A=2$ arc sin n^{-1}, of Figure 1. Obviously, for this condition of grazing incidence and emergence, $(A+D)/2=90°$ and equation (9) shows that the limiting tolerance is $T_{2D}=\infty$. The undesignated dotted line, $D=2$ arc cos $2n(n^2+1)^{-1}$, is identical with the line of optimum prism angle which is similarly shown in Figure 1. This dotted line is also the iso-tolerance curve of ± 0.825 seconds in double deviation measurement which for all media is equivalent to unit error in the sixth decimal place of index, provided the prism angle has the optimum value, $A=2$ arc tan n^{-1}. When precise determinations of the partial dispersions are desired, even at some sacrifice of accuracy in the absolute values of the indices, it is evident that refracting angles should be chosen from the area above the undesignated dotted line. In selecting such angles it should be remembered, however, that there is a loss of intensity, and that there may be a serious increase in aberration, as the limiting condition of grazing emergence is approached.

From Figure 1 alone it appears that for the refractive angle of a prism of any given medium there exist equally favorable values above and below the optimum angular value for the prism, but Figure 2 shows that from this particular standpoint only the larger refracting angles should be chosen. It must be remembered, however, that there is a loss of intensity, and that there may be a serious increase in aberration, as the limiting condition of grazing emergence is approached.

It will be noticed that, except for media having low refractive indices, the tolerances in prism-angle measurement are less liberal than those for determinations of double deviation. This makes it apparent that, for the most accurate minimum-deviation refractometry of glass, it is important to choose only certain refractive angles readily measureable with the highest accuracy, or else to determine deviations for all three refracting angles of an equilateral prism polished on three sides and so almost eliminate error of prism-angle measurement. The latter course was followed, implicitly, by Hopkinson,[42] Macé de Lépiney,[43] and others, and explicitly, by Gifford,[44] who entirely avoided precise refractive angle determinations.

The exclusive use of equilateral prisms and the making of triple deviation measurements is, however, neither desirable nor practicable, even in precise refractometry. In determinations on liquids of low index, for example, the more favorable tolerances in angle measurement, together with the very considerable increase in sensitivity, both of which are gained by using large refracting angles, make it advantageous to use hollow prisms with an angle appreciably larger than 60°; and the resulting simplicity of prism construction and use is a factor worthy of mention. Certainly there is also, in the general practice of prism refractometry, a considerable demand for accurate single determinations, and it is therefore pertinent to carefully consider in detail these requisite tolerances for high precison. With reference to the possibility of working within the limits found to be necessary, it may be mentioned that in angle measurement by the use of a spectrometer a precision of the order of a few tenths of a second has been attained.[45] Brief references to particular methods of prism-angle measurement will be made in a future paper when the symmetrical use of apertures, the curvature of prism surfaces, and the accuracy of collimation are considered.

In this survey little attention need be given to errors made in the pointings of the telescope or to those made in settings with the micrometer microscopes. Whenever, in decreasing the magnitudes of these accidental errors, repetition becomes onerous, it is likely that such errors can be satisfactorily reduced by the substitution of larger apertures, by improving the quality of scale rulings, or by the use of optical systems which are more carefully designed and constructed. Frequently, however, the size of the prism itself determines the effective telescope aperture and, hence, the limit of precision attainable in a single telescope pointing. This is especially likely under the conditions of reduced width of beam which must exist at

[42] J. Hopkinson, loc. cit., p. 290.
[43] J. Macé de Lépinay, J. de Physique (2), **6**, p. 193; 1887.
[44] J. Gifford, Proc. Royal Soc., London, **70**, p. 329; 1902. (Note by R. T. Glazebrook.)
[45] O. Schönrock, Zeitschrift f. Instrumentenkunde, **40**, pp. 92-93; 1920; **46**, p. 174; 1926.

the oblique incidence and emergence of rays in minimum-deviation measurements, and prism size is given quantitative consideration in a forthcoming paper, particularly as an important contributing factor in the error of prism table orientation.

V. USE OF MULTIPLE MICROSCOPES IN MINIMIZING CIRCLE ERRORS

In considering the difficulties in reaching the requisite accuracy, either in refractive-angle or minimum-deviation measurements, the errors relating to the divided circle are of fundamental importance. No detailed reference to eccentricity is necessary, because most attempts at moderately high accuracy include the use of scale-reading devices at positions angularly equidistant on the circumference of the circle, and under these conditions errors due to eccentricity and to the ellipticity of the pivot are eliminated.[46] The marks themselves, however, usually have errors of position which are classed as periodic (systematic) and accidental (irregular) and are by no means negligible. Therefore, it is generally assumed necessary to calibrate a circle when the accuracy required is of the order of a second of arc or better; but, to avoid the labor of a complete calibration, a Fourier series approximately expressing the low frequency periodic errors as functions of the readings is often determined by the examination of a limited number of the circle divisions.[47] When this latter procedure is followed the resulting corrections, which are computed for application to the circle readings, include neither the accidental errors nor those of high frequency; and often, in order to eliminate such errors, it is still necessary, during the regular use of the instrument, to repeat all measurements on various parts of the circle.

1. SPECIAL USE OF AN UNCALIBRATED CIRCLE

It should be emphasized, however, that in measuring certain commensurable angles all positional errors of scale marks, both periodic and accidental, are completely eliminated from the mean result of a few determinations taken with proper circle orientations.[48] As an obvious example, consider the important case of a 60° prism for which accurate angle measurement is desired. When using only one microscope, a correct value for the angle may be reached by averaging

[46] William Chauvenet, Spherical Astronomy, **2**, p. 51 (Philadelphia); 1891. There may exist, however, certain errors of the pivot which are not so eliminated.

[47] A method of this kind which has recently received considerable attention is that of H. Heuvelink, Zeitschrift f. Instrumentenkunde, **45**, pp. 70-84; 1925. See also L. Fritz und W. Uhink, ibid., **48**, pp. 53-68; 1928.

[48] J. Macé de Lépinay (J. de Physique, (2) **6**, p. 193; 1887), in measuring a double deviation of 84°, used two series of measurements involving a 90° difference in azimuth, and he pointed out that the process would entirely eliminate graduation errors for a double deviation of 90°. See also Annales de Chimie et de Physique (6), **10**, p. 73, note 4, 1887.

three measurements made on equidistant portions of the circle. Only three scale marks are used, and, if perfect functioning of the eyepiece micrometer is assured, the only requirement concerning the positions of these marks is that they be approximately 120° apart so that they will appear in turn in the field of view of the microscope as required. This, of course, is because the entire positional error of each line affects the results twice, but with unlike signs, and is thus eliminated from the average for the series.

The use of several equidistant scale-reading devices is of considerable importance in this connection, on account of the way in which their number, m, is related to the number of necessary repetitions, r. With four microscopes, every measurement of a 90° prism angle is entirely free from the errors of graduation of the circle. After each quadrant rotation the marks utilized are the same four used initially, and the circle has become in a sense a perfect quadrant. In general, the circle becomes equivalent to a perfect arc of $360°/m$, and a convenient equation

$$r = x.\frac{360}{mA} \tag{10}$$

gives the condition for perfect measurement of an angle of $A°$, provided that to the proportionality factor, x, there is assigned the lowest integral value which will yield an integral value for r. Obviously, the scale should be rotated between measurements through an angle of $360°/mr$, and x is the required number of complete traverses on the circle or on its equivalent perfect arc.

This error-free use of an uncalibrated circle is more or less well known; but, possibly because it is somewhat time consuming and requires considerable care for its successful application, it seems that it is avoided, whenever possible, by the use of a more accurate circle or one supposed to be accurately calibrated. In precise refractometry, however, where even the best available instrument often leaves much to be desired from the standpoint of the accuracy attainable, this special use of a circle should be of service. Its comparative neglect in this and related fields, especially in prism goniometry where the use of commensurable angles such as 30°, 45°, 60°, and 90° is quite prevalent, is probably due to the apparent limitation of the procedure to exactly commensurable angles. In reality the practical value of the method is very great because of certain possibilities in connection with errors of the subdivision of the degree intervals of circles. Whenever these errors are approximately eliminated (see pt. 2 of this section) this special use of a circle extends quite satisfactorily to all angles within 1° of the strictly commensurable values. Furthermore, the systematic errors of the degree scale

marks are usually relatively unimportant over arcs of a few degrees; and, consequently, by a small number of repetitions, the mean results for many incommensurable angles may be rendered comparatively free from positional errors of the scale marks.[49]

Although the use of an uncalibrated circle in measuring double minimum deviations is, in general, less satisfactory than its use in measuring prism angles, a glance at Figures 1 and 2 shows that only one-half or one-quarter as much accuracy is required, particularly for work on 60° glass prisms. The possible use of dispersion equations also ameliorates the situation somewhat, especially if indices are determined for several different wave lengths. Furthermore, the means required to eliminate some of the various accidental errors, which in determinations of deviation are larger than in prism-angle measurement, may serve to minimize unknown errors of the circular scale. As an example of the latter possibility, reference may be made to the errors in telescope pointings. For all slit images, except those formed by using the brightest lines near the central portion of the visible spectrum, the precision of pointings is appreciably lower than for those made during prism-angle measurement; consequently, it is often desirable, especially if but few different wave lengths are used, to make a number of observations of each deviation, and these repetitions also reduce the deleterious effects of an imperfectly graduated scale provided a suitable observational program is followed. The accidental errors of graduation are, of course, reduced as the square root of the number of scale marks used, and, according to Woodward,[50] the periodic errors tend, in general, to be eliminated with repeated observations provided the circle is advanced each time through an arc of $360°/mr$, which is the same rule mentioned above when considering the strictly error-free measurement of commensurable angles.

Attention has already been called to the advantages of the optimum relationship between prism angle, A, and number of reading microscopes employed, namely, that condition expressed in equation (10) for making certain measurements entirely free from scale error. It should also be added that for any angular measurement the elimination of periodic error of given frequency becomes more nearly complete, and the process of elimination extends to periodic errors of higher frequency, as the number of scale-reading devices is increased.[51] Consequently, in the design of a spectrometer, it is pertinent to consider a device to permit the mounting of a variable number of equi-

[49] B. Walter (Annalen d Physik, **46**, p. 424; 1892), by an "Umkreisungsverfahren," repeated measurements of refracting angle and of deviation until within ±30° of the starting point on the circle and reduced the errors from 50 seconds, for some single measurements, to 3 seconds or less for an average result of a number of repetitions not exceeding seven.

[50] R. S. Woodward, Report, Chief of Engineers, U. S. A., Appendix MM, p. 1947; 1879.

[51] Wm. Chauvenet, loc. cit., p. 53. If the most important periodic errors are those of long period, they are often almost eliminated from the mean of the readings of only four microscopes. (See L. C. Martin, loc. cit., p. 53.)

distant microscopes around the circle. Such an arrangement would also greatly facilitate complete initial calibration of the scale, and subsequent recalibrations which may be required after cleanings, in the event that it should seem desirable to provide for accurate measurement of incommensurable angles without repetitions.

2. ELIMINATION OF DEGREE-SUBDIVISION ERRORS

The periodic errors of the divided circle which have just been considered are those, principally of relatively low frequency, which relate only to the marks representing even degrees. On some circular dividing engines, however, the auxiliary gear governing the subdivision of degree intervals causes a periodic error whose period includes only a few of these subdivisions; [52] that is, a comparatively very high frequency periodicity is superimposed on the long periods which have been previously considered. These errors in subdivision of degree intervals sometimes approach or even exceed in magnitude [53] the errors of the "degree" graduations, and the importance of their elimination in the special use of an uncalibrated circle has already been pointed out. The avoidance of such errors is necessary also in any use of a scale which, as frequently happens, has been calibrated for the "degree" graduations only. Fortunately, the periodicity of these degree-subdivision errors can be easily determined; and such errors can be automatically eliminated from the mean of the readings by using N microscopes which are displaced from their equidistant positions [54] by fractions of a degree not exceeding $N/2d$, where N is the number of scale marks in each error period and d is the number of subdivisions per degree. Even with less than N microscopes these errors can be very satisfactorily reduced.

If the microscopes are not displaced by these fractions of a degree but are allowed to remain equidistant, then for a given telescope pointing it is evident that each microscope reading, and also the average reading, will contain degree-subdivision error to approximately the same extent. In general, this error will be different for two successive pointings and thus cause an erroneous angle measurement. Furthermore, in repeating, if the circle is advanced in azimuth through an arc measured in integral error periods (of N scale marks each), an error of this nature is not decreased with the number of observations.

---

[52] Gustav Förster, Zeitschrift f. Instrumentenkunde, **33**, pp. 44–51; 1913.

[53] J. Macé de Lépinay, Annales de Chimie et de Physique (7), **5**, p. 218; 1895.

[54] In the elimination of the eccentricity, e, from the mean of the microscope readings, the maximum error due to the displacement of one of two microscopes over an arc of α degrees from its position diametrically opposite the second is $e \sin \alpha$. Thus, for example, a 10′ displacement can not cause such error in excess of $0.003e$, and the value of e seldom exceeds a few seconds on circles for precise work.

VI. MICROMETER ERRORS

Errors in the adjustment of the magnification of the microscopes, causing so-called error of the "runs" of the micrometers, are not sufficiently emphasized in prism goniometry. This may be due to the fact that the use of the necessary corrections is supposed to be well known, or possibly it is because such errors are minimized when both positive and negative "runs" are made; that is, when results are obtained from the means of readings on both scale marks which are found adjacent to the fiducial line in the microscope field. In using multiple microscopes and in repeating scale positions, however, such duplication of micrometer settings is not only unnecessary but may, in fact, lead to errors through vibrations communicated to the instrument during the time required for moving the cross hairs from mark to mark of the scale.

The matter can not always be handled with a simple fixed correction because, for example, differences in room temperature, possibly through effects produced on the oil film between the surfaces of a conical bearing, are quite sufficient to cause changes in the working distances of the microscopes and thus to result in appreciable variations in magnification. Similar variations may also be produced by mere reorientation of the circle or of the system carrying the microscopes, except under ideal adjustment of the bearings and mounting of the circle. Fortunately, frequent determinations of the average run correction may be made accurately and easily under the exact conditions of use by taking one half of all measurements with positive and the other half with negative runs, rather than always selecting the run of minimum length.[55] Indeed, in this way, by a proper balance of positive and negative runs for the repetitions included in an observational program, the error of the runs may be so minimized in the average results that the residual effects are negligible.

Progressive errors of the eyepiece micrometer screws and the distortion introduced by the optical systems of the microscopes will, to a large extent, be included in the error of the runs when the latter are determined under the conditions of actual use as above mentioned. When using multiple microscopes, the periodic error of the screws can be automatically eliminated from the mean readings by the proper adjustment of their individual zero-position drum readings, provided such periodic errors are somewhat similar for all the microscopes and are known roughly as functions of the drum readings. Another method which obviates the use of corrections for the periodic errors of the micrometer screws is based on the repetition of observations with the program of circle advance so chosen that at each

[55] References to negative as well as positive runs should not, of course, be construed as abrogating the use of the usual precautions to eliminate backlash.

micrometer the initial drum readings for each of the successive measurements are evenly distributed over one complete revolution of the screw.

VII. NONCONSTANT RESIDUAL MECHANICAL STRAINS IN THE INSTRUMENT

One additional topic will be mentioned in this résumé and discussion of certain goniometrical requirements in refractive index spectrometry. This is the need of good balance of all moving parts of the instrument and the necessity of freedom from residual horizontal stress components at the instant when a pointing is completed. These requirements must be fulfilled in order to avoid small creepings which may otherwise occur after pointings but before and during the various microscope settings.[56]

Such creepings are very likely to cause systematic rather than so-called accidental errors, and the writer has found that certain errors of the order of 0.5 second of arc in prism-angle measurement are explainable as the algebraic sum of torsional effects of the male and female members of the spectrometer cone bearing.

With a moving telescope and autocollimating eyepiece, the (stationary) prism table being supported from the upper part of the male cone and the (moving) microscope system from the lower part of the female cone, the prism does not remain exactly stationary, but turns through a small angle in the direction of the telescope rotation, whereas the microscope system "drags" [57] slightly with respect to the telescope. If the first effect predominates, the measured arcs are too large and the refracting angles as determined are, therefore, too small. In deviation measurements, only the second of these effects is present and again the values as observed are less than should be found, so that under such circumstances the computed indices of refraction may be either high or low, systematically, on account of torsional strain which varies during prism angle and deviation measurements.

Such results are viewed as due to the frictional contacts which cause strains of the cone members during their relative motion and also prevent their subsequent complete elastic restitution. If the residual strain varies in amount for successive telescope pointings, the result

[56] The writer is averse to the use of clamps and slow-motion screws in making telescope pointings, feeling that small harmful residual stresses are more likely to exist through the use of such devices than is the case when the moving system is induced to take the desired orientation by a number of slight finger taps which produce swings alternating in direction and gradually decreasing in amplitude. It is obvious, however, that, even with optimum instrumental conditions, this method of making observations is not advantageous unless great care is taken to avoid vibrations during the time interval between the telescope pointings and the microscope settings.

[57] The effects discussed have, however, no reference to "drag" through mechanical contact other than that between the conical surfaces.

of a measurement of an angle is correspondingly incorrect. Errors of this kind are sensitive to defects in the conical surfaces, to mechanical interadjustment of the cone members, and also to variations in room temperature, possibly in the latter case through the effect of temperature on the oil film between the surfaces.

In designing a new instrument it is probably possible to avoid such defects to the extent required in sixth decimal place refractometry. In using an old instrument the effect of these errors may be greatly minimized in prism angle measurement, and also in deviation measurements if the collimator permits, by making observations not only on the angles themselves but also on their explements as is sometimes done for similar reasons when using the method of repetitions in geodetic surveying. Frequently, however, it will be necessary to make a statistical study of data taken under various conditions in order to show that these and similar errors are not present or to outline a working plan for their satisfactory elimination.

WASHINGTON, October, 1928.

A NEW DETERMINATION OF THE MELTING POINT OF PALLADIUM

By C. O. Fairchild,[1] W. H. Hoover, and M. F. Peters

ABSTRACT

The melting point of palladium was determined by measuring with an optical pyrometer the ratio of brightness of the red light ($\lambda=0.6528\mu$) emitted by black bodies at the melting points of palladium and gold, respectively. The crucible method was shown to be more reliable than the wire method. Especial attention was given to the purity of the metals. The result obtained by the crucible method, when substituted in Wien's or Planck's equation, gives the melting point of palladium as 1,556.6° C. with an uncertainty of 1°. In the computations C_2 was taken as 1.432 cm deg. and the melting point of gold as 1,063° C. The average of the present result, and those of six previous determinations, is 1,553° ±0.7°. Estimating the uncertainty in C_2 as 0.002 and in the melting point of gold as 0.5°, it is concluded that the uncertainty in the value of the melting point of palladium on the centigrade thermodynamic scale is approximately 2°.

CONTENTS

	Page
I. Introduction	931
II. Methods	932
1. Optical pyrometer	933
2. Crucible method	934
3. Wire method	936
III. Summary of results obtained	941
1. Crucible method	941
2. Wire method	945
IV. Computations	947
V. Purity of metals used	954
1. Gold	954
2. Palladium	955
VI. Conclusion	959
VII. Appendix: Thermoelectric measurements	959

I. INTRODUCTION

When the latest determination of a physical constant is in good agreement with the best value derivable from all previous acceptable data, the situation is regarded as satisfactory. But when the modern investigator's result departs considerably from this figure, the uncertainty in the value of the physical constant is not decreased unless a reasonable explanation is offered.

[1] Since writing this paper Mr. Fairchild engaged in research work for a manufacturing establishment in Brooklyn, N. Y.

This has been the situation with the melting point of palladium since Hoffman and Meissner[2] in 1919 obtained 1,556° C. when the mean was less than 1,553° and the average departure of previous values from the mean was about 2°. Moreover, the value 1,550° obtained in 1910 by Day and Sosman,[3] using a gas thermometer, was considered by them to be good to +2°. Therefore it seemed well worth while to redetermine the value of this important fixed point of the high-temperature scale.

Since 1911 no investigator has undertaken to measure high temperatures with a gas thermometer, and there is little likelihood that such measurements above 1,500° C. will again be attempted. The experimental difficulties are too great. Radiation methods of measurement are to be preferred. Measurements of total radiation from a black body, with the application of the Stefan-Boltzmann law for the establishment of a high-temperature scale, are to be preferred on theoretical grounds to dependence on Planck's law and measurements with an optical pyrometer or spectrophotometer. However, a greater precision can be obtained in measurements with an optical pyrometer than in measurements with a total radiation pyrometer; moreover, there is an increasing belief in the validity of Planck's law for spectral distribution of radiation from a black body, and experimental data confirming the quantum theory are accumulating rapidly. The uncertainty in the value of C_2 of Planck's law has been reduced in recent years to the order of 0.002 in 1.432 cm deg., an uncertainty equivalent to about 1° C. at 1,550° C.

II. METHODS

The method used was, in brief, to compare by means of an optical pyrometer the brightness of a black body at the melting point of palladium with that of a black body at the melting point of gold. There were two modifications of the method—(1) crucible method and (2) wire method.

In the crucible method the pyrometer was sighted into a black body immersed in freezing or melting metal in a crucible. In the wire method a Lummer-Kurlbaum black-body furnace was employed. Its temperature was determined by the melting of a small bit of gold or palladium wire placed within it. The wire was fused in between the hot junction ends of a thermocouple so that its emf would show a halt at the melting point while the furnace temperature slowly rose.

From the brightness measurements, or pyrometric readings, the melting point of palladium is computed according to Wien's law, which is equivalent to Planck's law for light, and such a temperature,

[2] Hoffman and Meissner, Ann. d. Phys., **60**, p. 201; 1919.
[3] Day and Sosman, Am. J. Sci., **29**, p. 93; 1910; **43**, p. 521; 1912.

basing the calculation on the melting point of gold and the value of the constant C_2 of Wien's law.

1. OPTICAL PYROMETER

The particular instrument used in this work is shown in Figure 1. It was built at the Bureau of Standards for the purpose of studying the characteristics, sources of error, etc., of the disappearing-filament optical pyrometer. The design was developed to give high precision and reliability.

The study of the instrument extended over a period of years. Particular attention was paid to diffraction,[4] to the effects of lens imperfections, to diaphragms or stops, and to the pyrometer lamp.

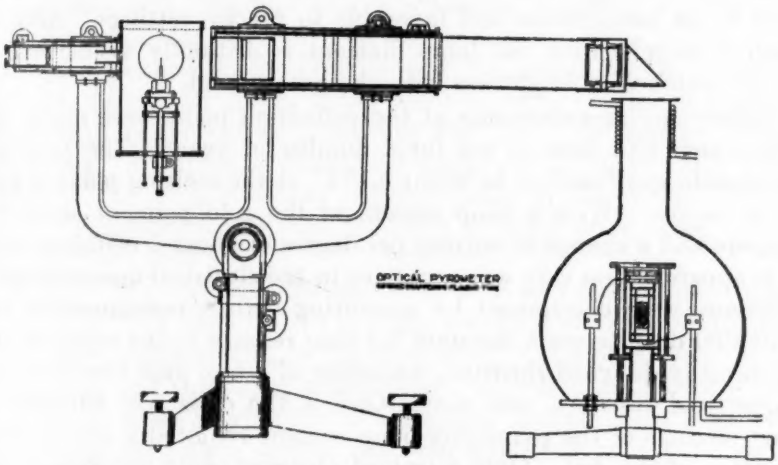

FIGURE 1.—*Optical pyrometer furnace and crucible of metal*

The front objective is an F3 lens computed at the bureau for this instrument. The pyrometer lamp used throughout the measurements reported here is a lamp provided with flat optical-glass windows fused to the lamp bulb. The lamp, after evacuating and baking, was aged or seasoned before any measurements were made. During the measurements the current-temperature characteristic of the lamp changed only slightly, the total change being equivalent to about 1° at 1,063° C. The change was gradual and was carefully watched or checked by repeated calibrations at the melting point of gold. The advantage of the flat windows is the elimination of the uncertain effects of striated blown bulbs, and the increase in precision obtained as a result of a well-defined and undistorted photometric field.

[4] Fairchild and Hoover, J. Opt. Soc. Am. and Rev. Sci. Inst., 7, No. 7, pp. 543-579; 1923.

The exit aperture of the pyrometer telescope during the present work was 0.04 radian. A larger aperture could not be used to advantage,[5] although so small an aperture makes necessary added precaution in keeping dust and dirt from the optical parts. The method used to make certain of the cleanliness of the optical path was to focus the eyepiece upon each glass surface of the system in turn with a bright background for illumination. Such a procedure was found to be essential.

Throughout the work the telescope was adjusted to give a magnification of the source of about 8 diameters, and of the pyrometer-lamp filament about 15 diameters. Such a magnification was selected to give, in conjunction with the 0.04 radian exit aperture and a red glass filter, a brightness of the photometric field which was found by trial to be comfortable and favorable to precise settings. Also, at such a magnification the lamp filament is distinctly visible and is easily matched in brightness with the background.

Before any measurements at the palladium point were made, the instrument had been in use for a number of years. The precision attainable was found to be about 0.1° C. at the melting point of gold or of copper. With a lamp current at the gold point of about 0.1 ampere and a change in current per degree of about 0.00015 ampere, it is apparent that care was necessary in the electrical measurements. Currents were determined by measuring with a potentiometer the potential drop across a standard 0.1 ohm resistor in the lamp circuit. A specially designed rheostat, consisting of a box with two dials and three fixed resistors, was used. One of the dials was adjusted so that settings of the pyrometer-lamp current required a considerable rotation of the dial. Only a trained observer could successfully use this fine-control dial. Settings of the current were always made by turning the dial slowly back and forth, causing the lamp filament to appear alternately darker and brighter than the background and then estimating the midpoint at which a photometric match appeared to be obtained. The dial of the rheostat worked smoothly and turned with slight effort. The observer had no knowledge of the current values of settings during a series of readings at a fixed or constant temperature of the furnace or crucible.

2. CRUCIBLE METHOD

The arrangement during measurements with the crucible method is shown in Figure 1. The pyrometer is provided with a total-reflection right-angled prism mounted upon the front end of the telescope. This prism was used in all measurements, even when sighting into the horizontal furnace shown in Figure 2, thus avoiding any

[5] See footnote 3, p. 932.

correction for its absorption. The furnace and crucible were small and mounted within an evacuated pyrex-glass globe having an optical-glass window. The furnace was made of alundum tubes and diaphragms and insulated with thoria. The insulated cover served as the upper diaphragm. Sides, bottom, and cover of the furnace were wound with platinum-rhodium alloy wire (20 per cent rhodium) to be heated electrically. "Sillimanite" porcelain crucibles, with an inner tube to serve as an immersed black body, were made by turning out the parts on a lathe, using for a cutting tool a crystal of carborundum. The porcelain was first fired to such a temperature that the lathe work was possible, and, after turning and cutting, the parts were fired again to a temperature slightly above the melting point of palladium. The crucibles barely withstood repeated melting and freezing operations, not only on account of the large difference in thermal expansion of the crucible and the palladium but probably because of slight shrinkage of the crucible during continued exposure to the high temperature. After this work had been finished Bowen and Greig [6] identified a eutectic of silica and alumina which melts at 1,545° C. This discovery fully accounts for the relatively short life of the crucibles and their tendency to crack after long heating at 1,550° to 1,560° C.

In order to prove that the immersed tube in a sillimanite crucible was a good black body, such a crucible, was filled with gold and heated in another separate furnace not illustrated. The brightness of this black body at the melting point of gold was compared directly with that of one made of graphite in a graphite crucible filled with gold. The results were quite satisfactory, and when this porcelain crucible finally failed a second crucible was not made.

Owing probably to the high thermal conductivity of gold, less trouble is experienced in obtaining freezing and melting points which agree than is the case with palladium. A necessary procedure in both cases is to heat the melting furnace uniformly. The diaphragms in the furnace shown in Figure 1 were designed to promote uniformity of temperature in the furnace, and hence in the melting or freezing metal. Under such conditions melts and freezes of both gold and palladium agreed invariably to a few tenths of 1° and frequently agreed to less than one-tenth of a degree.

The heating and cooling currents required by the furnace were determined by trial and slowly changed during the life of a furnace. Occasionally the duration of a melt or freeze was too short, and satisfactory observations were not obtained. The crucibles used in the final series at the palladium point held a charge 1.8 cm deep and 1.3 cm in diameter. The inner tube joined to the bottom of the crucible

[6] J. Am. Cer. Soc., 7, No. 4, p. 238; 1924.

had an inner diameter of 1.2 mm and an outer diameter of about 2 mm. This size of crucible and quantity of metal was sufficient to give a constant temperature at melting or freezing for over 30 minutes in the case of gold and nearly as long in the case of palladium. Usually the time during which constant readings were obtained was about 15 minutes.

3. WIRE METHOD

The type of furnace used in the investigation by the wire method is shown in Figure 2. It is essentially a Lummer-Kurlbaum experimental "black body" and is, in a general way, the same as the furnaces

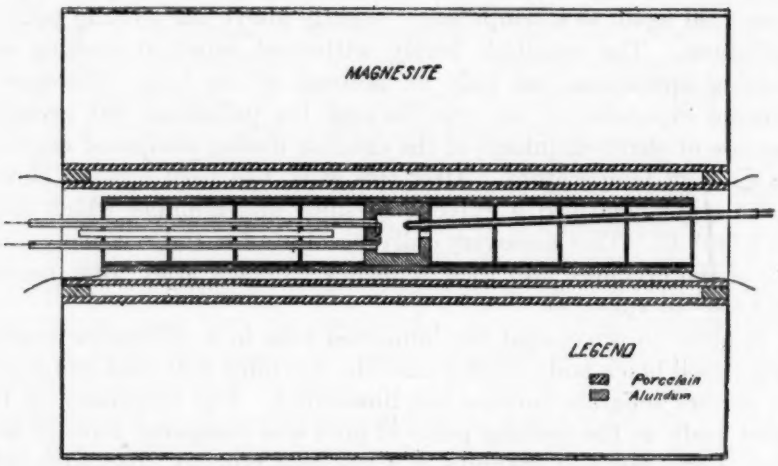

FIGURE 2.—*Black-body furnace showing control couple, test couple, and diaphragms used in wire method*

used by Hyde and Forsythe,[7] and by Hoffman and Meissner. It consists of two coaxial tubes each wound with platinum—20 per cent rhodium wire and insulated, outside of a small air space, with a refractory oxide. The larger of the two inner tubes was covered over its middle part with platinum foil in place of wire, thus compensating for the lower loss of heat from that part. This outer heating coil was shunted near one end for adjusting relative heating of front and rear of the furnace. The inner coil was wound nearly uniformly over the whole length, with a slight crowding of turns near the ends. Over this coil the space was filled with a pure grade of fused alumina called "R R Alundum" (ground to 120 mesh), a material of high thermal conductivity.

The inner tube was filled with a series of flat-bottomed, cylindrical cups of alundum placed end to end, ground to fit the tube and with bottoms drilled out with holes to serve as diaphragms and courses for

[7] The Gold Point Palladium Point Brightness Ratio, Astrophys. J., 51, p. 244; 1920.

tubes holding thermocouples. The result is a central cavity with a small opening, and a conical series of openings limiting the radiation. It may be supposed that the inner middle cavity of this furnace was at a uniform temperature, maintained in such condition by preventing much radiant heat from escaping through the small hole in the cavity.

An older construction of such a furnace is shown in Figure 3. The system of diaphragms in this furnace leads to decided departures from black-body conditions. This was found to be the case by the authors in 1916, and by others, including Hoffman and Meissner. These two workers tried blackening the side walls or "black wall" of their furnace and showed by such means that the side walls were, in general, hotter than the back wall when the furnace was apparently uniformly heated and the innermost opening was invisible.

The various methods employed to bring such a furnace (fig. 2 or 3) to the melting point of palladium (or gold) differ in details. Hyde and Forsythe controlled the furnace with a thermocouple led in from the rear and placed with its hot junction within the inner chamber or touching the "back wall" from behind and noted, by the

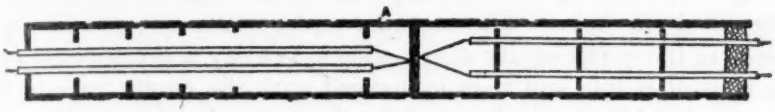

FIGURE 3.—*Older construction of black-body furnace shown in Figure 2*

ringing of an electric bell, the instant of melting through (apart) of a bit of fine palladium or gold wire welded or fused to the tips of two platinum wires led into the furnace from the front through the central diaphragms. Hoffman and Meissner did likewise except that the moment of melting was determined by observing a halt in the rise of emf of a thermocouple, used in place of the two platinum wires. Thus the possibility of obtaining a high reading during a rise of the wire above its melting point before melting apart was removed. Hoffman and Meissner observed that melting apart occurred in many cases a degree or so above the melting point. It does not follow, however, that such was the case with the experiments of Hyde and Forsythe, who used a finer and longer wire. Nevertheless, the "halt" method is more certain and exact. Apparently no attempt was made by any of these writers to adjust the furnace to a uniform temperature by means of actual measurement of the temperatures of various parts. Uniformity was adjudged by disappearance of the outline of the innermost opening. The measurements of brightness were made by sighting into the front of the furnace held at a constant temperature as indicated by the control couple. This couple was calibrated in a preliminary experiment by observing its emf at the

moment of melting of the gold or palladium wire inserted from the front. There is necessarily some uncertainty as to the constancy of the relation between the melting point and the emf of the control couple, and also as to the effect of alternate insertion and removal of the porcelain insulating tubes and couple through the front diaphragms. The radiation from the front openings is greater during the brightness measurements than when the openings are partly filled by the "melt" elements. Thus the relative temperatures of front and rear of the furnace may be disturbed.

In the procedure followed by the authors temperature uniformity was controlled according to actual measurements and was not disturbed by alternate insertion and removal of the melt couple. Furthermore, no primary dependence was placed upon the constancy of the control couple.

The furnace was heated to a temperature slightly below a melting point (1,060° or 1,550°) and maintained until a steady state was reached. A control couple inserted from the rear served to indicate this condition. A second couple was inserted through holes shown in Figure 2, either in front or rear, while in the opposite end an empty tube filled the holes. The second couple, whose hot junction was placed in the center cavity or the adjacent cavity was compared with the control couple and then exchanged with the empty tube in the other end. Allowing a few minutes for a steady state to be again reached, a second comparison would give the relative temperatures of two cavities or portions of the furnace. Through such a series of measurements adjustments were made until the middle three cavities were apparently at the same temperature.

Only longitudinal temperature gradients were smoothed out by such means, and no indication was obtained of the existence or magnitude of radial gradients. The average temperature of a given cavity was estimated and adjusted. In each case the couple extended well into the cavity, almost touching or reaching the next wall. Unavoidable errors attend such measurements. First, the insertion or exchange of tubes disturbs the temperature distribution. Second, the thermocouple is, in general, inhomogeneous and gives an emf dependent on the condition of that part of it traversing the gradients at the ends of the furnace. Third, radial gradients in temperature, if present, finally render impossible a measurement of the temperature of a cavity. No single value can represent the temperature of the cavity, which is not uniformly heated, and a thermocouple inserted into the cavity will indicate a temperature above the coldest part and below the hottest part, but not, except by accident, a temperature truthfully representing the intensity of radiation issuing from the hole in the experimental black body.

By means of the series of diaphragms only a part of this radiation is allowed finally to escape, the remainder being reflected back by the diaphragms and partly replaced by radiation from the diaphragms into the hole in the inner cavity or black body. The radiation finally leaving the furnace arises mainly in the "back wall" of the inner cavity and is partly made up of light reflected by the back wall from the side walls and front of the cavity. Thus the brightness of the "black body" depends to some extent upon the emissivity of the back wall. It is impracticable to overcome this difficulty by blackening the back wall, because materials used for blackening (such as chromium oxide) are not sufficiently refractory to use at high temperatures; that is, while the melting points of some such materials may be well above 1,550° C., they are too volatile to be used adjacent to a thermocouple or the bit of palladium put into the furnace.

Temperature uniformity is increased markedly by decreasing the size of the radiating opening, but this alone can not result in a perfect black body. A corresponding decrease in the size of each of the series of openings in the diaphragms must accompany a reduction in the inner hole in order to decrease the radiation from the front wall of the inner cavity.

Having observed, before the present work was begun, that certain forms of furnaces were not sufficiently "black," the furnace was built of alundum, a comparatively good conductor of heat, and the innermost hole was made as small as practicable—about 3 mm in diameter. The cups or crucibles used to form the inner cavity and adjacent diaphragms were ground into the furnace tube, fitting it so tightly that long heating at high temperatures has resulted in permanent fusion of crucibles and tube except at the relatively colder ends of the furnace. Fortunately this did not occur until the final form of furnace had been assembled.

Preliminary measurements by the wire method were made to compare the brightness of the Lummer-Kurlbaum black body at the melting point of gold with that of a "black body" immersed in the crucible of gold. So far as we can learn such a direct comparison of the two methods has not been made before. While Hoffman and Meissner used both methods, their reported results do not include direct comparison of two black bodies at a supposed single temperature.

The first measurements at the gold point by the wire method gave a brightness exceeding by the equivalent of 2° the brightness observed by the crucible method. Inasmuch as the measurements by the crucible method included measurements on both porcelain and graphite "black bodies" which were in practically exact agreement, we sought an explanation for the discrepancy in the wire method.

It hardly seems necessary to remark that the assumption of nearly perfect blackness of the tubes immersed in metal in the crucibles does not lead to the conclusion that the Lummer-Kurlbaum black body provided a brightness greater than that of a black body. The supposition is, on the other hand, that the observed brightness in the latter instance is too great because the "average" or equivalent temperature of the inner cavity is higher than that of the bit of metal melting within it. In case the side walls of this cavity are hotter than the back wall, the brightness of the back wall may be greater than that of a perfect black body at the temperature of the back wall on account of reflection of light coming from the side walls. A bit of palladium wire held near the back wall on the axis of the furnace will remain always at a temperature below that of the side walls.

In the first arrangement of diaphragms in the furnace shown in Figure 2 there was a series of openings through the diaphragms close to one side of the furnace tube. We found that a thermocouple inserted through these holes into the inner cavity indicated a temperature 2° higher than when inserted along the axis of the furnace. This does not show that the side walls are 2° hotter than the center, but that they are more than 2° hotter than the center. In all measurements we were careful to keep all holes in the diaphragms closed except those in the centers. If a couple was withdrawn, an empty tube replaced it. The holes were made only slightly larger than the tubes.

Having found a departure from ideal black-body conditions, we replaced the parts forming the inner cavity by a single alundum piece made as follows: Two crucibles of different diameters and same height were placed one within the other with bottoms opposed, thus forming a complete inclosure. The crucibles were cemented together with alundum cement in such a way as to provide sides, front, and rear walls about 6 mm thick. One 3 mm hole was drilled through the front wall and two holes through the back wall to fit the protection tubes for a thermocouple. The inner cavity was then somewhat smaller, but we hoped this would be more than offset by the effect of more uniform temperature resulting from thick walls.

Into the inner cavity was led a thermocouple through holes just bordering the central holes left open for observations. The hot junction of this couple was about midway between the axis of the furnace and the side wall of the cavity. A bit of gold or palladium wire 0.5 mm in diameter and 2 mm long joined the elements of this "melt" couple at the "hot junction."

Observations with the optical pyrometer were taken by one observer while another observer controlled the furnace and observed the emfs of the melt couple and control couple. Having adjusted the inner

three cavities to apparently the same temperature, a degree or so below the melting point, with the furnace held constant by means of the control couple, the melt couple was inserted and the furnace current adjusted to give a rate of rise of temperature of about 1° in three minutes. Observations were made with the optical pyrometer during the time immediately preceding the melt and finally at the moment of melting, while simultaneous readings were taken of the emf of the melt couple. All but the final reading of the optical pyrometer were corrected to the melting point. The corrections could be made with an accuracy of 0.1° or better. In thus checking the melt couple immediately after optical measurements all chance of change in the melt couple was avoided, and no dependence was placed upon the control couple, which could not readily be renewed and which continually developed inhomogeneity during the work.

The thermoelectric measurements required in the wire method are described in an appendix. The precision obtained was well within that attainable in the optical measurements.

III. SUMMARY OF RESULTS OBTAINED

1. CRUCIBLE METHOD

In this section the results are expressed in terms of the current passing through the pyrometer lamp when it was matched in brightness from time to time with a black body at the melting point of palladium, viewed through a sector disk, and with a black body at the melting point of gold.

With a knowledge of the constants to be used in the application of Wien's law, a sector disk was made having a transmission approximately equal to the ratio of brightness for red light of black bodies at the melting points of gold and palladium, respectively. The disk was made of aluminum carefully hammered flat, with two sector openings edged with steel knife-edges ground or "lapped" straight. While it was intended to obtain a disk of a selected transmission, the size of the openings was such that only a rough approximation could be made without many trials. Inasmuch as a correction would have to be made in any case for the incorrect transmission of the disk, the first value found was considered close enough and was eventually found to be so. The transmission of the disk was measured on a circular dividing engine at different points along the radii and the transmission computed for the section or, rather, zone of the disk to be used. This transmission was found to be 0.7829 per cent, with a probable accuracy of better than 0.0008 per cent. When the pyrometer lamp was matched in brightness with a black body at the palladium point through this disk the current through the lamp corresponded to a temperature about 1,301° K., 35° below the melting point of gold.

This interval was determined with an accuracy of 0.1°. For this purpose the lamp was calibrated with reference to gold as a fiducial point, for the range 1,000° to 1,700° K. and an equation of current versus temperature computed. In the region of 1,300° the calibration was carefully checked by sighting through sector disks into a black body at the gold point. From this equation, $\frac{di}{dt}$, the rate of change of current with temperature, for different temperature intervals, was computed. For the interval 1,300° to 1,336°, $\frac{di}{dt}$ was found to be 0.0001414 ampere per degree.

Corrections were applied to the measurements for change in the pyrometer lamp from the initial calibration, for impurity of the palladium melted repeatedly in crucibles, and for room temperature. The transmission of the red glass filter and a glass absorption screen used in many of the measurements depended upon the temperature of the room. The absorption glass was not appreciably heated by radiation from the furnace, because of the interposition of the glass window of the furnace, a thick glass prism, and the front objective lens of the pyrometer telescope.

The temperature coefficient of spectral transmission of the red glass filter was determined by the colorimetry section of the Bureau of Standards. The authors determined the coefficient for the absorption glass pyrometrically. The two determinations were made for a 30° interval in room temperature. Temperature of the laboratory varied from 22° to 42° C. during the different series of measurements.

After an extensive study of methods of melting pure palladium sponge, a small crucible of the metal was taken for a preliminary trial of the method. The results obtained with this crucible were not satisfactory. The furnace was not heated uniformly, the crucible failed after two melts and two freezes, and during the last freeze the inner tube within the crucible broke and tipped out of alignment. The 31 readings obtained in this series were not included with later results, because the melting and freezing points were not sharply defined. Even under such circumstances, however, the crucible method appears to advantage, for the series gave for the melting point of palladium 1,554°, a value found later to be in good agreement with the final mean.

A new furnace and new crucible were made, designed to eliminate the faults found in the first instance. A little increase in diameter of both permitted an increase in the strength of the inner tube, which was about 2 mm outside diameter. The heating elements of the new furnace were changed to promote uniformity of temperature, which was also helped by a better system of diaphragming.

Before taking observations on the black body in this crucible of palladium many melts and freezes of gold in both sillimanite and graphite crucibles were made. As a mean of 156 readings at the gold point the current through the pyrometer lamp numbered F10 was 0.11542 ampere. Within experimental error no difference was found between the black bodies of graphite and of porcelain. Refer to Table 1.

TABLE 1.—*Current through pyrometer lamp, gold point, crucible method*

Date	Current (ampere)		Number of readings	Secular mean	Remarks
	Melt	Freeze			
September, 1922	0.11543	0.11543	18	0.11543	New graphite crucible.
	----------	.11543	11	.11543	Do.
	.11543	.11544	20	----------	Do.
	----------	.11544	12	.11544	Do.
November, 1922	.11542	.11543	20	----------	New porcelain crucible.
	.11542	.11541	18	----------	Do.
	.11545	.11540	13	----------	Do.
	.11542	.11543	34	----------	Do.
	.11541	----------	10	.11542	Do.
December, 1922	.11542	----------	8	----------	Do.
	.11542	.11541	13	.11542	Do.
	.11546	.11546	18	----------	After using lamp at high temperature.
	.11545	.11542	18	.11545	
January, 1923	.11548	.11542	17	----------	Same crucible.
March, 1923	.11546	.11546	15	.11545	Do.
July, 1923	.11556	.11556	22	----------	Lamp again used at high temperature.
	.11556	.11555	13	----------	Another new graphite crucible.
	.11555	.11554	18	.11555	Same crucible.
September, 1923	.11558	.11556	28	.11557	Do.

Measurements with lamp F13, not given in the table, gave for the gold in a graphite crucible as a mean of 28 readings 0.28296 ampere through the lamp, and for the sillimanite crucible 0.28293 ampere. The difference is equivalent to about 0.1° and is not significant.

After these measurements the new cruicible of palladium gave very satisfactory results. (See Table 2.) The melting and freezing points were sharply defined and agreed with each other. Readings were taken with sector disk No. 3 and with absorption glass No. 2, which had been very carefully compared. The precision of this comparison was ample to allow their alternative use. After 20 readings with the absorption glass and 66 with the sector disk the lamp F10 was checked at the gold point, giving again the value 0.11542 ampere, as shown in the table. Two weeks later 18 readings with the palladium crucible gave a mean agreeing with the previous values.

TABLE 2.—*Summarized data in terms of current through pyrometer lamp (amperes)*

Date	Gold point				Palladium point									Remarks
	Secular mean crucible method	Wire method	Corrected for change lamp	Number of readings	Absorption glass	Sector disk	Corrections: Room temperature	Corrections: Lamp change	Corrections: Melting point	Corrected value	Furnace gradient		Number of readings	Method	
											Front	Rear			
											°	°			
August, 1922	0.11494			81		0.11005							31	Crucible	Preliminary, data not used.
December, 1922	.11542			156	0.11743	.11041	0	0	+0.00005	0.11046			9	do	Data used for comparison of absorption glass and sector.
	.1542				.11739	.11037	0	0	+.00005	.11042			11	do	
	.1542					.11040	0	0	+.00005	.11045			10	do	Top of furnace visibly cool.
	.1542					.11042	0	0	+.00005	.11047			17	do	New furnace cover, giving apparently uniform temperature of furnace.
	.11542					.11042	0	0	+.00005	.11047			13	do	
	.1542					.11041	0	0	+.00005	.11046			15	do	
	.1542					.11040	0	0	+.00005	.11045			11	do	Succeeded by check at gold point.
	.1542			21		.11041	0	0	+.00005	.11046			18	do	Do.
	.11545			36		.11046	0	−.00003	+.00005	.11048			15	do	Crucible removed and Pd examined for change in purity.
March, 1923	.1545	0.11567	0.11564	14											Preliminary, thin wall, black body.
	.1545	.11548	.11545	7											New thick walls. See text, furnace temperature quite uniform, opening always invisible.
	.1545	.11549	.11546	10											
	.1545	.11555	.11552	10											
	.11545			32	.11736	.11034	+.00004	−.00003	0	.11035	−10	+3	5	Wire	Data not used, but opening nearly invisible.
	.1545				.11745	.11043	+.00004	−.00003	0	.11044	−2	+2	8	do	
July, 1923	.1555			53	.11754	.11052	+.00004	−.00013	+.00003	.11046			16	Crucible	Crucible removed and Pd examined.
	.1555	.11559	.11546	42											Two series furnace O. K.
August, 1923	.1555				.11773	.11071	+.00008	−.00013	0	.11066	+.3	+2.3	28	Wire	Data used for comparison with sector.
	.1555					.11064	+.00013	−.00013	0	.11064	+.3	+2.3	10	do	
	.1555				.11771	.11069	+.00009	−.00013	0	.11065	+2.6	+2.0	10	do	
	.1555				.11755	.11053	+.00009	−.00013	0	.11049	−1.4	+2.8	15	do	
	.1555					.11062	+.00012	−.00013	0	.11061	−.6	+2.2	15	do	

The next check at the gold point followed after considerable use of the lamp for other purposes, during which use the lamp changed slightly, now requiring 0.11545 ampere, mean of 36 readings. During the same day that this check was made the last observations with the palladium crucible then in hand were made. The mean of 15 readings was slightly higher than the previous results. This ended the observations with this crucible.

Nearly a year later, after measurements by the wire method another crucible was made and filled with palladium. This was melted in the same furnace as before. Lamp F10 had changed to require 0.11555 ampere at the gold point. But one melt and one freeze of the palladium were observed for the purpose of demonstrating the reproducibility of the results obtained by the crucible method. The palladium was removed from the crucible without further melting, to be examined for impurities. The results were in satisfactory agreement with those obtained the year before.

After making all corrections to measurements, as described above, the final weighted mean current for F10 sighting into the palladium crucible through sector disk No. 3 is 0.11047 ampere. This is 0.00495 ampere below the standard current of 0.11542 ampere for the gold point. The lower reference temperature is obtained from $\frac{di}{dt}=0.0001414$ ampere per degree and is found to be 1,301.1° K.

Employing the methods given in a later section to calculate the melting point of palladium from the measured ratio of brightness "from gold to palladium," the result is found to be 1,826.6° K., or 1,553.6° C., for $C_2=1.432$ cm deg.

2. WIRE METHOD

The initial brightness measurements by this method were made at the gold point, using a Lummer-Kurlbaum furnace as described in a section above. Referring to Table 2, the first result is found to be 0.11567 ampere as a mean of 14 readings. This is 0.00022 ampere above the value obtained with the crucibles of gold and is equivalent to a difference of nearly 2°. There seems to be no doubt that the brightness of this furnace was greater than that corresponding to a black body at 1,063° C. The furnace was very uniformly heated, according to thermocouple measurements of the temperatures of the three middle cavities. It was at this stage of the work that, as stated before, the side walls of the middle cavity were shown to be at least 2° hotter than the temperature indicated by a couple whose hot junction was near the axis of the furnace tube and close to the back wall of this cavity. After replacing the parts forming the middle cavity with the single-piece inclosure with 6 mm walls,

further measurements were in much better agreement with the crucible values but did not give satisfactory reproducibility.

The first two runs with the thick-walled inner cavity, of 7 and 10 readings, respectively, gave mean currents of 0.11548 and 0.11549 ampere through the pyrometer lamp. While these values are only a fraction of a degree above the crucible results, the third run of 10 readings gave 0.11555 ampere. This was a real discrepancy, for a subsequent check with a crucible (sillimanite) of gold showed that the pyrometer lamp had not changed.

Immediately after the third run the furnace was heated to the melting point of palladium. Late in the evening of that day the furnace was brought to a steady and fairly uniform temperature. Two runs with palladium wire were made. In the first the front cavity was much too cold, according to actual measurements, although the middle diaphragm or innermost opening was almost invisible. A low result was obtained. In attempting to adjust the furnace to uniformity it was found that when the indicated temperatures signified uniformity the innermost opening appeared darker than the surrounding front of the diaphragm. Readings were then taken with the gradient as given in Table 2, and the result, 0.11044 ampere, was in fair agreement with those of the crucible method.

In July, 1923, two sets of measurements at the gold point, when the furnace was apparently very uniformly heated, gave as a mean of 42 readings 0.11546 ampere, a result 0.00004 ampere above the crucible values. The first set gave 0.11549 and the second 0.11543, variations from the mean quite like those obtained before. The variations could not be correlated with the slight temperature gradients in the furnace, such as were indicated by thermoelectric measurements before and after the brightness measurements.

When the furnace was heated to the palladium point, attempts were repeated to adjust it for equality of temperature in the middle three cavities; again we found that the innermost opening appeared dark under such conditions. Adjustments of the furnace were made, of course, by trial, and the measurements with the optical pyrometer proceeded when the furnace was in various states of nonuniformity, as given in the last five lines of Table 2. There is not much certainty as to the accuracy of the figures in the column headed "Furnace gradient." Possibly they are accurate to less than 1°. That they do not correctly represent the true temperature gradients there can be no doubt. However, they are consistent with the results obtained with the optical pyrometer; that is, the colder the front cavity, the lower the pyrometer reading, while the rear temperature remained according to measurements, 2° to 3° high. It is possible that further study of the wire method would disclose a

procedure and furnace design which would eliminate the effects shown here. However, it is well established that there is too much radiation escaping from the innermost cavity of the furnace as built for this work. It seems probable that with the present design the inner cavity is necessarily too cold when the furnace is adjusted to uniformity as described above. Perhaps the addition of heating elements in the diaphragms themselves would alter this condition. It would be very difficult to manipulate the furnace, in such case, at 1,550° C. Time and effort are better spent with the crucible method. At best, the wire method appears as a good but not perfect substitute. Taking the data obtained and making allowance for the departure from black-body conditions, considerable support is given to the opinion that the crucible method furnishes a nearly perfect black body but there is no way of selecting a satisfactory mean of the wire-method results. The indicated temperatures of the front and rear cavities are not those of the front and rear walls of the innermost cavity. Moreover, the side walls are in all probability hotter than the diaphragms.

A weighted mean of the results of the wire method is 0.11060 ampere for the palladium point and 0.11547 ampere for the gold point. The latter value is 0.00005 above the crucible value for gold. This difference of 0.00005 may properly be subtracted for the purpose of comparing the methods, from 0.11060 giving 0.11055 ampere for the final result from the wire method. This is 0.00008 above the crucible result, corresponding approximately to 1.1° in the melting point of palladium.

Although the difference of 1° in the results from the two methods is small, the evidence is clearly against averaging the two. The final result, therefore, will be based on the crucible method alone.

IV. COMPUTATIONS

In order that the measurements with an optical pyrometer may be interpreted as a determination of the melting point of palladium, it is necessary to base the high-temperature scale upon Planck's (or Wien's) law for the spectral distribution of radiation from a black body and at least one previously known temperature or fixed point. The value of the constant C_2 in Wien's law

$$J = c_1 \lambda^{-5} e^{\frac{-c_2}{\lambda \vartheta}} \tag{1}$$

is involved, and also a computation of the effective wave length, λ_e, of the light transmitted by the red glass filter of the pyrometer. The equation for computing one temperature from a known temperature is conveniently put in the form

$$\frac{1}{\vartheta_2} - \frac{1}{\vartheta_1} = \frac{\lambda_e \log T}{c_2 \log e} \tag{2}$$

derived from Wien's law, in which ϑ_2 and ϑ_1 are the two temperatures involved, T is the transmission of a sector disk or ratio of black-body brightnesses corresponding to the temperatures ϑ_2 and ϑ_1 and e is the Napierian base.

The computations following are based on $C_2 = 1.432$ cm deg., on $\vartheta_1 = 1301.1°$ K. as found in the experimental results obtained by the crucible method, on $T = 0.7829$ per cent, and λ_e.

The remaining quantity with which we are concerned is λ_e. The effective wave length or mean effective wave length λ_e is a function of the transmission of the red glass filter, visibility of radiant energy, and spectral distribution of radiant energy. The variation of λ_e with temperature of the black-body radiation is so slight that only approximate values of black-body temperatures are required for the computation of λ_e for any given interval of temperature.

All the photometric observations included in this report were made with the right eye of one of the writers, C. O. F., for whom visibility had been measured by two groups of workers.[8] The relative visibility for this eye as determined in the two cases is given in Table 3, together with the mean visibility for many eyes and the ratios of the two sets of measurements.

TABLE 3.—*Relative visibility versus wave length*

λ micron	V for C. O. F. by —			V many eyes by —		
	Coblentz, 1917	Gibson, 1923	Ratio	Coblentz	Gibson	Ratio
0.61	0.613	0.534	1.15	0.557	0.511	1.09
.62	.470	.431	1.09	.427	.387	1.10
.63	.338	.319	1.06	.302	.270	1.08
.64	.220	.2154	1.02	.194	.184	1.05
.65	.135	.1343	1.01	.115	.113	1.02
.66	.076	.0784	.97	.0645	.0642	1.00
.67	.040	.0427	.94	.0338	.0349	.97
.68	.020	.0223	.90	.0178	.0178	1.00
.69	.0090	.0112	.80	.0085	.0092	.92
.70	.0051	.0056	.91	.0040	.0045	.89
.71	.0025	.00273	.92	.00203	.00220	.92
.72	.0011	.00137	.80	.00097	.00108	.90
.73	.00055	.000686	.80	.00048	.00051	.94
.74	.00033	.000345	.96	.00028	.00026	1.08
.75	.00020	.00021	.95	.00020	.00014	1.43

It might be supposed that the mean of the values in the second and third columns of Table 3 should be used in our calculations. This is not the case, however. Other groups of workers have reported their results of determinations of the relative visibility for many eyes. It is apparent that the visibility for C. O. F. as given in the table could be corrected to values consistent with the mean visibility for the human

[8] Coblentz and Emerson, B. S. Sci. Paper No. 303; 1917. Gibson and Tyndall, B. S. Sci. Paper No. 475; 1923.

eye as determined by all published measurements. The data of Gibson are so close to such a mean that this correction is unnecessary, so we have used the values in the third column. Moreover, while Coblentz used a flicker photometer, Gibson's photometric arrangement resembled that of optical pyrometry.

The difference in λ_e computed from V (C. O. F.) as determined by Coblentz and by Gibson is 0.0011μ, equivalent to 1.2° in the calculated melting point of palladium. The uncertainty in the final result arising from an uncertainty in λ_e is discussed later.

The spectral transmission of the red glass used as a filter was measured by the colorimetry section of the Bureau of Standards. These measurements were made both photometrically and radiometrically and at two different temperatures of the red glass. The change in λ_e with room temperature was found to be 0.000089μ per degree, equivalent to a change of 0.09° in the palladium point per degree change in room temperature under the conditions of the work.

The mean effective wave length of the red glass screen for a certain temperature interval θ_1 to θ_2 is defined as that wave length at which the ratio of black-body radiation intensity at the two temperatures is equal to the ratio of integral luminosity; that is, λ_e is that wave length at which

$$\frac{J_2}{J_1}=\frac{L_2}{L_1}=\frac{\int_0^\infty J_2(\lambda,\vartheta_2)\,R(\lambda)\,V(\lambda)\,d\lambda}{\int_0^\infty J_1(\lambda,\vartheta_1)\,R(\lambda)\,V(\lambda)\,d\lambda} \tag{3}$$

in which the quantities J, R, V, and L are, respectively, radiant energy, transmission of screen, visibility, and luminosity. The mean effective wave length can be defined also from its relation to the effective wave length λ_L. This quantity is defined as that wave length at which the rate of change of radiant energy at a given temperature is equal to the rate of change of integral luminosity. It can be shown that the reciprocal of the mean effective wave length, λ_e, for a certain temperature interval ϑ_1 to ϑ_2 is equal to the average value of the reciprocal of the effective wave length, λ_L, for the interval $1/\vartheta_1$ to $1/\vartheta_2$; that is

$$\frac{1}{\lambda_e}=\frac{\int_{1/\vartheta_1}^{1/\vartheta_2}\frac{1}{\lambda_L}\,d\left(\frac{1}{\vartheta}\right)}{\frac{1}{\vartheta_2}-\frac{1}{\vartheta_1}} \tag{4}$$

The relation between $1/\lambda_L$ and $1/\vartheta$ is found to be practically linear and approximately

$$\lambda_e=1/2\,(\lambda_{L1}+\lambda_{L2})$$

The two methods of computing λ_e are found to agree exactly. We present here only the calculations by the former method, which is, in this particular instance, slightly shorter. The calculation of integral luminosities is made by tabular integration of JRV products, since it is not practicable to express R (λ) in anylitical form, and an analytical expression for V (λ) is somewhat awkward to use.

The tabular integration is performed most conveniently by Simpson's rule. The use of this rule permits the use of wider intervals of abscissas than a simple step-by-step method.

Table 4 gives the values of JRV from which the integrals in equation (3) are computed. The constant C_1 of Wien's equation has been omitted, and only relative values of luminosity are obtained. Simpson's rule is stated as

$$A=\frac{h}{3}\left[(y_o+y_n)+4(y_1+y_3+\ldots)+2(y_2+y_4+\ldots)\right]$$

in which h is the width of strips and y_o and y_n are the first and last ordinates.

From Table 4, L_2 is found to be 695.02×10^{-7} and L_1 is 543.04×10^{-9}.

$$\frac{L_2}{L_1}=T=127.99$$
$$\log T=2.107176$$

From equation (2)

$$\lambda_e=\frac{C_2\log e}{\log T}\left(\frac{1}{1,300}-\frac{1}{1,825}\right)=0.6531_0 \text{ microns}$$

Computations using narrower strips and more digits give $\lambda_e=0.6531_1\mu$, and the step-by-step method gives from the table $\lambda_e=0.6530_0\mu$. The visibility data from Coblentz give $\lambda_e=0.6519\mu$.

A great many computations have been made for this particular temperature interval, many other temperatures, and for various sets of data on visibility and red-glass transmission. Among these were computations of the errors arising from low accuracy in visibility data of the far red, and in data on red-glass transmission near the short wave-length limit. The values in Table 4 have been shortened to approximately the significant figures, and the number of wave lengths used have been limited to the minimum, the table being carefully trimmed down to the least number of figures which will give λ_e to the nearest unit in the fourth place.

The question as to what accuracy is required in the measurements of spectral transmission of the red glass is easily answered by computations. For example, the effective wave length at 55°, room

TABLE 4.—*Relative spectral luminosity of black body, at 1,300 and 1,825° K., through 3 mm Corning H. T. red glass*

[For C_2=1.432 cm deg.]

Wave length, micron	*V* visibility C. O. F., by Gibson	*R* transmission of red glass, 25° C.	*VR*	$J_1 \times 10^8$ for 1,300° K.	$J_2 \times 10^8$ for 1,825° K.	$J_1VR.\ 10^9$	$J_2VR.\ 10^7$
0.615	0.485	0.000	0.00000	18.92	32.71	0	0
.620	.431	.014	.0060	20.99	34.81	1.27	2.10
.625	.375	.085	.0319	23.24	37.00	7.41	11.79
.630	.319	.250	.0798	25.69	39.28	20.49	31.33
.635	.263	.520	.1368	28.34	41.65	38.76	56.96
.640	.2154	.655	.1411	31.21	44.11	44.03	62.23
.645	.173	.730	.1263	34.30	46.66	43.31	58.92
.650	.1343	.780	.1048	37.63	49.29	39.42	51.64
.655	.101	.798	.0806	41.22	52.02	33.22	41.93
.660	.0784	.809	.0634	45.07	54.84	28.59	34.78
.665	.057	.815	.0465	49.21	57.74	22.86	26.82
.670	.0427	.819	.0350	53.64	60.74	18.76	21.24
.675	.030	.823	.0247	58.37	63.83	14.41	15.76
.680	.0223	.826	.0184	63.43	67.00	11.68	12.34
.685	.0156	.828	.0129	68.82	70.27	8.89	9.08
.690	.0112	.830	.0093	74.56	73.62	6.93	6.84
.695	.0078	.830	.0065	80.68	77.07	5.22	4.99
.700	.0056	.830	.00465	87.16	80.60	4.05	3.75
.705	.0040	.830	.00332	94.05	84.22	3.12	2.80
.710	.00273	.828	.00226	101.3	87.92	2.29	1.99
.715	.00188	.826	.00155	109.1	91.71	1.69	1.42
.720	.00137	.825	.00113	117.2	95.58	1.32	1.08
.725	.00096	.824	.00079	125.8	99.54	1.00	.79
.730	.000686	.823	.00057	135	103.6	.76	.59
.735	.00049	.822	.00040	144	107.7	.58	.43
.740	.000345	.821	.00028	155	112	.44	.32
.745	.00028	.820	.00023	165	116	.38	.27
.750	.00021	.819	.00017	176	121	.30	.21
.755	.00015	.818	.00012	188	125	.23	.15
.760	.00011	.816	.00009	200	129	.18	.12
.765	.000078	.815	.000065	213	134	.14	.09
.770	.00005	.814	.000041	226	139	.09	.06

temperature of the red glass, is found to be 0.0027 greater than at 25°, a change of less than 0.5 per cent, while the changes in spectral transmission are very marked, as shown in Table 5, particularly from 0.62μ to 0.65μ.

TABLE 5.—*Transmission of red glass*

λ	T=25°	T=55°
μ		
0.615	0	0
.62	0.104	0.004
.63	.250	.130
.64	.655	.550
.65	.780	.750
.66	.810	.794
.67	.820	.810
.68	.826	.818

The uncertainty in λ_e arising from uncertainties in the data in Table 5 can be scarcely more than a few units in the fourth place, our estimate being 0.0003μ. The uncertainty arising from errors

in visibility is possibly somewhat larger, but we believe it is considerably less than 0.0003. The observer's eye is slightly red sensitive, but is otherwise normal, and apparently stable in spectral sensitivity or visibility.

Although the computation of λ_e appears somewhat involved, there is good reason to believe that λ_e is as well known as would be the case with a spectrophotometer, the slits of which must be opened to such a width as to afford the same brightness as that obtained with the optical pyrometer, in order to obtain the same photometric precision. We are supported in this statement by Forsythe and would call attention to the following statement by Hoffman and Meissner:

> As was indicated by a separate very careful investigation, the ratio of brightness at the two melting points, determined with these two slit widths (collimator slit 0.2 mm, ocular slit 0.3 mm) differed from the ratio with the slits reduced to infinitely small width, only by a negligible amount.

The absorption glass[9] employed during some of the series of measurements is a screen made up of three different-colored glasses, the combined effect of which is a transmission which approximates an exponential function of wave length. The three glasses used are Corning G171 IZ (2.57 mm thick), G554 CP (3.07 mm thick), and Jena F3815 (0.175 mm thick). The screens give a perfect color match of filament and background when sighting into a black body with the pyrometers, using a red glass in the eyepiece. Of course a very dense red glass gives by itself such a color match, but for many purposes it is desirable to use a red glass screen not too dense. The glass described above as having an effective wave length about 0.653μ is sufficiently selective to give an almost perfect color match with the sector disk used at the palladium point and at the same time transmit enough light to promote ease in obtaining a photometric match. When using the absorption glass, a greater precision is possible because of more perfect disappearance of the filament than can be obtained using a sector disk of low transmission. Another advantage of the absorption glass is that in combination with the red glass it has a lower room-temperature coefficient than the sector disk and red glass combination.

The calibration of such an absorption glass or screen can be accomplished by comparison with a sector disk or by using two known temperatures. In the present case the screen was compared with a sector disk. The comparison results in a determination of the constant A in

$$A=\frac{1}{\vartheta_2}-\frac{1}{\vartheta_1}=\frac{\lambda_e \log T}{C_2 \log e}$$

The constant A for such a glass is not affected by small changes in the λ_e of the red glass screen used in conjunction with it, so that

[9] Foote, Mohler, and Fairchild, J. Wash. Acad. Sci.; November, 1917.

further measurements with the glass can be made without close attention to effective wave length. A full discussion of the theory and usefulness of this type of absorption device is not properly included here. Its use introduced no significant errors and does not enter into a discussion of the accuracy of the final results.

The sector disk used was made by mounting steel knife-edges on openings in an aluminum disk. The disk was carefully balanced and hammered flat. The steel knife-edges were ground and polished as straight as possible. Their straightness was examined on a linear dividing engine and found to be accurate to 1μ or better throughout. Before measurements on the dividing engine were made, the knife-edges were aligned with the center of the disk. The angles were measured at three radii and the transmission of the disk at a particular radius taken where the apertures of the pyrometer were placed with reference to the slits in the disk. The accuracy in the determination of the transmission of the sector disk was better than 0.1 per cent of the transmission. Dividing engine measurements were made before and after rotating the sector disk at high speed (5,000 r. p. m.) to be certain that no slip of the knife-edges would take place.

The effects of diffraction by a sector disk have been made the subject of study by two of the writers,[10] from which study we were able to avoid error from loss of light by diffraction.

The calculation of the palladium melting point from the equation

$$\frac{1}{\theta_2}-\frac{1}{\theta'_1}=\frac{\lambda_e \log T}{C_2 \log e}$$

is made as follows:

λ_e from Table 4 is 0.65310μ for room temperature $=25°$ C.

$\lambda_e=0.65283$ for 22° C., the temperature on which the calculations are based.

$T=0.007829$, $-\log T=+2.1063$.

$C_2 \log e=6{,}219.1$.

$\theta'_1=1{,}301.1°$ K. as found on page 1 for a lamp current of 0.11047 ampere.

$\theta_1=1{,}063°$ C.

$$\frac{1}{\theta_2}-\frac{1}{1{,}301.1}=-0.00022110.$$

$\theta_2=1{,}826.6°$ K. $=1{,}553.6°$ C.

Using these values, the ratio of brightness, R, of a black body at the melting point of palladium to that of a black body at the melting point of gold is obtained from the equation

$$\log R=\frac{C_2 \log e}{\lambda_e}\left(\frac{1}{\theta_2}-\frac{1}{\theta_1}\right)$$

$$R=82.25$$

[10] See footnote 3, p. 932.

One might suppose that a recalculation of λ_e from Table 4 is required if another value than 1.432 is used for C_2, but it can readily be shown that a change in C_2 has a third-order effect on λ_e. Hence, the palladium point may be computed for any value of C_2 from the equation above.

V. PURITY OF METALS USED

The metals used in these series of measurements were of such a high purity that chemical analyses were not attempted. The methods used to determine the quality of the metals are described below.

1. GOLD

The gold for filling the crucibles was obtained from the United States assay office at New York. It was very pure but was less pure than a sample obtained from the United States Mint at San Francisco, which was used as a standard for comparison. The latter sample under spectroscopic examination showed slight traces of copper, silver, and calcium. The assay-office gold contains traces of the same metals, each impurity being present in such a small quantity that estimates were placed at about 0.001 per cent or less for each.

A comparison of the melting points of the different samples of gold was made by the wire method. In applying this method a high accuracy of comparison was obtained by careful manipulation of the furnace and by the use of new well-annealed thermocouples. The thermoelectric circuits were made as free as possible from stray emfs and the measurements made on a Diesel horst potentiometer with a galvanometer of high sensitivity (15 mm per microvolt). A precision of better than 0.2 microvolt in the measurement of the emf of the thermocouple was obtained without difficulty. The gold from the assay office was found to have a melting point approximately 0.01° high. Two other samples of gold were at hand, one from a merchant and one from the Nela Research Laboratory. The former melted 0.28° low and the latter 0.17° high.

Owing to the remarkable consistency of the results obtained in observations with the optical pyrometer upon crucibles of gold, it has been unnecessary to test the contents of a crucible after use. In fact, the original graphite crucible of gold is still intact and is in use. One of the ingots from a sillimanite crucible was examined and showed no change in melting point.

We may consider it a well-established fact that the gold was sufficiently pure. It is highly probable that in the future this metal will always be readily available in so pure a state. This is fortunate because gold is not equaled by any other metal in the properties which make it useful for a pyrometric fixed point. It does not oxidize nor carbonize, nor absorb gases when melted either in air or a reducing

atmosphere. Also, it has a very high thermal conductivity, which is a valuable property for obtaining sharply defined melting and freezing points as they are indicated by a thermocouple or optical pyrometer.

2. PALLADIUM

Palladium sponge, lot No. 3, was prepared by W. H. Swanger from metal obtained from the United States assay office at New York. This metal had been prepared by an electrolytic process and was about 99.0 per cent pure. Four hundred and twenty grams were used in the preparation of palladium No. 3. The metal, in the form of wire about 4 mm in diameter, was dissolved in aqua regia made up from 4 volumes of hydrochloric acid (sp. gr. 1.18), 1 volume of nitric acid (sp. gr. 1.42), and 2 volumes of water. After the metal was dissolved the solution was evaporated to remove most of the excess of nitric acid. It was then diluted with water containing some hydrochloric acid and treated with an excess of ammonia without previously filtering off the small insoluble residue. The treatment with ammonia produced a precipitate of $[Pd(NH_3)_4]Cl_2.PdCl_2$ (Vauquelin's salt) which dissolved in excess of ammonia on digestion on the steam bath. The solution of tetramminepalladous chloride $[Pd(NH_3)_4]Cl_2$ was now filtered from the precipitated impurities, of which the predominant constituent was iron hydroxide.

The original insoluble matter was, of course, removed at the same time. To the filtered solution, normally yellow but in this case green because of the presence of copper, a slight excess of hydrochloric acid was added, thereby precipitating nearly all of the palladium as dichlordiamminepalladium $Pd(NH_3)_2Cl_2$. This precipitate was filtered off, washed, and redissolved by the addition of ammonium hydroxide. The ammoniacal solution was filtered and the palladium salt again precipitated by the addition of hydrochloric acid to a slight excess. This cycle was repeated twice more. In the last operation gaseous ammonia was led into the suspension of the salt in water instead of adding ammonium hydroxide. This precaution was taken to avoid contaminating the solution with impurities which might be present in the ammonium hydroxide.

The final salt was well washed, thoroughly drained on a Büchner funnel, and dried in an air oven. It was reduced to sponge by ignition in porcelain containers under an atmosphere of hydrogen. To avoid having the final sponge saturated with hydrogen the sponge was taken from the atmosphere of hydrogen while it was still warm. It oxidized slightly on cooling in the air but was reduced by moistening with a few drops of formic acid and warming sufficiently to evaporate the excess of acid. Subsequent spectrographic examination of samples prepared from this sponge indicated the absence of all of the

other platinum metals as well as the impurities found chemically in the original material.[11]

The mother liquors from the various operations were examined for impurities. The principal foreign metals found were copper, lead, silver, iron, and platinum. Small amounts of bismuth, antimony, tellurium, and silicon were also found.

Palladium sponge, lot 4, was prepared from scrap palladium obtained from various experiments with portions of palladium from lot 3 and possibly from other lots of pure palladium. It was dissolved in aqua regia and once precipitated as dichlordiamminepalladium in the manner previously described. This salt was ignited to sponge, which was then redissolved in aqua regia. The solution was filtered from traces of insoluble matter, treated with one-third its volume of concentrated nitric acid and with sufficient ammonium chloride solution to precipitate nearly all of the palladium as ammonium chloropalladate $(NH_4)_2PdCl_6$. This precipitation occurred after digesting for a short time on the steam bath. The precipitation of palladium in this way is not quantitative, but under good conditions a larger yield of palladium is obtained than in the precipitation of dichlordiamminepalladium. The use of ammonium chloropalladate in the purification of palladium is less common than the precipitation of dichlordiamminepalladium. One possible advantage is that the salt is precipitated from an acid solution. In the precipitation of palladium from an ammoniacal solution, silver chloride present in the solution would also be precipitated by the addition of hydrochloric acid.

The red salt $(NH_4)_2PdCl_6$, obtained as described, was ignited to sponge in an atmosphere of hydrogen. The sponge was redissolved in aqua regia and the palladium once more precipitated as ammonium chloropalladate in the manner described. This salt was ignited to the sponge known as lot 4.

Impurities found when examining the mother liquors were silver, iron, copper, and nickel, as well as a small amount of silica. Examination of samples from this lot, by means of the spark spectrograph, revealed no traces of the impurities or of the metals of the platinum group. Melt No. 138 was made from this sponge. This melt, made in a crucible of powdered lime, showed the principal calcium lines rather strongly. Hydrogen present in the palladium sponge probably caused some reduction of the lime in contact with the molten palladium.

In the beginning it was intended to apply three tests for comparative purity—(1) spectroscopic, (2) thermoelectric, and (3) melting

[11] The spectrographic method used is described in B. S. Sci. Paper No. 444, Practical Spectrographic Analysis.

point. These tests could be carried out best after preparation of the metal in the form of wire or rod. Hence the problem of successful melting of the pure metallic sponge immediately presented itself. Furthermore, we intended to use a sillimanite porcelain crucible in the final determinations of the melting point, and for that reason we prepared samples melted in sillimanite. Being previously informed that palladium absorbs oxygen readily when molten, and believing that melting the metallic sponge in a vacuum would result in the retention of oxidizable impurities or the absorption of reduced elements from the crucible, we prepared to melt the sponge in air and freeze the metal in pure nitrogen. A number of attempts showed that oxygen absorbed above the melting point was eliminated exceedingly slowly while the metal was held molten in an atmosphere of pure nitrogen. The contents of a crucible upon freezing usually gave off a small quantity of gas generating a pressure which cracked the crucible. It is not certain that this gas was oxygen. It may have been nitrogen. During these trials a number of fairly solid ingots were obtained and were drawn into rods and wire. One such ingot was found under spectroscopic examination to be purer than any other but is listed as No. 3 in the table below. This sample and No. 138 contained only calcium, so far as known, but No. 138 was the most negative thermoelectrically and possibly the purest.

There may be some doubt as to the relative purity of the samples Nos. 1, 2, and 3 in the table, but there is a difference of only 0.1° in the melting points. Sample No. 2 was obtained from Doctor Sosman, of the Geophysical Laboratory, and was cut from the ingot which Day and Sosman have retained since their measurements with a nitrogen thermometer. Spectroscopic examination showed a trace of copper and more calcium than sample No. 3, but the melting point was nearly identical with that of No. 1. The precision of the melting point comparisons is very nearly 0.1°.

The table following is presented for various reasons. It shows that an extensive investigation was made, and that a sufficiently pure metal was obtained. A fairly consistent relation between relative melting points and thermoelectric power is apparent. The statement by Adams [12] that impure palladium usually melts higher than the pure metal is not confirmed.

Samples Nos. 8 and 11 were cut from ingots left after the observations on the melting point by the crucible method. We have used the corrections of 0.4° and 0.7° in the two cases for the following reason. It was found that palladium sponge melted in sillimanite gave a metal spectroscopically pure, when the melting was done in air (freezing in nitrogen). Samples Nos. 8 and 11, however, were

[12] Day and Sosman, The Dictionary of Applied Physics, "Abs. Scale of Temp.," Macmillan & Co.; 1922.

prepared by melting the sponge in sillimanite in a vacuum; in fact, in the crucible used for the temperature measurements as shown in Figure 1. (This procedure eliminated the possibility of the cracking of crucibles by evolution of gas from the freezing metal.) Whatever impurity entered the metal must have resulted from the reduction of the material of the crucible by impurities in the sponge. Subsequent examination showed the introduced impurities to be traces of aluminum, iron, silicon, and a greater amount of titanium. Furthermore, the crucible was filled by repeated melting of charges of compressed sponge, and no measurements were made until the metal had been in contact with the crucible for a considerable length of time. Of course the sponge used was tested separately, sample No. 1 (138) representing this lot of sponge (see Ann. d. Physik, 1919), and the values given are theirs and versus their purest sample. No. 15 contained platinum.

Summary of estimated errors

Source of error	Equivalent in degrees
Transmission of sector disk	0.2
Effective wave length	.3
Photometric matching	.2
Brightness of experimental black bodies	.3
Impurity of metal	.1
Total	1.1

A very conservative estimate of the uncertainty is 1°. We believe that the probability that the error is greater than 0.5° is very small.

Waidner, Mueller, and Foote [13] have reviewed the work of various investigators of the melting point of palladium, and their summary is given in Table 6, in which the values have been recorrected to $C_2 = 1.432$ cm deg.

TABLE 6.—*Comparison of samples of palladium*

No.	Sample	Difference in melting point	E. M. F. at melting point	Metal melted in—
		° C.		
1	No. 138	0	0	Lime.
2	D. & S., 1923	0	----------	Magnesia.
3	B. of S., 1923	−0.1	+54	Sillimanite.
4	D. & S. 2	−.2	180	Magnesia ?.
5	G 2	−.3	160	Lime.
6	4 remelted	−.4	250	Sillimanite.
7	W 1	−.4	205	Lime.
8	B. of S., 1923	−.4	----------	Sillimanite.
9	Nela	−.6	----------	(?).
10	G 1	−.6	490	Lime.
11	B. of S., 1922	−.7	550	Sillimanite.
12	N. Y. A. Office	−2.3	2,500	Lime ?.
13	Heraeus	+.9	3,800	(?).
14	Kahlbaum	+1.0	5,200	(?).
15	H & M [a]	+9.5	5,600	(?).

[a] No. 15 was an impure sample found by Hoffman and Meissner.

[13] Pyrometry Symposium, Bull. A. I. M. M. E.; 1919; also published by the institute as a book Pyrometry.

TABLE 7.—*Melting point of palladium*

[C_2=1.432 cm deg. M. P. of gold=1,063° C.]

Investigators	Method	Melting point
		°C.
Nernst and Wartenberg, 1906	Ratio of brightness Pd/Au, Wanner pyrometer.	1, 552
Waidner and Burgess, 1907	Disappearing filament pyrometer and sector disk.	1, 550
Day & Sosman, 1910	Gas thermometer	1, 550
Hyde, Cady, and Forsythe, 1915	Ratio of brightness Pd/Au, disappearing-filament pyrometer.	1, 557
Mendenhall, 1917	Ratio of brightness Pd/Au, spectral pyrometer.	1, 553
Hoffman and Meissner, 1919	Ratio of brightness Pd/Au, spectrophotometric.	1, 556
Present authors	Ratio of brightness Pd/Au, disappearing-filament pyrometer.	1, 553. 6
Mean		1, 553. 1±0. 7

VI. CONCLUSION

The melting point of very pure palladium has been redetermined by measuring the relative brightness of black bodies at the melting points of gold and palladium and calculating the upper temperature by means of Wien's law, which is equivalent to Planck's law, for light and such a range of temperature. The measurements were made with an optical pyrometer sighted into a black body immersed in freezing metal. The precision attained was about 0.1° at the gold point or 0.2° at the palladium point. The result is $1{,}553.6 \pm 0.5°$ C., based on 1,063° C. for the melting point of gold and 1.432 for C_2 in Planck's law. On this basis the mean of all accepted data is 1,553.1°, with a "probable error" of 0.7°. If we consider the uncertainty of 0.5° in the melting point of gold and 0.002 in the value for C_2 (accepting Planck's law), we may finally conclude that the melting point of palladium is $1{,}553 \pm 2°$ on the centigrade thermodynamic scale.

It has become almost universal practice to take 1,063° C. as the melting point of gold. The earlier work of Hollorn and Day [14] resulted in the value 1,064°, while the later work of Day and Sosman led to the value $1{,}062.6° \pm .8°$. It is obvious that an accuracy of the order of 0.1° was not attained, and that if the value is to be given to the nearest degree, then 1,063° is logically indicated as the proper choice.

VII. APPENDIX

1. THERMOELECTRIC MEASUREMENTS

Throughout this work all electrical measurements were made with potentiometers. Part of the time a Leeds & Northrup type K slide-wire potentiometer was employed, and for more accurate work

[14] Ann. d. Phys., **307**, p. 527; 1900.

a Diesselhorst 5-dial potentiometer was used. It is out of place here to describe in detail well-established methods of measuring small emfs. Attention is directed here to the special problems arising.

No special difficulty was met in measuring emfs of thermocouples at the melting point of gold. New, homogeneous couples of platinum and platinum, 10 per cent rhodium alloy, made at the Bureau of Standards were used exclusively.

A new couple, well annealed and inserted in a clean 2-holed porcelain tube, was cut at its hot junction, and a bit of gold wire was welded to both elements. The weld was made in such a way that a minimum of strain remained in the two legs of the couple, so that the gold would not part at the melting point. The couple with its gold tip was inserted into the furnace just below the melting point, and after a steady state was reached the heating rate was adjusted to about 0.3° per minute. The slow rise of emf of the couple was observed in the drift of a line of light across a galvanometer scale. When the melting point was reached, the drift ceased—the emf remained constant—for a fraction of a minute and then continued with a slight increase caused by the slight lag of the couple behind the furnace temperature. Frequently the gold parted a degree or so above the melting point. Occasionally the furnace was manipulated so successfully that the gold was made to freeze without having been more than a few tenths of a degree above its melting point. The freezes checked the melts fairly well but were not taken during any optical measurements. When the gold parted, the galvanometer swung freely back to zero, indicating an open circuit.

A precision of measurement was attained which made it possible to compare thermoelectrically the melting points of different samples of gold to 0.02° corresponding to 0.2 microvolt from the couple. It was possible to detect the melting range of samples which melted only a few tenths of a degree from the melting point of the purest samples.

Such a precision was, also attained in measurements at the palladium point, but not without practice and a study of the difficulties encountered. These were, in particular, (1) deterioration of thermocouples, which became inhomogeneous, and (2) electrical leakage from the furnace to the thermoelectric circuit through refractory insulation. The most refractory procelains become fairly good conductors above 1,450° C., and considerable leakage could occur when part of the furnace was 110 volts above the ground potential. Were it not that this leakage occurred over only a short length of the couple circuit, measurements could scarcely be made at all.

First, we found that by using new annealed couples, by leaving them in the 2-holed tubes after their use had begun, and by clipping from

the end 1 cm or so after each melt that trouble with inhomogeneity was almost eliminated. It was necessary, however, to insert the couple to the same depth in the furnace each time in order to obtain satisfactory results.

Leakage caused more trouble. At first we found that at the moment of melting the emf did not always remain constant but rose and fell erratically. This was found to be caused by changes in the positions of the wires of the couple when they were relieved from a strained position by melting of the palladium. If the weld was properly made, the erratic changes at the melting point were small but were not eliminated. We tried grounding the couple and shielding it from the furnace with an intermediate grounded shield without material success.

A notable difference between gold melts and palladium melts was that when the palladium melted through, the galvanometer in the circuit was thrown violently off the scale instead of coming to a balance as on open circuit. Reversing the heating current of the furnace reversed the high potential across the galvanometer, plainly indicating the presence of leakage from the furnace winding to the couple. Believing that chemical action or electrolysis might be playing a part, we carried out a few simple tests as follows:

A couple whose hot junction had been cut open was inserted into the furnace at about 1,550° C. and emfs across the outer terminals observed under different conditions. Reversing the furnace current reversed the emf. Then we noticed that opening the heating circuit suddenly, removing high potential from the furnace, did not result in zero emf across the terminals of the couple. In one instance this emf was in excess of 1 volt but dropped so rapidly that no accurate measurement was possible.

A new couple open at the end in a new porcelain tube was inserted in the furnace at 1,550° C., and immediately afterwards the furnace current was rapidly reversed by hand, thus preventing appreciable electrolysis. After the couple had become practically as hot as the furnace, the current was suddenly cut off. The galvanometer across the outer terminals of the couple thereupon indicated no emf. After closing the furnace-heating circuit and allowing the current to pass for a minute in one direction and then again opening the circuit, the galvanometer indicated a high potential, which quickly dropped in value.

In order to obtain high precision in electrical measurements at the palladium point—that is, measurements to tenths of a microvolt—we found it best to reverse the furnace current by hand while the emf of the couple was indicating the melting of the palladium. (No steady source of alternating current was conveniently available.)

Quite satisfactory measurements were obtained which were certainly consistent to 0.5 microvolt, by exercising care in repeating melts without change in any detail. Many samples of palladium were compared as to melting point, and in a few cases of purest material special care was used.

It must not be supposed that difficulties met in thermoelectric measurements have any bearing on the results obtained with the optical pyrometer. The optical-pyrometer measurements were followed immediately by the check of the thermocouple at the melting point, without disturbing the melt couple in any way. The precision obtained in comparing different samples of palladium was necessary in identifying the purest metal but was greater than necessary in the measurements of brightness.

WASHINGTON, November 24, 1925.

A NEW SEISMOMETER EQUIPPED FOR ELECTROMAGNETIC DAMPING AND ELECTROMAGNETIC AND OPTICAL MAGNIFICATION (THEORY, GENERAL DESIGN, AND PRELIMINARY RESULTS)

By Frank Wenner

ABSTRACT

An elementary discussion is given of the principles involved in the functioning of seismometers equipped for electromagnetic damping and electromagnetic and optical magnification. These principles are then used in the development of an equation giving the relation between angular displacement of the winding of the galvanometer and the linear displacement of the ground. This equation, which is a linear differential equation of the fourth order, contains terms representing the reaction of the galvanometer upon the motion of the steady mass of the seismometer, a point which has previously been neglected and which is of importance unless the seismometer is made much larger than that for which there is any real need. A solution of this equation is given for the case of a sustained harmonic displacement of the ground. Also the corresponding equation and solution are given for the case of tilting of a horizontal-component instrument.

A procedure which may be followed in the development of a general design for a seismometer, to give approximately a specified performance, is illustrated by a concrete example. In this design the steady mass is about 500 g; the arrangement is such that the period may be determined and the damping adjusted from the recording station, which may be at a distance from the seismometer; and the magnification and its variation with the period of earth displacements, in the range from 2.5 to 60 seconds, is substantially the same as is given by a seismometer of the ordinary type having a magnification for short-period displacements of 1,250, a period of 12.5 seconds, and critical damping.

Preliminary results obtained with an experimental seismometer constructed substantially in accordance with this design are given, and a photograph of the instrument is shown.

CONTENTS

	Page
I. Introduction	964
II. Fundamental relations	966
1. Electrodynamic relations	966
2. Electromagnetic relations	967
3. Electromagnetic damping	968
4. Electromagnetic magnification	968
5. Electromagnetic damping with direct connection between seismometer and galvanometer	972
6. Electromagnetic damping with bridged circuit and ideal galvanometer	974
7. Electromagnetic magnification with bridged circuit and ideal galvanometer	974
8. Distribution of currents in bridged circuit	975

	Page
III. Equations of motions	976
1. Equation of motion of steady mass of seismometer	976
2. Equation of motion of the coil of the galvanometer	977
3. General seismometer equation	978
IV. A particular solution of the general seismometer equation	979
V. Tilting of horizontal-component seismometer	982
VI. General design	983
1. Statement of the problem	983
2. Constants of the galvanometer and electromagnetic magnification required	985
3. Moment of inertia	986
4. Displacing constant	986
5. Restoring constant	987
6. Damping constant with circuit open	987
7. Electrodynamic constant	988
8. Resistances of seismometer winding and bridge	988
VII. Performance to be expected	990
VIII. Detailed design and construction	995
IX. Summary	997
X. Appendix—symbols	998

I. INTRODUCTION

This paper presents some results of work on the development of seismometers, which is a part of an investigation initiated by the Carnegie Institution of Washington, and in which among others the Bureau of Standards and the Coast and Geodetic Survey are cooperating. Other work on the development of seismometers, which constitutes a part of the same investigation, is described in a paper [1] by Anderson and Wood. That paper described a new type of seismometer of high sensitivity employing only optical magnification and intended primarily for the registration of near-by earthquakes. This paper pertains to the development of seismometers of high sensitivity employing electromagnetic as well as optical magnification, sometimes referred to as galvanometer registration, and intended primarily for the registration of distant earthquakes.

The application of electromagnetic magnification to seismometry began to receive serious consideration about 20 years ago. In 1907 Galitzin published a paper [2] on the electromagnetic registration method. However, he referred to this method in an earlier paper [3] in which he gave results obtained with an experimental equipment on a shaking table. In 1907 Goldschmidt [4] described a plan for a seismometer using electromagnetic magnification in conjunction with mechanical magnification by means of a pointer galvanometer for producing the record on a smoked paper. As no further reference to this plan has been

[1] Anderson and Wood, Bull. Seis. Soc. Am., **15**, p. 1; 1925.
[2] Galitzin, Comp. Rend. d. sea. d. l. Comm. Sism. Per., **3**, pt. 1; 1907.
[3] Galitzin, Comp. Rend. d. sea. d. l. Comm. Sism. Per., **1**, pt. 3; 1904.
[4] Bull. Mens. Soc. Bel. D'Elec., **24**, p. 605; 1907.

found, presumably no instrument was constructed in accordance with it, or, if so, its performance was found to be unsatisfactory.

In 1909 Grunmach [5] described a seismometer, using electromagnetic magnification in conjunction with optical magnification and photographic registration, which was designed for and used in the study of vibration caused by operating machinery. This seismometer was used with a galvanometer of very short period, and therefore the characteristics of the system were such that it would give but a slight response to displacements having periods longer than one second. In other respects the equipment was not suitable for use in the usual teleseismic observations. Galitzin published a description of his vertical-component instrument [6] in 1910 and of his horizontal-component instrument [7] in 1911. He also published several other papers [8] and gave a series of lectures.[9] These papers and lectures are devoted mainly to the application of electromagnetic magnification to seismometry. He not only developed and used seismometers employing electromagnetic and optical magnification, electromagnetic damping, and photographic registration, but has given a fairly complete theory applicable to the instruments which he developed.

However, he did not take into consideration the reaction of the galvanometer upon the seismometer, except in an indirect and very incomplete way. He recommends that the period of the seismometer be adjusted to coincidence with that of the galvanometer and that the damping of the seismometer be adjusted with the galvanometer connected. With the rather large steady mass (5 kg or more) which he used, the galvanometer could affect the motion of the steady mass of the seismometer only to a nearly negligible extent. With the much smaller steady mass (1 kg or less) which I propose to use, it is necessary that the various reactions of the galvanometer upon the seismometer be taken definitely into consideration. Therefore, a theory more general than that given by Galitzin will be developed. In addition, the principles involved in electromagnetic damping and electromagnetic magnification will be discussed in an elementary way. A general design for a seismometer differing radically from any previously described will be developed and some idea given as to the performance to be expected from an instrument constructed in accordance with this design. Finally, a photograph of an experimental seismometer and parts of records obtained with it will be shown.

That this presentation of the subject may not be unnecessarily complicated no attempt will be made to state relations with extreme

[5] Grunmach, Phys. Zs., **10**, p. 853; 1909.
[6] Galitzin, Comp. Rend. d. sea. d. l. Comm. Sism. Per., **4**, pt. 2; 1910.
[7] Galitzin, Comp. Rend. d. sea. d. l. Comm. Sism. Per., **4**, pt. 1; 1911.
[8] Galitzin, Comp. Rend. d. sea. d. l. Comm. Sism. Per., **1** to **4**; 1902-1911. Comp. Rend. d. sea. d. l. Acad. d. Sci., Paris, **150**, pp. 642, 816, 901, 1041, 1727; 1910. Bull. d. l. Acad. Imp. d. Sci. d. St. Petersburg; 1909 and 1910.
[9] Vorlesungen über Seismometrie, published by B. A. Teubner; 1914.

exactness. For example, electric currents will be assumed to be in phase with the electromotive forces which cause them though the circuits are inductive, moments or torques caused by air friction will be assumed to be proportional to the relative velocity of parts of the apparatus, static friction and hysteresis will be assumed to be negligible, and the torque required to hold the steady mass in a displaced position will be assumed to be proportional to the displacement. Further, attention will be given mainly to the electrical, the electromagnetic, and electrodynamic relations, since seismologists generally may not be so familiar with these as with the mechanical and optical relations.

II. FUNDAMENTAL RELATIONS

Before proceeding to set up an equation giving the relation between the angular displacement of the coil of the galvanometer and the linear displacement of the ground, it will be to our advantage to refer to or establish a number of relations which, except for limitations of the type just referred to, may be considered as exact. It will also be to our advantage to refer to or establish other relations which must be considered as approximations or as applicable only in limiting or ideal cases. Both the more exact relations and the approximate relations will, in general, be stated in the form of equations or mathematical expressions, but to distinguish the one from the other the former will be designated by numbers and the latter by letters. It may be of assistance to the reader to know the need for both exact relations and approximate relations. The exact relations lead to expressions which are too complicated to be used in the development of a general design for a seismometer, and the approximate relations can not be relied upon to give definite information as to the performance to be expected from an equipment having known structural constants.

The symbols used will be explained as they are introduced and in connection with the more important equations. Most of them will also be explained in an appendix.

1. ELECTRODYNAMIC RELATIONS

The mechanical force acting between a conductor and a magnetic field when there is an electric current in the conductor is given by the equation

$$F = HIi \tag{1}$$

Here F is the mechanical force in a direction perpendicular to both the direction of the axis of the conductor and to the magnetic field, H is the component of the magnetic field perpendicular to the axis of the conductor, I is the length of that part of the conductor which is within the magnetic field, and i is the current in the conductor. (See

fig. 1) From equation (1) it follows that the moment or torque acting between a coil of insulated wire mounted, as shown in Figure 2, and the magnet is given by the equation

$$T = AHni \tag{2}$$

Here T is the torque, A is the area of the winding, H is the component of the magnetic field in the plane of the coil and perpendicular to the axis of rotation, and n is the number of turns of the coil. The product AHn will be referred to as the electrodynamic constant and designated as g. Therefore

$$T = gi \tag{3}$$

2. ELECTROMAGNETIC RELATIONS

If the conductor shown in Figure 1 is permitted to move perpendicular to its axis and to the magnetic field, either as the result of the

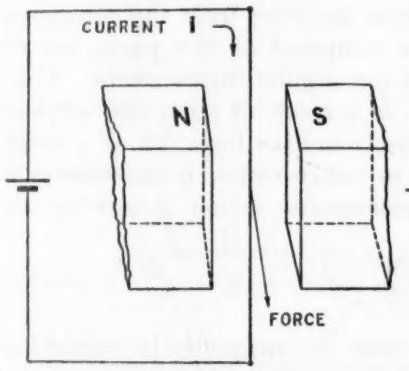

FIGURE 1.—*Electrodynamic interaction between a straight conductor and a magnetic field*

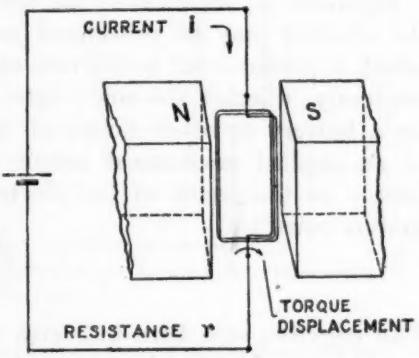

FIGURE 2.—*Electrodynamic interaction between a coiled conductor and a magnetic field*

force produced by the current or as a result of an applied mechanical force, there is developed in the conductor an electromotive force

$$e_i = -Hl\frac{\delta x}{\delta t} \tag{4}$$

Here $\delta x/\delta t$ is the rate of displacement of the conductor with respect to the magnet. If the conductor moves as a result of the current, the direction of this electromotive force is opposite to the electromotive force which causes the current, so it is sometimes referred to as a "back" electromotive force.

For the arrangement shown in Figure 2, it follows that

$$e_i = -g\frac{\delta\theta}{\delta t} \tag{5}$$

where $\delta\theta/\delta t$ is the rate of angular displacement of the coil. As the current, i, in the coil is equal to the total electromotive force in the circuit divided by the resistance,

$$i=(e+e_i)/r \tag{6}$$

Here e is the electromotive force of the battery or other source of electric power, e_i is the electromotive force developed within the coil, and r is the resistance of the circuit. From equations (3), (5), and (6) it follows that

$$T=\frac{ge}{r}-\frac{g^2\delta\theta}{r\delta t} \tag{7}$$

It should be understood that here T is only the torque resulting from the current in the winding and that an additional torque may be applied mechanically.

3. ELECTROMAGNETIC DAMPING

Equation (7) shows that the torque resulting from the current in the winding may be considered as composed of two parts, one of which is proportional to the rate of the angular displacement. Consequently, whether the coil rotates as a result of a current supplied by a battery or other source of electromotive force, or as a result of an applied mechanical torque or other cause, it experiences a torque as the result of the electromagnetic action caused by the motion equal to

$$-\frac{g^2\delta\theta}{r\delta t}$$

The negative sign here indicates that this torque is in opposition to the motion or tends to retard the motion. As the ratio of the retarding torque to the rate of angular displacement is the damping constant, it follows that that part of the damping constant resulting from electromagnetic action in the insulated electric circuit is equal to g^2/r. Other parts of the damping constant may be contributed by air friction, electric currents inducted in the frame on which the coil is wound, as in some galvanometers, in a separate copper plate associated with another magnet such as is used in some seismometers, etc.

4. ELECTROMAGNETIC MAGNIFICATION

If the electric circuit includes two insulated windings each so arranged that it is free to move in the field of a magnet as shown in Figure 3, the motion of either develops an electromotive force in the circuit. The resulting current not only causes a torque tending to retard the motion of the winding which is caused to move as the result of an applied mechanical torque, but also a torque tending to displace the other winding. Therefore if a torque is applied to either

winding, both are rotated, and consequently both develop an electromotive force. However, these two electromotive forces are not in the same direction but tend to cause currents in opposite directions through the electric circuit.

It will be convenient to think of the winding on the left as attached to the steady mass of the seismometer in such a way as to rotate about the axis of suspension, and of the magnet as being attached to the support of the seismometer; and of the winding on the right as located in the galvanometer and as having a mirror attached to it for indicating or recording photographically its angular displacements. If a torque is applied to the winding on the left—that is, to the moving system of the seismometer—and the resulting angular displacement

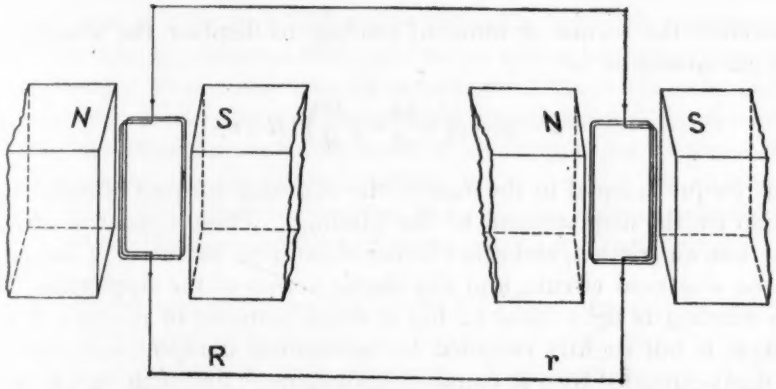

FIGURE 3.—*Two coiled conductors connected in series, each associated with a magnetic field*

One of these coiled conductors may be thought of as attached to the steady mass of a seismometer and the other as being in the galvanometer and having a mirror attached for recording its motions photographically

of each winding is considered as positive, the total electromotive force, e_t, in the circuit is given by the equation

$$e_t = G\frac{\delta\phi}{\delta t} - \frac{g\delta\theta}{\delta t} \tag{8}$$

Here G and ϕ are the electrodynamic constant and the angular displacement of the winding of the seismometer with respect to its support, and g and θ are the electrodynamic constant and angular displacement of the winding of the galvanometer. For the arrangement shown in Figure 3,

G = the area times the number of turns of the winding, times the field strength of the magnet.

For the arrangement which is to be used in a seismometer, the winding will be circular and located at a distance from the axis of rotation,

and the magnetic field will be radial toward the axis of the winding so that

G = the circumference times the number of turns of the winding times the field strength of the magnet times the distance from the center of the winding to the axis of rotation.

The current i in the circuit is the total electromotive force $G\frac{\delta\phi}{\delta t}-g\frac{\delta\theta}{\delta t}$ divided by the resistance of the circuit $R+r$, or

$$i=\left(G\frac{\delta\phi}{\delta t}-g\frac{\delta\theta}{\delta t}\right)/(R+r) \tag{9}$$

Therefore the torque or moment tending to displace the winding of the galvanometer is

$$T=gi=g\left(G\frac{\delta\phi}{\delta t}-g\frac{\delta\theta}{\delta t}\right)/(R+r) \tag{10}$$

This torque is equal to the sum of the opposing torques brought into action by the displacement of the winding. These consist of inertia reaction, air friction, and other forms of damping exclusive of damping in the electrical circuit, and the elastic action of the suspension. If the winding is light (that is, has a small moment of inertia), if the motion is but slightly retarded by mechanical damping and there is no short-circuited turn to cause electromagnetic damping, and if there is but slight constraint by the suspensions, the torque required to produce the motion $\delta\theta/\delta t$ is small. If, in addition, both G and g are fairly large and $R+r$ is small, experience shows that, for conditions such as are met in teleseismic observations, $G\frac{\delta\phi}{\delta t}-g\frac{\delta\theta}{\delta t}$ is very small in comparison with either $G\frac{\delta\phi}{\delta t}$ or $g\frac{\delta\theta}{\delta t}$, or that

$$G\frac{\delta\phi}{\delta t}=g\frac{\delta\theta}{\delta t} \text{ approximately} \tag{A}$$

From this it follows by integration that

$$\frac{\theta}{\phi}=\frac{G}{g} \text{ approximately} \tag{B}$$

To the extent that these conditions are realized, the angular displacement of the winding of the galvanometer will be proportional to, and in phase with, the displacement of the steady mass with respect to its support, and the electromagnetic magnification will be equal to

$$\frac{G}{g} \tag{C}$$

A galvanometer giving an angular deflection at all times very nearly proportional to the angular displacement of the steady mass of the seismometer will be considered as ideal. The motion of the winding of such a galvanometer would be that necessary to develop a back electromotive force at every instant very nearly equal to the potential difference applied at its terminals or the electromotive force developed in the seismometer winding in case of a direct connection, as shown in Figure 3. Consequently, the current through the winding would be extremely small. For the galvanometer to give an exact duplication on a magnified scale of the motion of the seismometer winding with respect to its support, it would be necessary for the galvanometer to develop a back electromotive force exactly equal to the potential difference applied across its terminals. This in no case can be fully realized, and if it could would not be desirable, since the performance would then be the same as with mechanical and optical magnification. It is assumed that what may be considered ideal is that the galvanometer give a fairly accurate magnified reproduction of the displacement of the steady mass with respect to its support for frequencies of importance in teleseismic observations, but not follow the extremely short-period disturbances resulting from traffic, moving machinery, etc., nor the long-period disturbances resulting from temperature changes, etc.

The actions and reactions taking place in electromagnetic magnification are of such importance in connection with the theory and especially in connection with the design of seismometers of the type under consideration that it may be well to repeat a part of what has just been said in a somewhat different way. If each of the two windings is arranged to rotate about an axis parallel to its plane and passing through its geometric centers perpendicular to the field of its magnet, as shown in Figure 3, any rotation of either winding causes a change in the magnetic flux through it or a change in the magnetic flux linking the circuit, and the other winding tends to move in such a way as to keep the flux linking the circuit constant.

The change in the flux linking the circuit, assuming that only one of the windings is rotated, would be equal to its area, times the number of turns, times the field strength, times the angular displacement. Therefore the other winding tends to turn in the opposite direction by an amount such as to make its area times the number of its turns, times the field strength of its magnet, times its angular displacement, equal to that of the first. This is not only the action that tends to take place but actually would take place if the second winding had no moment of inertia, no damping, and no spring or other device tending to hold or bring it to a definite position. It is also the action which would take place if the electrical resistance of the circuit could be made zero or negligibly small. Further, if the

product of the area and number of turns of each of the windings times the field strength of each of the magnets is large, the inertia, damping, and restraint of each of the windings are small; and the resistance of the circuit is small, the relative motions of the two windings would be substantially the same as though they were mechanically connected in such a manner that any rotation of either would be duplicated by the other in reversed direction except that the magnitudes of the rotations would be in the inverse ratio of their electrodynamic constants. For example, if the two windings had equal areas and moved in equal magnetic fields but had turns in the ratio of 2 to 1, the one having the smaller number of turns would move through twice the angle moved through by the other.

In practice it is not possible to construct a galvanometer having a negligible moment of inertia, negligible damping and negligible restraint by the suspensions, a negligible resistance, or an extremely large electrodynamic constant. However, it is possible to construct a galvanometer having such relations between its structural constants that for the purpose of design it may be assumed that the angular displacement of its winding will be a magnified duplication of the angular displacement of the steady mass of the seismometer with respect to its support.

5. ELECTROMAGNETIC DAMPING WITH DIRECT CONNECTION BETWEEN THE SEISMOMETER AND GALVANOMETER

In the preceding section it was pointed out that the current in the circuit is equal to

$$\left(G\frac{\delta\phi}{\delta t}-g\frac{\delta\theta}{\delta t}\right)/(R+r)$$

If this current is brought about by the application of a mechanical torque tending to displace the winding of the seismometer with respect to its magnet, the resulting electrodynamic action is not only a torque

$$g\left(G\frac{\delta\phi}{\delta t}-g\frac{\delta\theta}{\delta t}\right)/(R+r)$$

tending to displace the winding of the galvanometer, but a torque

$$G\left(G\frac{\delta\phi}{\delta t}-g\frac{\delta\theta}{\delta t}\right)/(R+r) \tag{11}$$

tending to retard or damp the motion of the winding of the seismometer. However, it has just been assumed that the winding of the galvanometer should move in such a way as to develop a back electromotive force very nearly equal to the potential difference impressed across its terminals, or in this case that $G\frac{\delta\phi}{\delta t}$ and $g\frac{\delta\theta}{\delta t}$ should

be very nearly equal. Therefore the current must be very small, and consequently it can cause only a slight retardation of the motion of the winding of the seismometer. Thus, it will be seen that the desired performance of the galvanometer has the effect of practically destroying electromagnetic damping in the system. In fact, a satisfactory performance of both galvanometer and seismometer can not be obtained if the only provision for damping is in a simple series circuit, such as that showing in Figure 3.

The necessary damping may be obtained electromagnetically by the use of either of two fairly simple means. One of these means consists in the use of two circuits in the seismometer—one, which may consist simply of a copper plate, for producing the desired damping and the other for connection to the galvanometer to produce the desired electromagnetic magnification. The other means consists of the use of a bridge or shunt across the circuit as shown in Figure 4.

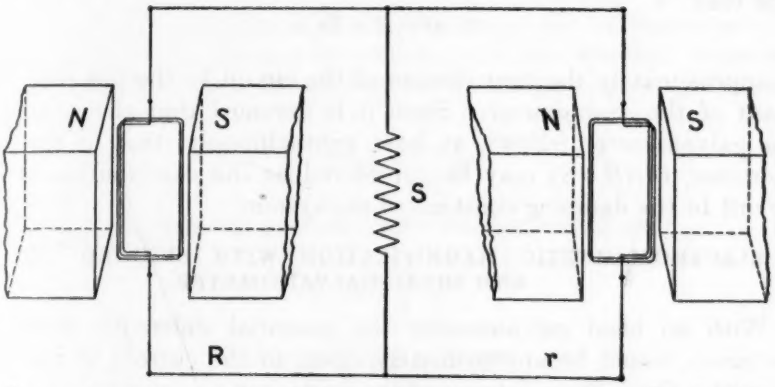

FIGURE 4.—*Bridge circuit used with the seismometer, the design of which is to be developed later*

Here R represents the resistance of the seismometer winding and the leads connecting it to the recording station; r represents the resistance of the galvanometer winding, suspensions, and leads; S represents the resistance of the bridge or shunt, the adjustment of which serves to bring about an optimum damping of the system

With this arrangement the electromotive forces induced in the windings tend, in general, to cause currents in opposite directions in them but in the same direction through the bridge. Therefore whenever there is a motion of the windings there will be a current in one or both, and consequently electromagnetic damping of the system. By a suitable choice of the resistance of the bridge, provided the apparatus is properly designed, this damping may be adjusted to an optimum value. The former of these means is used in the apparatus designed by Galitzin and similar apparatus designed by Wilip, but as compared with it the latter has a number of advantages, especially if the steady mass of the seismometer is made small. For this reason it will be presumed that the latter will be used though the analysis which will be made is applicable in either case.

6. ELECTROMAGNETIC DAMPING WITH BRIDGED CIRCUIT AND IDEAL GALVANOMETER

With an ideal galvanometer—that is, a galvanometer developing at every instant an electromotive force very nearly equal to but in opposition to the potential difference impressed across its terminals—there is but little current through its winding. Consequently the current through the seismometer winding is

$$G\frac{\delta\phi}{\delta t}/(R+S) \text{ approximately} \tag{D}$$

Here S is the resistance of the bridge. From this and equation (3) it follows that the retarding torque is

$$G^2\frac{\delta\phi}{\delta t}/(R+S) \text{ approximately} \tag{E}$$

and that

$$G^2/(R+S)$$

is approximately the contribution of the circuit to the damping constant of the seismometer. Since it is assumed that the motion of the galvanometer follows, at least approximately, that of the seismometer, $G^2/(R+S)$ may be considered as the contribution of the circuit to the damping constant of the system.

7. ELECTROMAGNETIC MAGNIFICATION WITH BRIDGED CIRCUIT AND IDEAL GALVANOMETER

With an ideal galvanometer the potential difference across its terminals would be approximately equal to the current in the seismometer times the resistance of the bridge, or

$$G\frac{\delta\phi}{\delta t}\frac{S}{R+S}$$

and this is approximately equal to the electromotive force developed in the winding of the galvanometer or

$$g\frac{\delta\theta}{\delta t}$$

that is

$$G\frac{\delta\phi}{\delta t}\frac{S}{R+S}=g\frac{\delta\theta}{\delta t} \text{ approximately} \tag{F}$$

from which it follows that the electromagnetic magnification is

$$\frac{G}{g}\frac{S}{R+S} \text{ approximately} \tag{G}$$

8. DISTRIBUTION OF CURRENTS IN BRIDGED CIRCUIT

In a part of the above discussion it was assumed that the galvanometer would give an ideal performance. However, any galvanometer which might be used in connection with a seismometer must be expected to give a performance differing from this, at least slightly slightly under the most favorable conditions and greatly if the period of the disturbance is very short or very long. Consequently it is necessary that the relation between the currents and the electromotive forces be established without reference to the performance of the galvanometer.

The current in the seismometer winding which would result from an electromotive force developed only in its winding would be

$$G\frac{\delta\phi}{\delta t}/[R+rS/(r+S)] \tag{12}$$

and the fractional part of this passing through the galvanometer would be $S/(r+S)$; that is, if the winding of the galvanometer were clamped so as to prevent its motion while the winding of the seismometer were moved, the current in the seismometer winding would be

$$G(r+S)\frac{\delta\phi}{\delta t}/Q^2 \tag{13}$$

and the current in the galvanometer winding would be

$$GS\frac{\delta\phi}{\delta t}/Q^2 \tag{14}$$

where

$$Q^2=rR+rS+RS \tag{15}$$

Likewise the current in the galvanometer winding resulting only from an electromotive force in its winding would be

$$-g\frac{\delta\theta}{\delta t}/[r+SR/(S+R)] \tag{16}$$

and the fractional part of this current passing through the seismometer winding would be $S/(R+S)$; that is, if the winding of the seismometer were clamped so as to prevent its motion while the winding of the galvanometer were moved in the direction in which it would move as a result of as positive displacement of the winding of the seismometer, the current in the galvanometer winding would be

$$-g(R+S)\frac{\delta\theta}{\delta t}/Q^2 \tag{17}$$

and the current in the seismometer winding would be

$$-gS\frac{\delta\theta}{\delta t}/Q^2 \tag{18}$$

However, as the apparatus is used both windings move and consequently both develop electromotive forces. Therefore if I is the current in the seismometer winding resulting from the electromotive forces developed in both windings, it follows from equations (13) and (18) that

$$I=G(r+S)\frac{\delta\phi}{\delta t}/Q^2-gS\frac{\delta\theta}{\delta t}/Q^2 \tag{19}$$

and if i is the current in the galvanometer winding resulting from the electromotive forces developed in both windings, it follows from equations (14) and (17) that

$$i=GS\frac{\delta\phi}{\delta t}/Q^2-g(R+S)\frac{\delta\theta}{\delta t}/Q^2 \tag{20}$$

Equations (19) and (20) will be used in the next section in establishing the relation between displacements of the support of a seismometer or the ground, and displacements of the winding of a galvanometer when a seismometer and galvanometer are connected as shown in Figure 4. Other parts of what has preceded will be used later in the development of a general design for a seismometer.

III. EQUATIONS OF MOTION

Having considered some of the electrical, electromagnetic, and electrodynamic relations, it is in order to set up the equation of motion of the steady mass of the seismometer, the equation of motion of the coil of the galvanometer, and the general seismometer equation; that is, the equation giving the relation between the motion of the coil of the galvanometer and the displacement of the support of the seismometer.

1. EQUATION OF MOTION OF STEADY MASS OF SEISMOMETER

With no externally applied moments or torques, no motion of the support of the seismometer, and with the electric circuit open, the equation of motion of the seismometer may be written as follows:

$$K\frac{\delta^2\phi}{\delta t^2}+D\frac{\delta\phi}{\delta t}+U\phi=0 \tag{21}$$

Here K is the moment of inertia of the steady mass about the axis of rotation.

D is the damping constant or the ratio of the retarding torque to the angular velocity. It includes all forms of damping present when the electric circuit is open.

U is the restoring constant or ratio of the restoring torque to the angular displacement.

ϕ is the angular displacement; and

t is the time.

This is the equation of motion of a freely swinging pendulum for small amplitudes. It is developed in textbooks on physics, mechanics, and seismometry.

If the seismometer is moved linearly in a direction perpendicular both to the axis of rotation and to a line passing through the axis of rotation and the center of mass, and if the angular displacement ϕ resulting from this displacement is taken as positive, to prevent an angular displacement it would be necessary to apply a torque $-LM\frac{\delta^2 X}{\delta t^2}$. Here

L is the distance from the axis of rotation to the center of "steady" mass.

M is the mass of the moving system.

X is the displacement of the support.

Consequently the torque resulting from the displacement or rather the acceleration of the support of the seismometer is

$$LM\frac{\delta^2 X}{\delta t^2} \tag{22}$$

If, in addition, the circuit is closed so that a current may flow as a result of the electromotive forces induced in the winding of the seismometer and the connected galvanometer, there is an additional torque supplied through the winding of the seismometer. This torque is equal to

$$-GI \tag{23}$$

where G is the electrodynamic constant of the seismometer and I is the current in the seismometer winding.

If, therefore, there is a motion of the support of the seismometer and the resulting motion of the steady mass is permitted to cause a current in the winding, the equation of motion of the steady mass with respect to its support is

$$K\frac{\delta^2\phi}{\delta t^2}+D\frac{\delta\phi}{\delta t}+U\phi=LM\frac{\delta^2 X}{\delta t^2}-GI \tag{24}$$

2. EQUATION OF MOTION OF THE COIL OF THE GALVANOMETER

The equation of motion of the coil of the galvanometer may be written as follows:

$$k\frac{\delta^2\theta}{\delta t^2}+d\frac{\delta\theta}{\delta t}+u\theta=gi \tag{25}$$

Here

k is the moment of inertia of the moving system,
d is the damping constant with the circuit open,
u is the restoring constant,
g is the electrodynamic constant,
θ is the angular displacement,
t is the time, and
i is the current through the winding.

It may be noted that in equations (24) and (25) the terms GI and gi have opposite signs. The difference in sign results from the assumption that the relative motion of the winding and support of the seismometer is the primary cause for the current in the seismometer winding and that the current in the galvanometer winding is the primary cause for its motion with respect to its support. The other difference between these two equations results from the assumption that the axis of rotation of the moving system of the galvanometer passes through its center of mass so that a linear acceleration of the support of the galvanometer has no tendency to cause an angular displacement.

3. GENERAL SEISMOMETER EQUATION

With a bridged circuit such as is shown in Figure 4, expressions for I and i are given by equations (19) and (20). Substituting these in equations (24) and (25) gives

$$K\frac{\delta^2\phi}{\delta t^2}+[D+G^2(r+S)/Q^2]\frac{\delta\phi}{\delta t}+U\phi=LM\frac{\delta^2 X}{\delta t^2}+\frac{GgS}{Q^2}\frac{\delta\theta}{\delta t} \tag{26}$$

and

$$k\frac{\delta^2\theta}{\delta t^2}+[d+g^2(R+S)/Q^2]\frac{\delta\theta}{\delta t}+u\theta=\frac{GgS}{Q^2}\frac{\delta\phi}{\delta t} \tag{27}$$

It may be noted that each of these equations contains a term representing electromagnetic damping in the circuit, that the former contains a term representing the effect of the motion of the galvanometer winding upon the relative motion of the steady mass and support of the seismometer, and that the latter contains a term representing the effect of the relative motion of the steady mass and its support upon the motion of the galvanometer winding.

With seismometers of the type under consideration the user will wish to know the ratio of the displacements as shown on the record, which will be proportional to the angular displacements of the winding of the galvanometer, to displacements of the ground, but need not be concerned with the relative motion of the steady mass with respect to its support. Consequently equations (26) and (27) may be combined in such a way as to eliminate ϕ, $\frac{\delta\phi}{\delta t}$ and $\frac{\delta^2\phi}{\delta t^2}$. To do this it is only necessary to differentiate the equations and make the proper substitutions.

Differentiating equation (26) gives

$$K\frac{\delta^3\phi}{\delta t^3}+[D+G^2(r+S)/Q^2]\frac{\delta^2\phi}{\delta t^2}+U\frac{\delta\phi}{\delta t}=LM\frac{\delta^3 X}{\delta t^3}+\frac{GgS}{Q^2}\frac{\delta^2\theta}{\delta t} \tag{28}$$

Differentiating equation (27) gives

$$k\frac{\delta^3\theta}{\delta t^3}+[d+g^2(r+S)/Q^2]\frac{\delta^2\theta}{\delta t^2}+u\frac{\delta\theta}{dt}=\frac{GgS}{Q^2}\frac{\delta^2\phi}{\delta t^2} \tag{29}$$

Differentiating equation (29) or equation (27) a second time gives

$$k\frac{\delta^4\theta}{\delta t^2}+[d+g^2(R+S)/Q^2]\frac{\delta^3\theta}{\delta t^3}+u\frac{\delta^2\theta}{\delta t^2}=\frac{GgS}{Q^2}\frac{\delta^3\phi}{\delta t^3} \tag{30}$$

Equations (27), (29), and (30) contain expressions for $\frac{\delta\phi}{\delta t}$, $\frac{\delta^2\phi}{\delta t^2}$, $\frac{\delta^3\phi}{\delta t^3}$, which when substituted into equation (28) give

$$\frac{\delta^4\theta}{\delta t^4}+m\frac{\delta^3\theta}{\delta t^3}+n\frac{\delta^2\theta}{\delta t^2}+o\frac{\delta\theta}{\delta t}+p\theta=q\frac{\delta^3 X}{\delta t^3} \tag{31}$$

and this will be referred to as the general seismometer equation. Here

$$\begin{aligned}
m&=\frac{D}{K}+\frac{G^2(r+S)}{KQ^2}+\frac{d}{k}+\frac{g^2(R+S)}{kQ^2}\\
n&=\frac{Dd}{Kk}+\frac{u}{k}+\frac{U}{K}+\frac{dG^2(r+S)+Dg^2(R+S)}{kKQ^2}\\
o&=\frac{dU+Du}{Kk}+\frac{Ug^2(R+S)+uG^2(r+S)}{kKQ^2}\\
p&=\frac{Uu}{Kk}\\
q&=\frac{LMgGS}{KkQ^2}
\end{aligned} \tag{32}$$

The general seismometer equation (31) is a fourth-order linear differential equation with constant coefficients. It is much more complicated than the second-order linear differential equation with constant coefficients, which is usually given for the relation between the relative displacement of the steady mass and the support of the seismometer when the latter is subjected to accelerations. Therefore, no attempt will be made to get a solution of it except for the case of a sustained harmonic displacement of the support; that is, of the ground. This, however, will suffice to show how the magnification and phase angle depends upon the constants of the seismometer, the constants of the galvanometer, the resistance of the bridge, and the frequency or period of the disturbance.

IV. A PARTICULAR SOLUTION OF THE GENERAL SEISMOMETER EQUATION

In deriving a particular solution of the general seismometer equation the complex number or vector notation will be used; that is, it will be assumed that the displacement X is the real part of the expression

$$\mathfrak{R}\cos(\omega t+\alpha)-j\mathfrak{R}\sin(\omega t+\alpha) \tag{33}$$

This may be written

$$X = \mathfrak{R}[(\epsilon^{j(\omega t+\alpha)} + \epsilon^{-j(\omega t+\alpha)})/2 + (\epsilon^{j(\omega t+\alpha)} - \epsilon^{-j(\omega t+\alpha)})/2]$$

$$= \mathfrak{R}\epsilon^{j\alpha}\epsilon^{j\omega t}$$

$$= X\epsilon^{j\omega t} \text{ (real part only).} \tag{34}$$

Here $\omega = 2\pi$ times the frequency or 2π divided by the period of the earth displacement.

t = the time from any arbitrary starting point.

α = the phase angle and depends upon the starting point of t.

$j = \sqrt{-1}$.

ϵ = the base of the Napierian logarithm.

$\boldsymbol{X}$ = a complex quantity equal in magnitude to the amplitude of the earth displacement and containing the phase angle α.

Since X is a harmonic function of time, derivatives of X, and the angular displacement of the galvanometer winding and its derivatives, are harmonic functions of time and all have the same frequency or period. Consequently the angular deflection of the galvanometer winding is given by the equation

$$\theta = \Theta\epsilon^{j\omega t} \text{ (real part only)} \tag{35}$$

where Θ is a complex quantity equal in magnitude to the amplitude of the deflection of the galvanometer winding and containing a phase angle β, differing in general from the phase angle α. Successive differentiation of equation (35) gives

$$\frac{\delta\theta}{\delta t} = j\omega\Theta\epsilon^{j\omega t}$$

$$\frac{\delta^2\theta}{\delta t^2} = -\omega^2\Theta\epsilon^{j\omega t} \tag{36}$$

$$\frac{\delta^3\theta}{\delta t} = -j\omega^3\Theta\epsilon^{j\omega t}$$

$$\frac{\delta^4\theta}{\delta t^4} = \omega^4\theta\epsilon^{j\omega t}$$

Differentiation of equation (34) three times gives

$$\frac{\delta^3 X}{\delta t^3} = -j\omega^3 X\epsilon^{j\omega t} \tag{37}$$

Substituting these expressions for Θ and its derivatives and the derivative of X in equation (31) gives

$$[\omega^4 - j\omega^3 m - \omega^2 n + j\omega O + p]\ \Theta\epsilon^{j\omega t} = -j\omega^3 q X\epsilon^{j\omega t}$$

or

$$\Theta/X = -j\omega^3 q/[\omega^4 - j\omega^3 m - \omega^2 n + j\omega o + p] \tag{38}$$

The amplitude of displacements as shown on the record is equal to Θl where l is the effective length of the galvanometer pointer. Since the record is to be produced photographically by means of a light beam reflected from a mirror attached to the galvanometer winding, usually l is equal, at least approximately, to twice the distance between the mirror and the recording paper. Consequently the magnification M_x—that is, the ratio of the displacements shown on the record to the displacements of the ground—is equal to $\Theta l/X$. Therefore

$$M_x = -j\omega^3 ql/[\omega^4 - j\omega^3 m - \omega^2 n + j\omega o + p]$$

Replacing m, n, O, p, and q by their equivalents, as given by equation (32), gives

$$M_x = \frac{MLGgSl}{\begin{array}{l}(Dk + dK)Q^2 + G^2 k(r + S) + g^2 K(R + S) \\ -[(Du + dU)Q^2 + G^2 u(r + S) + g^2 U(R + S)]/\omega^2 \\ + j\omega kKQ^2 \\ -j\,[(Dd + uK + Uk)Q^2 + G^2 g^2 + G^2 d(r + S) + g^2 D(R + S)]/\omega \\ + juUQ^2/\omega^3\end{array}} \tag{39}$$

This equation will be used in determining the performance characteristics of a seismometer equipment having structural constants corresponding to those of the general design to be developed later and may be used for this purpose in cases in which the structural constants are determined experimentally. This equation may also be used in determining the performance characteristics of a seismometer equipment of the Galitzin type, providing the structural constants are known or determined experimentally. However, in such cases there may or may not be a bridge or shunt across the terminals of the galvanometer. If no shunt is used, S is infinite, so terms not containing S may be neglected and the equation simplified by dividing both numerator and denominator by S. It should be noted that Q^2 contains S and that in this case

$$Q^2/S = R + r$$

Equation (39) applies only after the displacement has continued for a sufficiently long time for a steady state to be reached and does not give any indication as to how long that is. Therefore the equa-

tion gives directly but little information concerning the relation between the displacement shown on the record and the displacement of the earth just after the beginning or end of a disturbance or the beginning or end of a phase. However, if the apparatus is so designed that the performance of the galvanometer approximates what has been referred to as ideal and the system is properly damped, the effect of transients will be substantially the same as for properly damped seismometers having mechanical or mechanical and optical magnification.

Equation (39) might be rationalized, but to do so would make it more rather than less complicated. Calculations may be made by first substituting numerical values, then summing the real and imaginary (those containing j) terms separately, squaring each, adding and extracting the square root. The ratio of the sum of the imaginary terms to the sum of the real terms multiplied by -1 is the tangent of the angle by which the displacements shown on the record lag in phase behind the displacements of the ground.

V. TILTING OF HORIZONTAL-COMPONENT SEISMOMETER

The discussion given above is applicable to both vertical and horizontal component instruments. With either, the tilting or rotation accompanying seismic disturbance having a distant origin have but slight or negligible effect. However, with horizontal-component instruments the long-period tiltings of local origin, such as changes in the level of the pier on which the instrument is mounted, either as the result of temperature changes, gradual settling, or change in position of large masses near it, have a marked effect. Likewise the change in the stiffness of the spring of a vertical-component instrument as a result of gradual weakening or as a result of temperature changes has a marked effect. It will, therefore, be of interest to see how apparatus of the type under consideration behaves for such disturbances.

If a horizontal-component seismometer is subjected to tilt about a horizontal axis through the center of its steady mass and normal axis of rotation instead of a linear acceleration, the equation of motion of the steady mass with respect to its support has the term $ML\frac{\delta^2 X}{\delta t^2}$ replaced by the term $ML\mathfrak{g}\psi$ where $\mathfrak{g}$ is the acceleration of gravity and ψ is the angle of tilt. Therefore, $LM\mathfrak{g}\frac{\delta\psi}{\delta t}$ may be substituted for $LM\frac{\delta^3 X}{\delta t^3}$ in the general seismometer equation (31). Since for a harmonic disturbance

$$\frac{\delta^3 X}{\delta t^3} = -j\omega^3 \boldsymbol{X} e^{j\omega t} \tag{40}$$

and

$$\frac{\delta\psi}{\delta t} = j\omega\Psi e^{j\omega t}$$

the magnification of tilts, M_ψ, is the same as the magnification of displacements, M_x, except for the factor $-\mathfrak{g}/\omega^2$. The magnification of tilts, therefore, may be obtained by multiplying the right-hand member of equation (39) by $-\mathfrak{g}/\omega^2$. This gives

$$M_\psi = \frac{-MLg\mathfrak{g}GSl}{\begin{array}{l}\omega^2[(Dk+dK)Q^2+G^2k(r+S)+g^2K(R+S)] \\ -(Du+dU)Q^2+G^2u(r+S)+g^2U(R+S) \\ +j\omega^3kKQ^2 \\ -j\omega[(Dd+uK+Uk)Q^2+G^2g^2+G^2d(r+S)+g^2D(R+S)] \\ +juUQ^2/\omega\end{array}} \qquad (41)$$

Here the minus sign in the numerator of the right-hand member signifies that 180° is to be subtracted from the phase angle when determined as explained above.

In cases in which the magnification and phase angle of displacements have already been calculated, the magnification and phase angle of tilts may be obtained by multiplying the calculated values by $\mathfrak{g}/\omega^2$ and adding 180°.

As used here, M_ψ is not strictly a magnification, since it is equal to the amplitude of the linear displacement shown on the record divided by the amplitude of the angle of tilt instead of a ratio of two similar quantities.

VI. GENERAL DESIGN

1. STATEMENT OF THE PROBLEM

Equations (39) and (41) show how the magnification and phase angle of earth displacements and earth tilts depend upon the various structural constants of the seismometer and galvanometer, the resistance of the bridge, the distance between the galvanometer mirror and the recording paper, and the period of the disturbance. It might appear, therefore, that simply by a suitable choice of values for these almost any performance desired might be obtained. However, in such apparatus values which may be taken for certain of the constants are more or less definitely limited by values taken for other constants. A case in point is the ratio of the moment of inertia to the restoring constant. If this is made greater than 4, the period is longer than 12.5 seconds, and, in general, it can not be made more than two or three times this without the instrument becoming definitely unstable. Likewise, with the galvanometer, the electrodynamic constant can not be increased indefinitely while both the electrical resistance and moment of inertia of the winding are kept below definite limits. There are many such limitations, so while it would be possible to select a set of values for the various constants to give, for example, the same magnification for displacements of all periods, difficulties would be encountered in either or both the con-

struction and use of the apparatus. Therefore, in deciding what not only should be considered as a good performance but one that may be within the possibility of attainment, we shall be guided mainly by the experience of others.

It seems that except for the shifting of the rest point or general lack of stability, and in some cases the response to short-period disturbances of local origin, the usual type of seismometer having a high static magnification, a very long period, and critical or near-critical damping would give the type of record desired for teleseismic observations. Difficulties in maintaining a suitable stability increase both as the magnification is increased and as the period is increased, so that usually with a magnification of as much as 400 it is not practicable to have the period longer than about 10 seconds. With electromagnetic magnification there can be a gradual shift in the position of the steady mass without a corresponding shift in the position of the galvanometer winding. The difficulties arising from a moderate lack of stability are therefore much less, and consequently a somewhat longer period and a considerably higher magnification may be used. In fact, this constitutes one of the main advantages to be gained by the use of electromagnetic magnification. It will, therefore, be assumed that the free period is to be 12.5 seconds and the combined optical and electromagnetic magnification is to be such that the displacements shown on the record will be approximately the same as would be given an ordinary type of seismometer having the same period, critical damping, and a static magnification of 1,000.

Galvanometers known as the fluxmeter type, which have been on the market for a number of years, have such relations between their constants that for conditions such as are met in teleseismic observations they give approximately the ideal performance referred to above; that is, their characteristics are such that when connected to a suitably designed winding on a seismometer they should give a reasonably accurate record of the displacements of the steady mass with respect to its support. In fact, except for minor defects, which need not be considered here, they seem to be nearly as good as any which might be made, especially for the purpose. It will, therefore, be assumed that a particular one of these galvanometers is to be used without change and that the problem is to so design the seismometer that when used with this galvanometer the performance will approximate that just stated, except that the record should have the appearance of much greater stability of the rest or zero position, and the magnification of very short period displacements should be relatively small. Further, it will be assumed that the seismometer should be small in size, reasonably inexpensive to construct, be fairly rugged, and require but few adjustments and these of a type easily made.

2. CONSTANTS OF GALVANOMETER AND ELECTROMAGNETIC MAGNIFICATION REQUIRED

It now becomes necessary to consider the magnitude of the various constants affecting the performance of the apparatus and, therefore, to decide upon a system of units. While the equations given above may be used with any consistent system of units, that which will be used is based on the centimeter as the unit of length, the gram as the unit of mass, the second as the unit of time, and the magnetic permeability of air (or vacuum) as the unit of magnetic permeability.

In this system of units the structural constants of the galvanometer as determined from five independent measurements of its performance are as follows:

$$k = 1.62$$
$$d = .05$$
$$u = .318$$
$$g = 623{,}000$$
$$r = 10^{10}$$

Also the focal length of the mirror is such that the distance between the mirror and the recording paper can conveniently be made 1 m. Consequently it may be presumed that

$$l = 200$$

If the steady mass remained strictly at rest, the magnification M_x would be equal to

$$\frac{l}{L} \times \frac{\Theta}{\Phi}$$

where l/L may be referred to as the optical magnification and Θ/Φ is the electromagnetic magnification, which will be designated as h.

l is the effective length of the galvanometer pointer which, with the optical system to be used, is equal to twice the distance between the galvanometer mirror and the recording paper.

L is the distance from the center of the steady mass to the axis of rotation.

Θ is equal in magnitude to the amplitude of the angular deflection of the galvanometer winding.

Φ is equal in magnitude to the amplitude of the angular deflection of the moving system of the seismometer with respect to its support.

Since l equals 200 cm for M_x, to equal 1,000 it would be necessary for the electromagnetic magnification h to equal 1,000 $L/200$ cm or 5 L/cm. However, the steady mass is displaced when the support is displaced both because all of the steady mass can not be concentrated at the same distance from the axis of rotation and because of the moment of inertia of the galvanometer, and the resulting loss in

magnification, in proportional parts, is equal to the displacement of the steady mass divided by the displacement of the support.

An assumption as to how much should be allowed as the loss in magnification resulting from these two causes constitutes a starting point in the development of a general design for a seismometer. For the present, it will be assumed that this loss will amount to 50 per cent. As the design progresses, this assumption may be revised and the design started anew should it be found that it is unreasonable. This loss in magnification can be compensated for by doubling the electromagnetic magnification; that is, by making it 10 L/cm instead of 5 L/cm.

3. MOMENT OF INERTIA

With an ideal galvanometer, the reactions between the galvanometer and the seismometer are substantially the same as though there were a direct mechanical connection between them. Consequently the loss in magnification [10] because of the moment of inertia of the winding of the galvanometer is the same as would result if h^2k/L^2 grams could be added to the steady mass at a distance L from the axis of rotation without in any way affecting the displacing constant, ML. Since $h=10L$/cm and $k=1.62$, h^2k/L^2 is equivalent to 162 g. Therefore, if the loss in magnification because of the moment of inertia of the galvanometer winding is not to be excessive, the steady mass must be large in comparison with 162 g. However, there is not much to be gained by making it larger by a factor of more than 5, and in order that the cost may not be unnecessarily large it is desirable to keep the steady mass small. Therefore 500 g will be taken as representing what seems to be a fair compromise between somewhat conflicting requirements.

If the steady mass is taken as 500 g and placed with its center at a distance of 20 cm from the axis of rotation, which seems might be convenient, the moment of inertia will be somewhat greater than 500×20^2. It must be somewhat greater than this, since the steady mass must include the winding and various supports, as well as the steady mass proper, all of which can not be placed at the same distance from the axis of rotation. It will, therefore, be assumed that the moment of inertia K of the moving system of the seismometer is to be 2.5×10^5 g cm^2. With L equal to 20 cm, the optical magnification as defined above becomes 10 and the electromagnetic magnification h becomes 200.

4. DISPLACING CONSTANT

With a steady mass of 500 g and the distance from the center of mass to the axis of rotation equal to 20 cm the displacing constant ML equals 10,000 g cm.

[10] Reid, The California Earthquake of Apr. 18, 1906, 2, p. 155; 1910.

Since $K=2.5\times10^5$ and this, in effect, is increased by h^2k or 0.648×10^5, and $ML^2=2\times10^5$, the loss in magnification on account of a lack of concentration of the steady mass and on account of the moment of inertia of the galvanometer winding is $(3.148-2)/3.148$, or 37 per cent. Therefore the assumption made above that the loss in magnification from these two causes would amount to 50 per cent was somewhat over liberal, but scarcely so much as to justify a revision of the values selected for the steady mass and moment of inertia.

5. RESTORING CONSTANT

According to the pendulum formula, the free or undamped period, T_0, is given by the equation

$$T_0=2\pi\sqrt{K/U} \tag{42}$$

Since it has been assumed that the free period would be adjusted to 12.5 seconds and the value 2.5×10^5 has been selected for the moment of inertia K, it is necessary that the restoring constant

$$\begin{aligned}U&=4\pi^2\times2.5\times10^5/12.5^2\\&=6.25\times10^4\text{ g cm}^2/\text{sec.}^2\end{aligned}$$

6. DAMPING CONSTANT WITH THE CIRCUIT OPEN

No effort will be made to damp the motion of the steady mass with the circuit open. There will, however, be some damping because of air friction, etc., but this probably will amount to not more than one-tenth that which would be required to produce critical damping.

The equation for the motion of the seismometer with the circuit open and no driving torque is

$$K\frac{\delta^2\phi}{\delta t^2}+D\frac{\delta\phi}{\delta t}+U\phi=0$$

as given above, equation (21), and for the motion to be critically damped it is necessary that[11]

$$D=2\sqrt{KU} \tag{43}$$

Since

$$K=2.5\times10^5\text{ and }U=6.25\times10^4$$

for critical damping it would be necessary that $D=25\times10^4$. It will, therefore, be considered that $D=25\times10^3$ g cm^2/sec. This value for D will have but a slight effect upon the performance of the apparatus, so it would make but little difference if by change it should be larger or smaller by as much as 100 per cent.

7. ELECTRODYNAMIC CONSTANT

What has preceded fixes the electromagnetic magnification at 200. With an ideal galvanometer the electromagnetic magnification is equal to $\frac{G}{g}\frac{S}{R+S}$, so if $S=2R$, which seems reasonable, it is necessary since $g=623{,}000$, that $G=1.5\times623{,}000\times200=1.87\times10^8$ dyne cm/E. M. U. current.

8. RESISTANCES OF SEISMOMETER WINDING AND BRIDGE

For the system to be critically damped, assuming the galvanometer to give an ideal performance, it is necessary that[11]

$$D'+G^2/(R+S)=2\sqrt{K'U'} \tag{H}$$

or

$$R+S=G^2/(2\sqrt{K'U'}-D')$$

where

$$D'=D+h^2d$$
$$K'=K+h^2k$$
$$U'=U+h^2u$$

Here D', K', and U' represent the combined effects of the damping constants with the circuits open, the moments of inertia, and the restoring constants of the galvanometer and seismometer.

Substituting for D, d, G, K, k, U, u, and h the values given above gives for $R+S$

$$12.3\times10^{10}\text{ E. M. U. resistance (or 123 ohms).}$$

Since it is assumed that S is to be equal to 2 R, it follows that R may be taken as 4.1×10^{10} and S as 8.2×10^{10}.

The selection of a proper value for S is of considerable importance, since it determines the damping and the damping to a considerable extent determined the performance. In the use of the apparatus, the proper resistance for the bridge will be determined experimentally and so should present no difficulty, but the problem here is to determine in advance what the resistance of the bridge should be to give critical damping. The procedure followed above is based on the assumption that the galvanometer would develop a back electromotive force equal to the potential difference applied across its terminals, while it is known that this will be only approximately true. Therefore a second approximate calculation will be made based on the assumption that the galvanometer and the seismometer have the same period. This permits the consideration of the bridge as made up of two

[11] See general design of critically damped galvanometers. B. S. Sci. Papers, **19** (No. 278), pp. 216–219; 1916, for discussion of conditions giving critical damping.

conductors in parallel, one connected to the galvanometer and of the proper resistance to critically damp the galvanometer, and the other connected to the seismometer and of the proper resistance to critically damp the seismometer. Assuming the resistance of the seismometer winding and connecting line to be 4.1×10^{10}, this leads to a value for the resistance of the bridge differing by but a few per cent from that stated above. As the galvanometer has a period of about 14 seconds, and it is assumed the seismometer will be adjusted to a period of 12.5 seconds, 8.2×10^{10} may be considered a proper value to use for the bridge in making an advance determination of the performance characteristics of the apparatus.

In the construction of a seismometer in accordance with this design, the value taken here for R should be looked upon as an upper limit for the resistance of the seismometer winding. If it is made less than 4.1×10^{10} in adjusting the bridge to given critical damping, it may be expected that it will become somewhat more than 8.2×10^{10}, and this will give some increase in the magnification and make the performance characteristics approach more nearly to those of the usual type of seismometer.

The procedure followed here has led to the following set of values for the structural constants of the seismometer and resistance of the bridge:

$$\begin{aligned} LM &= 10^4 \\ K &= 2.5\times10^5 \\ D &= 2.5\times10^4 \\ U &= 6.25\times10^4 \\ G &= 1.87\times10^8 \\ R &= 4.1\times10^{10} \\ S &= 8.2\times10^{10} \end{aligned}$$

Here all values are in c g s mechanical or electromagnetic units.

This design is based on the supposition that the galvanometer gives an ideal performance, though it is known that it gives only approximately such a performance. Therefore it should be expected that a seismometer constructed in accordance with it will give only approximately the performance specified above.

It should be noted that in the development of this design no reference has been made to the general seismometer equation (31) or to its solution for the case of a sustained harmonic displacement, equation (39). Equation (39) and equation (41), which gives the magnification of tilts, will serve to give more definite ideas concerning the performance to be expected and may be used to show the effects of various modifications in the design, especially if modifications may be made in the galvanometer as well as the seismometer.

VII. PERFORMANCE TO BE EXPECTED

Having thus arrived by a rather indirect procedure and to some extent by guessing at a set of values for the intrinsic or structural constants of the seismometer, it is in order to see more definitely what should be expected of a seismometer constructed in accordance with this design, when used with a galvanometer having the constants stated above. Substituting the values given for the structural constants of the seismometer and the galvanometer, and the resistance of the bridge, in equations (39) and (41), and dividing numerator and denominator by 10^{27}, gives for the magnification of displacements

$$M_x = \frac{19{,}200}{17.4 - 4.07/\omega^2 + j1.86\omega - j15.76/\omega + j0.091/\omega^3} \tag{44}$$

and for the magnification of tilts

$$M_\psi = \frac{81.8 \times 10^6}{17.4\omega^2 - 4.07 + j1.86\omega^3 - j15.76\omega + j0.091/\omega} \tag{45}$$

The substitution in these equations of different values of ω in the range from 62.8 to 0.001, corresponding to periods from 0.1 to 6,280 seconds, gives the data for the magnification of displacements and tilts tabulated in Table 1. This table also contains data for the phase angle between the deflection as shown on the record and the displacement and tilt of the earth. A part of these data are shown graphically in Figures 5, 7, and 9.

TABLE 1.—*Data showing performance to be expected of seismometer constructed in accordance with general design developed above and used with galvanometer having constants stated above*

ω	T_e	M_x	$M_\psi \times 10^{-6}$	γ_x	γ_ψ
62.8	0.100	163	0.00004	−81.5	−261.5
15	.419	600	.00261	−57.1	−237.1
10	.628	790	.00775	−44.4	−224.4
5	1.26	1,050	.0457	−19.9	−199.9
4	1.57	1,097	.0675	−11.8	−191.8
3	2.09	1,132	.123	−1.1	−181.1
2.5	2.51	1,140	.178	5.6	−174.4
2	3.14	1,135	.2781	15.3	−164.7
1.67	3.80	1,120	.3935	21.7	−158.3
1.50	4.19	1,104	.4775	26.3	−153.7
1.00	6.28	1,000	.980	46.0	−134.0
.628	10.00	781	1.94	73.3	−106.7
.500	12.57	643	2.52	87.9	−92.1
.333	18.85	397	3.50	113.6	−66.4
.250	25.1	259	4.013	130.0	−50.0
.200	31.4	178	4.360	141.6	−38.4
.100	62.8	48.5	4.75	170.2	−9.8
.060	104.5	16.8	4.575	188.0	8.0
.030	209.5	3.60	3.96	212.3	32.3
.010	628	.193	1.89	247.0	67.0
.002	3,140	.00169	.413	264.8	84.8
.001	6,280	.00021	.207	267.4	87.4

Here

$\omega = 2\pi/T_e$.
T_e = the period of earth displacement.
M_x = the magnification of earth displacements.
M_ψ = the magnification of earth tilts.
γ_x = the phase displacement between the record and earth displacement, in degrees.
γ_ψ = the phase displacement between the record and earth tilt, in degrees.

Figure 5 shows the magnification of earth displacements having periods in the range from 0 to 30 seconds. The reduced magnification of short-period displacements, especially those below 2.5 seconds,

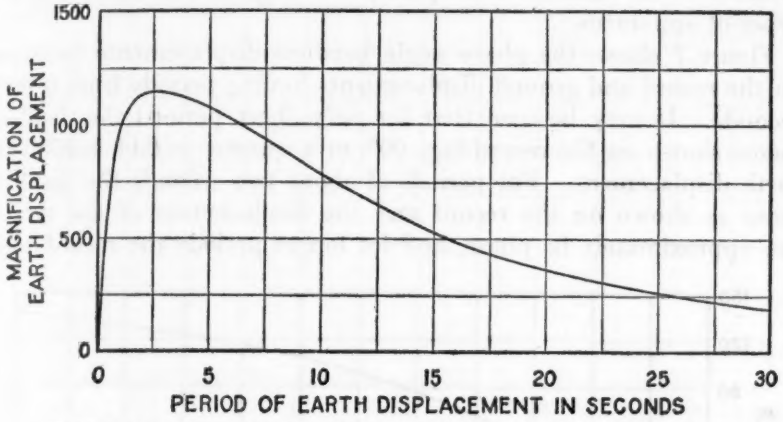

FIGURE 5.—*Magnification of earth displacements of different periods*

is one of the important advantages to be gained by electromagnetic magnification. In the range of periods from about 2.5 to 30 seconds, the magnification of earth displacements varies with the period much as it does with the usual type of seismometer having the same

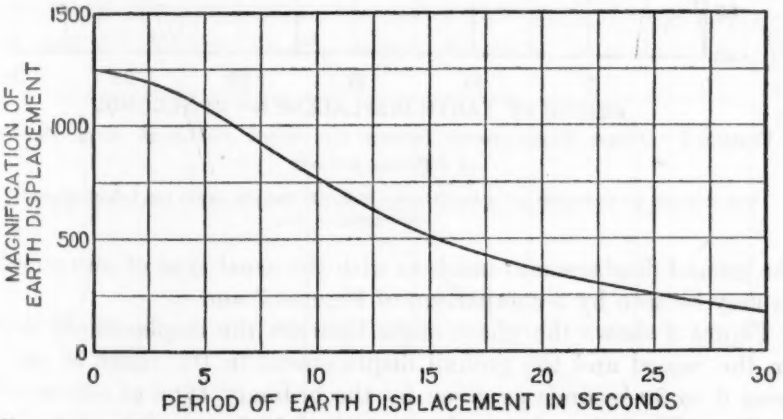

FIGURE 6.—*Magnification of earth displacements of different periods as given by a seismometer of the usual type having a static magnification of 1,250, a period of 12.5 seconds, and critical damping*

free period and critical damping, as may be seen by a comparison of Figures 5 and 6.

Figure 6 shows the magnification of earth displacements in the range of periods from 0 to 30 seconds as given by the ordinary type of seismometer having a free period of 12.5 seconds, critical damping, and a magnification of short-period displacements of 1,250. Here a

magnification of 1,250 is used instead of 1,000, that assumed in the development of the design, since it is found that this gives a closer correspondence between the two characteristic curves and so furnishes a better basis for a comparison of the performances of the two types of apparatus.

Figure 7 shows the phase angle between displacements as shown on the record and ground displacements having periods from 0 to 30 seconds. It may be seen that for very short periods the displacements shown on the record lags 90°, or a quarter period, behind the earth displacement. For periods of about two seconds the displacement as shown on the record and the displacement of the ground are approximately in phase, and for longer periods the record leads

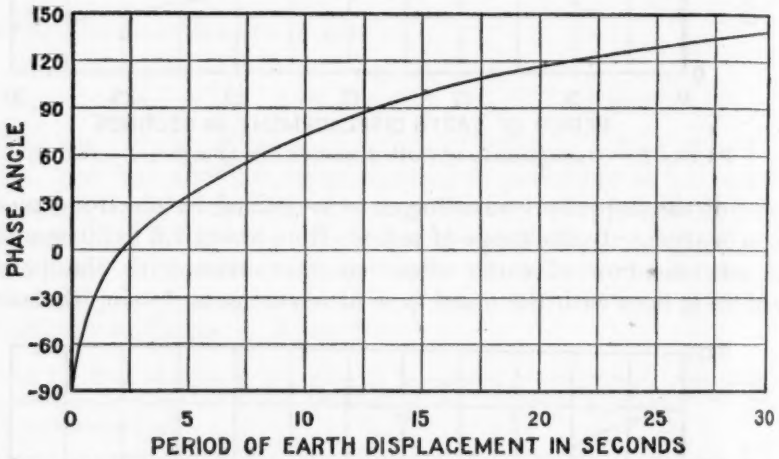

FIGURE 7.—*Phase displacements between the record and earth displacements of different periods*

The ordinates are in degrees and a negative sign indicates that the record lags behind the earth movement

the ground displacement much as with the usual type of seismometer, as may be seen by a comparison of Figures 7 and 8.

Figure 8 shows the phase angle between the displacement shown on the record and the ground displacement in the range of periods from 0 to 30 seconds as given by the ordinary type of seismometer having critical damping and a period of 12.5 seconds.

Figure 9 shows the magnification of tilts of the ground having periods from 6 to 6,000 seconds.

Figure 10 shows the magnification of tilts of the ground in the same range of periods as given by the ordinary type of seismometer having a free period of 12.5 seconds, critical damping, and a magnification of short-period displacements of 1,250.

In Figures 9 and 10 the periods are plotted on a geometric scale, the better to bring out the characteristics of the apparatus.

It will be seen that for the design under consideration the magnification of very long period earth tilts is much less than that given by the ordinary type of seismometer. This is an important advantage

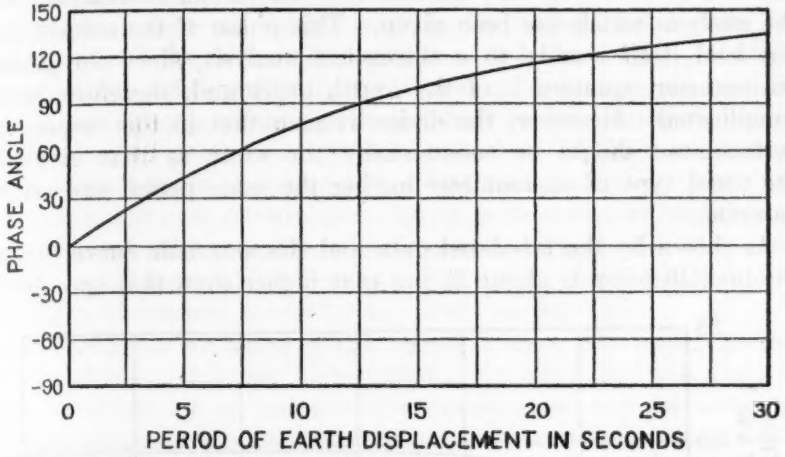

FIGURE 8.—*Phase displacements between the record and earth displacements of different periods as given by the usual type of seismometer having a period of 12.5 seconds and critical damping*

to be gained by electromagnetic magnification, since in many cases it is tilting, having in effect a period of several hours, which limits the magnification which can be used with a seismometer having a long period. It may be of interest, therefore, to note that for a

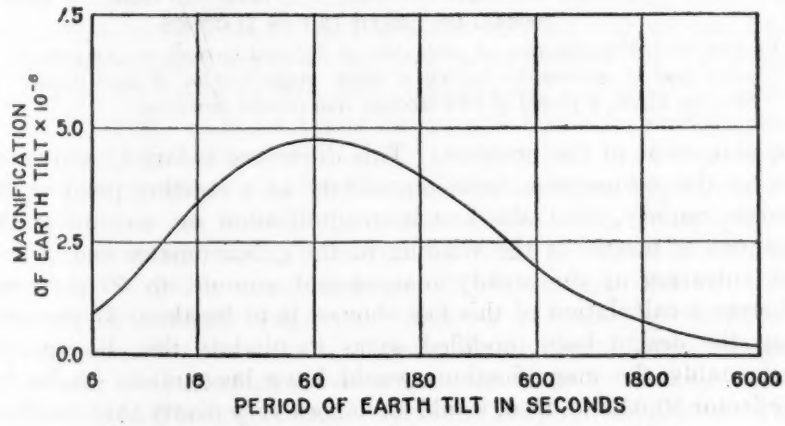

FIGURE 9.—*Magnification of earth tilts of different periods*

period of 6,000 seconds the magnification is only about 4 per cent of that of the ordinary type of seismometer having similar characteristics in the teleseismic range of periods. For disturbances of longer periods the magnification is inversely proportional to the period.

As to the performance which should be expected under conditions to be met in teleseismic observations—that is, where the displacement of the ground is more or less irregular instead of a sustained harmonic function of time—no very definite conclusions can be reached from the analysis which has been given. This phase of the subject does not lend itself readily to a theoretical analysis, since the general seismometer equation is of the fourth order and, therefore, rather complicated. However, the design is such that in this respect the performance should be substantially the same as that given by the usual type of seismometer having the same period and critical damping.

As shown by the tabulated data and characteristic curve (fig. 5), the magnification is about 25 per cent higher than that specified in

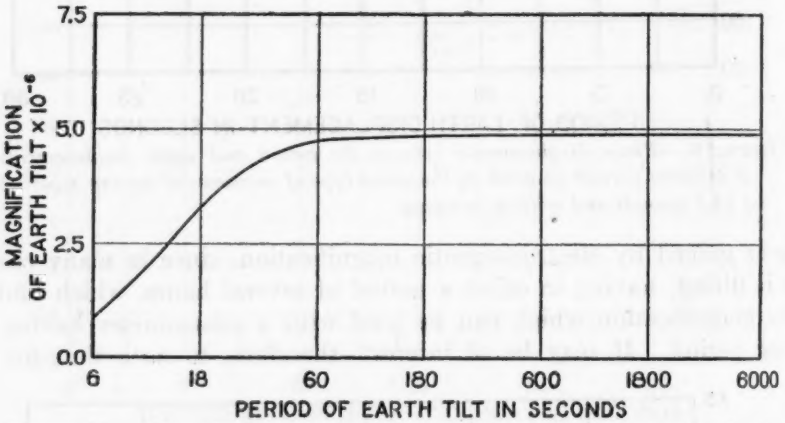

FIGURE 10.—*Magnification of earth tilts of different periods as given by the usual type of seismometer having a static magnification of earth displacements of 1,250, a period of 12.5 seconds, and critical damping*

the statement of the problem. This difference is largely accounted for by the assumption made tentatively as a starting point in the design, namely, that the loss in magnification on account of the moment of inertia of the winding of the galvanometer and lack of concentration of the steady mass would amount to 50 per cent, whereas a calculation of this loss showed it to be about 37 per cent. Had the design been modified so as to obviate this discrepancy, presumably the magnifications would have been made smaller by the factor 50/63 and, if so, would have been very nearly that specified. However, it is possible there may be no serious objection to the use of the higher magnification.

The reduced magnification of short-period displacements results mainly from the moment of inertia of the winding of the galvanometer and the resistance of the electrical curcuit. By changing the design of the galvanometer, a reduction of the resistance of the seismometer

winding, or both, it would be possible to materially increase the magnification of short-period displacements without making much change in the magnification of displacements having periods of 2.5 seconds and more. By making the bridge across the line connecting the galvanometer and seismometer highly inductive [12] and of low resistance, and the seismometer considerably larger, or the coil of the galvanometer considerably lighter, it would be possible to make the performance characteristics both for short and intermediate period displacements correspond very closely to those of the usual type of seismometer having the same period and same damping. However, this would make the construction slightly more expensive, the apparatus somewhat more complicated and much more subject to very short period disturbances of local origin. Further, it would result in only a slight improvement in records of distant earthquakes.

It would be an advantage if the magnification of tilts having periods of one minute and longer were materially reduced, and this could be brought about by stiffening the suspensions of the galvanometer winding, an increase of the resistance of the electrical circuit, or both. However, a stiffening of the suspensions or an increase of the resistance of the electrical circuit would have a detrimental effect upon the magnification of displacement of periods in the teleseismic range. It seems, therefore, that there are no obvious changes which should be made in this general design so it will be considered as completed.

VIII. DETAILED DESIGN AND CONSTRUCTION

The general design outlined above differs radically from any which, in so far as I know, has been used, and the analysis just made shows that an instrument constructed in accordance with it should give at least a fairly satisfactory performance, assuming, of course, proper attention to the detailed design and first-class workmanship throughout. It seemed, therefore, that it might be well to carry this project further to see what if any difficulties might be encountered in the detailed design and construction, to see more definitely what sort of performance such an instrument might give, and to see what difficulties might be encountered in its adjustments and use. Accordingly, a detailed design was made for a horizontal-component seismometer to have the values for the structural constants approximately the same as those given in the general design and an experimental instrument constructed approximately in accordance with this detailed design.

In the detailed design and construction no special effort was made to follow any particular general design strictly, since it was felt that considerable liberty might be taken without materially affecting the performance. However, care was taken to see that the structural

[12] Wenner, Phys. Rev., 19, p. 410; 1922.

constants should have such relative values that there would be no question but that critical damping and high magnification could be realized even should it be found necessary to adjust the apparatus so as to have a considerably shorter free period than that assumed in the statement of the problem. Further, where it was found convenient to make departures in a direction thought to be beneficial, this was done. As constructed, most of the constants have values smaller than those given by the general design. The largest departure is in the resistance of the seismometer winding, which is only about half as large. This lower resistance should result in making the performance characteristics approach more closely to those of the usual type of seismometer, having the same period and critical damping.

The experimental seismometer was shown at the meeting of the eastern section of the Seismological Society of America in May, 1927, and a photograph of it is reproduced in Figure 11. It has been installed on a pier located on undisturbed ground beneath the floor of a basement room of one of the buildings of the Bureau of Standards where conditions are not especially favorable for obtaining records of teleseismic disturbances. The galvanometer, recording camera, and bridge are located on the first floor of the same building, which permits of changing records without disturbing the seismometer. This also permits of a test to see that the motion of the steady mass is not obstructed, a determination of the period, and an adjustment of the damping without entering the room in which the seismometer is located. Parts of a few records obtained with this equipment are shown in Figures 12 to 16, inclusive. In these records the recording drum made one revolution per hour and the minute marks were made by momentarily increasing the intensity of the light source. A shutter was operated in the light beam as suggested by Anderson and Wood.[13] This gave exposures of about 0.07 second at intervals of about 0.6 second. Because of the limited space available for the recording apparatus, a lens was used to reduce the distance between the galvanometer mirror and the recording paper to about 80 cm. Therefore in the records the magnification is only 0.8 that which would have been obtained had the normal distance of 100 cm been used. The motion recorded is the N–S component. All save one of these records were made with a rather poor mirror on the galvanometer. The replacement of this mirror with one of good quality is giving much clearer and sharper records.

It is expected that a more complete description of the apparatus, a procedure for determining its structural constants, a procedure for making the adjustments, more definite information concerning its

[13] Anderson and Wood, Bull. Seis. Soc. Am., 15, p. 36; 1925.

FIGURE 11.—*Experimental seismometer constructed substantially in accord with the general design.*

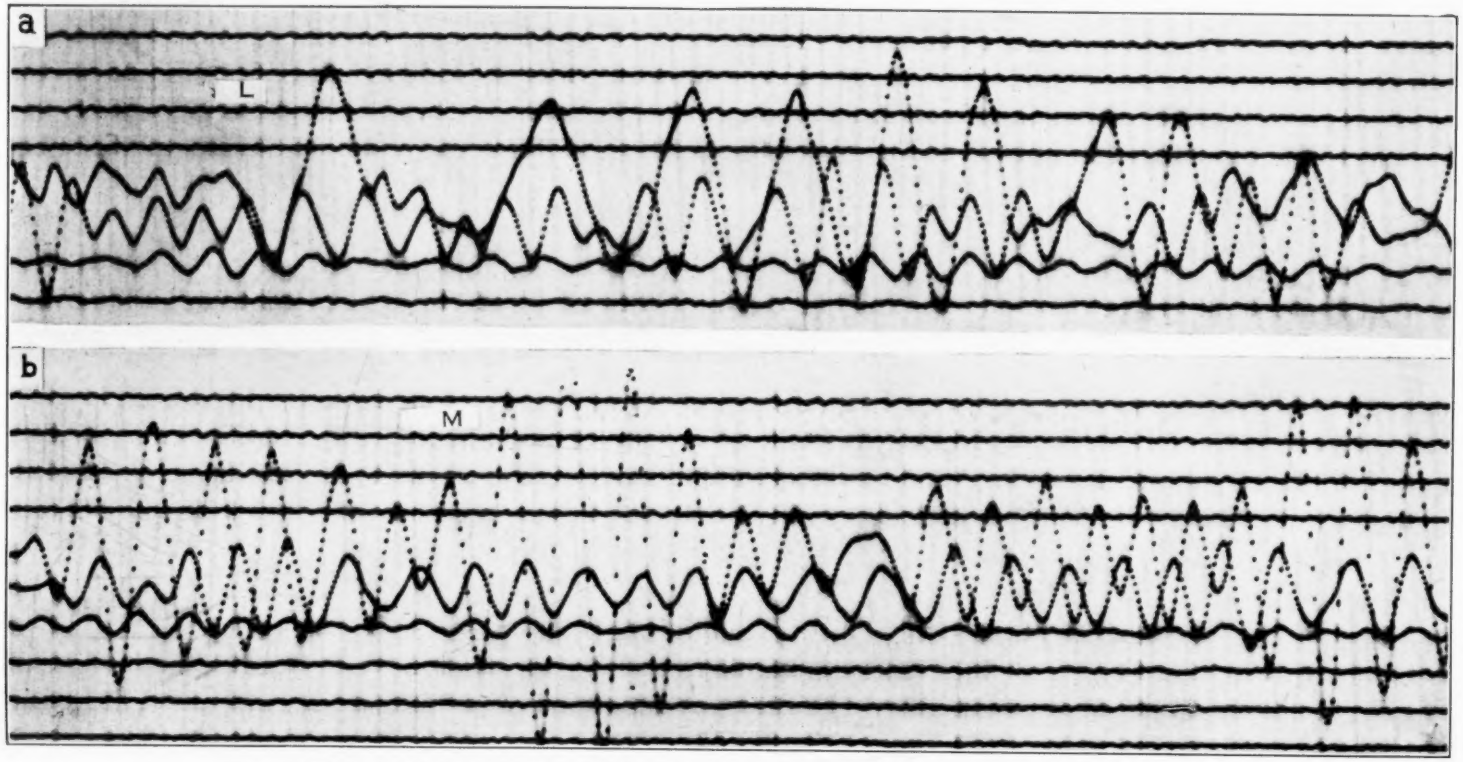

FIGURE 12.—*Parts of record of earthquake of March 16, 1928, near New Hebrides*

a shows L phase; *b* shows M phase

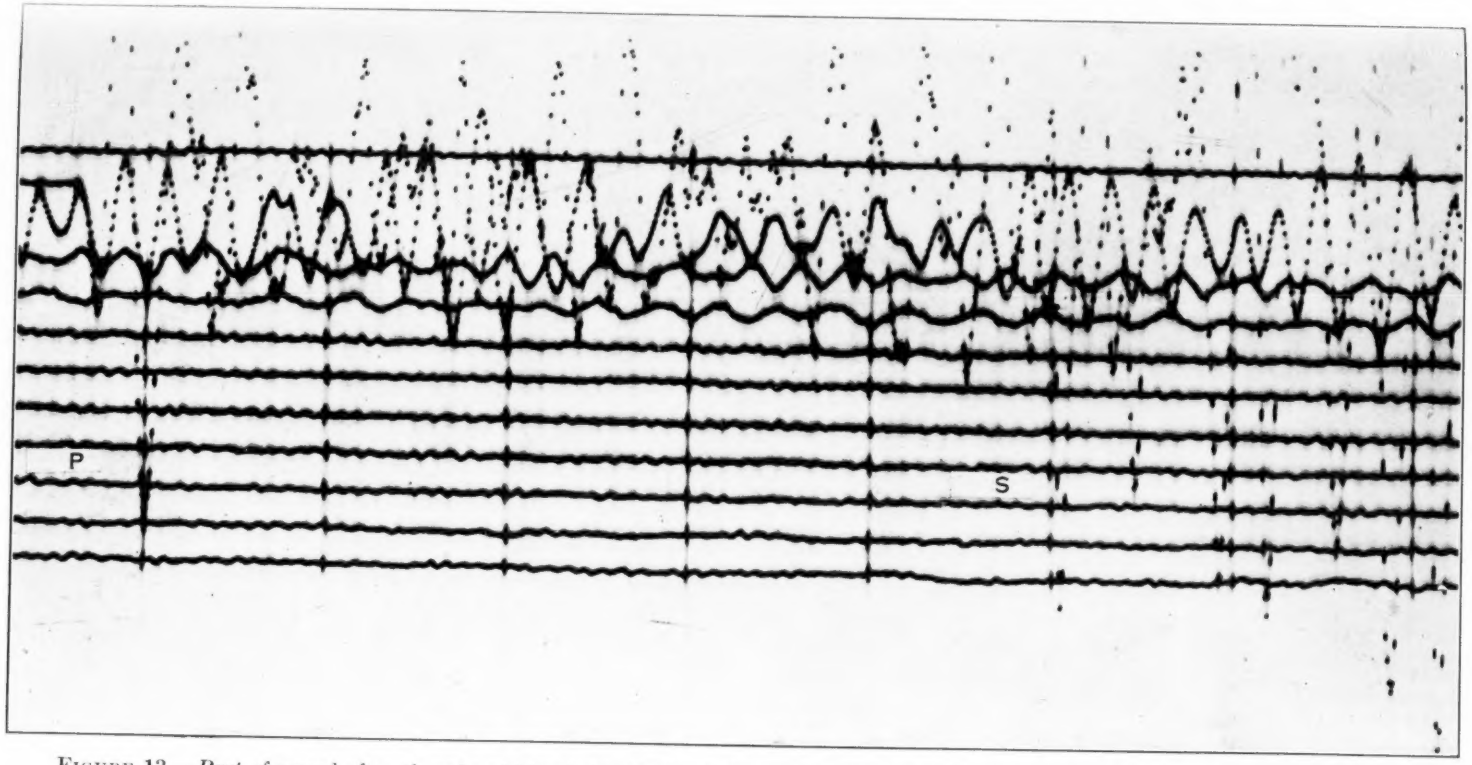

FIGURE 13.—*Part of record of earthquake of March 22, 1928, off the coast of southern Mexico, showing P, S, and other earlier phases*

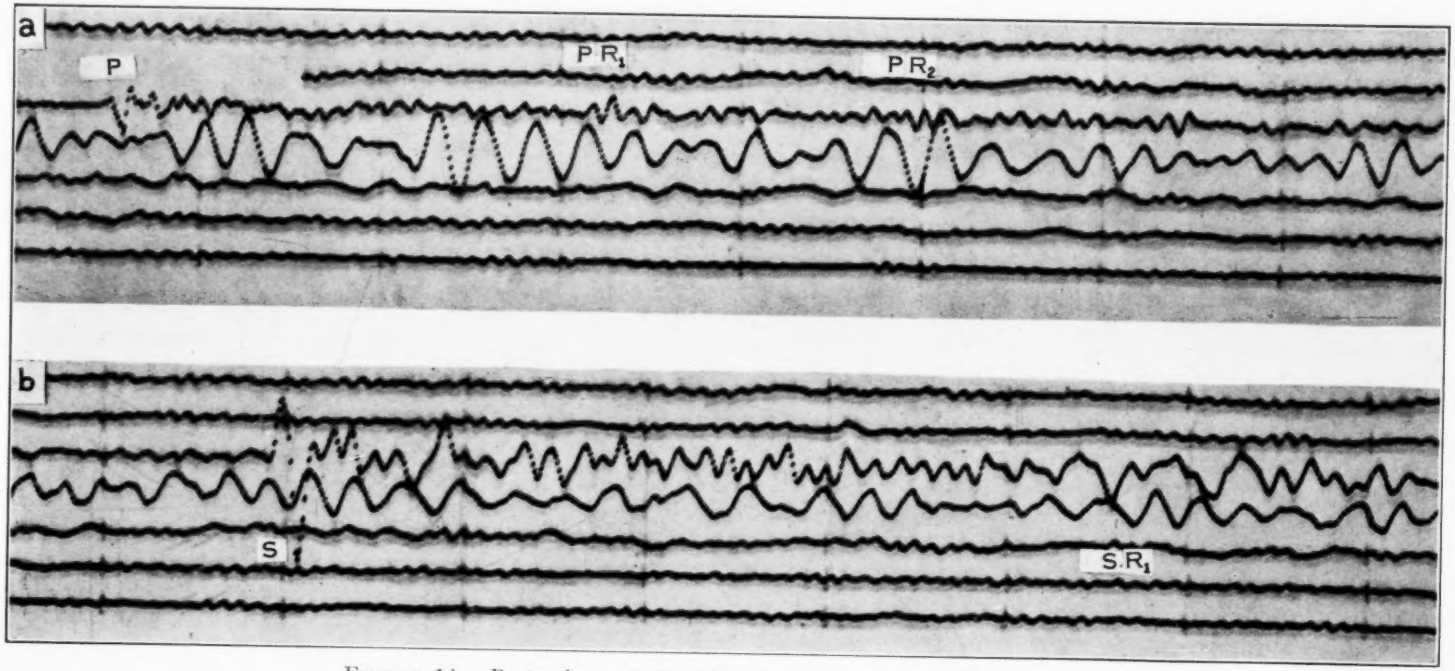

FIGURE 14.—*Parts of record of earthquake of April 18, 1928, in Bulgaria*

a shows P, PR_1, PR_2, and possibly other phases; *b* shows S, SR_1, and possibly other phases

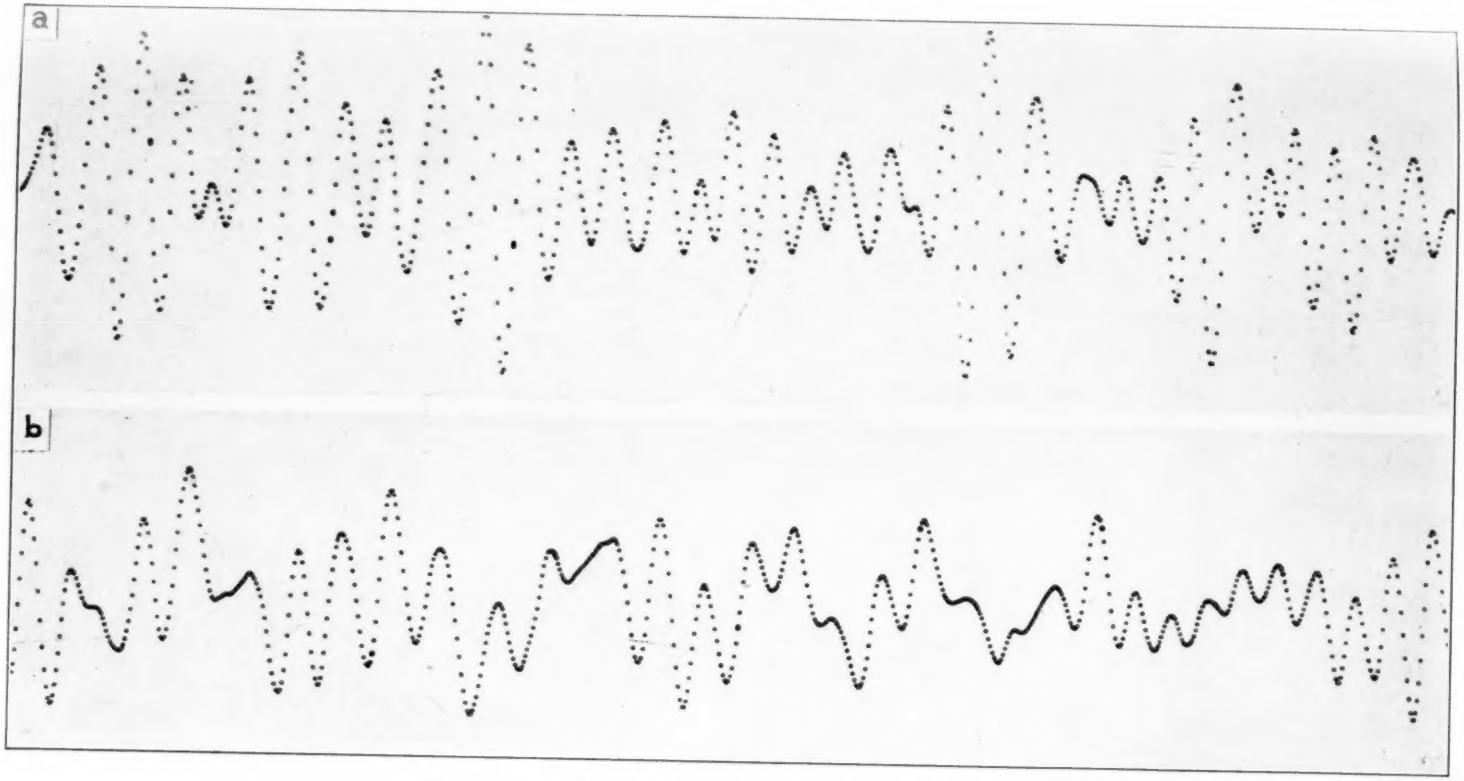

FIGURE 15.—*Parts of record of earthquake of June 17, 1928*

a, About 1 hour and 30 minutes after time of origin; *b*, about 1 hour and 45 minutes after time of origin

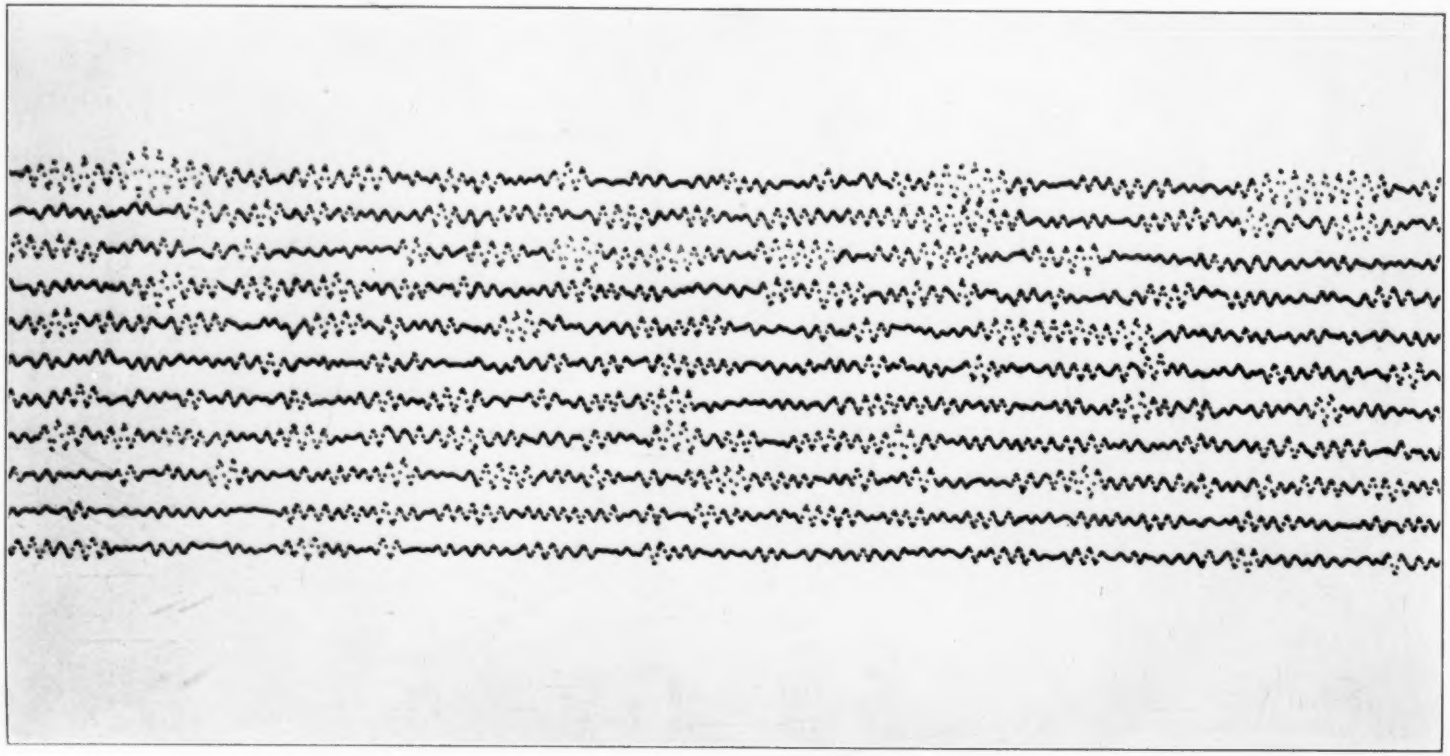

FIGURE 16.—*Part of record showing microseisms of considerably more than average intensity*

performance, and possibly suggestions for improving either or both the general design and the detailed design will be given in another paper.

IX. SUMMARY

1. An elementary discussion is given of the principles involved in electromagnetic damping and electromagnetic magnification.

2. It is shown that proper electromagnetic damping may be secured by the use of a bridge or shunt across the circuit connecting the seismometer and the galvanometer.

3. Expressions are derived for the current in the galvanometer winding and in the seismometer winding when both windings are developing an electromotive force and the circuit is bridged.

4. The equation is established for the motion of the steady mass relative to its support for the case in which the displacing torque arises both from an acceleration of the support and a current in the winding. From this and the corresponding equation for the motion of the winding of the galvanometer there is obtained a general seismometer equation; that is, an equation stating the relation between the angular displacement of the winding of the galvanometer and the linear displacement of the ground on which the seismometer is located.

5. The general seismometer equation which is a linear differential equation of the fourth order is solved for the case of a sustained harmonic displacement of the ground.

6. It is shown that by a slight modification of this solution it gives the relation between the deflection of the galvanometer winding or the displacements shown on the record and the angle of tilt of a horizontal-component seismometer.

7. A general design is developed for a seismometer to give at least approximately a specified performance. This general design permits of making the seismometer of small size, simple construction, and requires no special magnets for producing proper damping.

8. The damping of both the galvanometer and the seismometer is controlled by a single bridge or shunt across the line connecting the galvanometer and the seismometer. As this bridge may be located adjacent to the galvanometer, the period may be determined and the damping adjusted from the position of the galvanometer, which normally would be in a room other than that in which the seismometer might be located.

9. Characteristic curves for a seismometer of this general design and, for comparison, corresponding curves for the ordinary type of seismometer are shown.

10. Finally, a photograph of an experimental seismometer constructed substantially in accordance with this general design and parts of a few records obtained with it are shown.

X. APPENDIX—SYMBOLS

The symbols used in more or less separated parts of this paper and the quantities which they represent are as follows:

d, damping constant of galvanometer with circuit open.

D, damping constant of seismometer with circuit open.

g, electrodynamic constant of galvanometer.

$\mathfrak{g}$, acceleration of gravity.

G, electrodynamic constant of seismometer. The factors on which it depends are explained on page 970.

H, magnetic field strength.

h, the electromagnetic magnification or the ratio of Θ to Φ.

i, current usually in galvanometer winding.

I, current in seismometer winding.

j, square root of minus one.

k, moment of inertia of winding and mirror of galvanometer.

K, moment of inertia of moving system of the seismometer.

l, equivalent length of galvánometer pointer or twice the distance between the optical center of the galvanometer mirror or lens and the recording paper.

L, distance from center of mass of moving system of seismometer to the axis of rotation.

M, mass of the moving system of seismometer.

M_x, magnification of linear displacements of the support of the seismometer; that is, the ratio of displacement as shown on the record to displacements of ground.

M_ψ, magnification of angular displacements or tilts.

Q^2, defined by equation (15).

r, resistance, usually of the galvanometer winding and suspensions.

R, resistance of seismometer winding and connecting leads.

S, resistance of shunt or bridge across circuit connecting galvanometer and seismometer.

t, time.

T_o, the undamped period of the seismometer.

u, restoring constant of galvanometer.

U, restoring constant of seismometer.

x, linear displacement.

X, linear displacement of support of seismometer.

$\mathfrak{X}$, amplitude of linear displacement of support of seismometer.

$\boldsymbol{X}$, complex quantity equal in magnitude to amplitude of linear displacement of support of the seismometer and containing a phase angle depending upon the assumed origin of time.

ϵ, base of Napierian logarithm.

ϕ, angular deflection of moving system of seismometer.

Φ, complex quantity, equal in magnitude to amplitude of angular deflection of steady mass of seismometer, and containing a phase angle.

ψ, angle of tilt.

Ψ, complex quantity, equal in magnitude to the amplitude of angle of tilt and containing a phase angle depending upon the assumed origin of time.

θ, angular deflection, usually of moving system of galvanometer.

Θ, complex quantity, equal in magnitude to amplitude of angular deflection of moving system of galvanometer and containing a phase angle.

ω, 2π divided by period of earth displacement or tilt.

WASHINGTON, December 7, 1928.